Melanie Santos Matos

Degree in Medicinal Chemistry

Exploring the potential of natural extracts obtained from winemaking waste streams for cosmetic applications

Dissertation to obtain the Master Degree in
Biochemistry for Health

Supervisor: Ana Matias, PhD, iBET/ITQB-UNL
Co-supervisor: Ana Teresa Serra, PhD, iBET/ITQB-UNL

December, 2017

Melanie Santos Matos

Degree in Medicinal Chemistry

Exploring the potential of natural extracts obtained from winemaking waste streams for cosmetic applications

Dissertation to obtain the Master Degree in
Biochemistry for Health

Supervisor: Ana Matias, PhD
Co-supervisor: Ana Teresa Serra, PhD

December, 2017

Exploring the potential of natural extracts obtained from winemaking waste streams for cosmetic applications

Para ser grande, sê inteiro: nada
Teu exagera ou exclui.
Sê todo em cada coisa. Põe quanto és
No mínimo que fazes.
Assim em cada lago a lua toda
Brilha, porque alta vive.

(Ricardo Reis, heterónimo de Fernando Pessoa)

Acknowledgements

Em primeiro lugar, gostaria de agradecer à minha orientadora, Doutora Ana Matias, por me ter proporcionado a oportunidade de desenvolver este trabalho, dentro de um tema que me fascina, no laboratório de Nutracêuticos e Tecnologia de Processo de Bioativos do ITQB/iBET. Agradeço também por toda a orientação, motivação e apoio prestados, e pelo interesse demonstrado no meu trabalho.

Agradeço à minha co-orientadora, Doutora Teresa Serra, por todos os conhecimentos transmitidos, pelas palavras de incentivo e otimismo, e por estar sempre disponível para me ajudar.

Quero também agradecer a toda a equipa NBPT que tão bem me recebeu: Liliana, Carolina, Joana Guerreiro, Vanessa, Agostinho, Maria João, Ana Nunes e Ana Roda. Obrigada por toda a ajuda, simpatia e boa disposição. Devo um agradecimento especial:

À Liliana, por me ter transmitido todas as bases necessárias para começar o meu trabalho, pela enorme ajuda na realização da análise por HPLC, e por ter continuado sempre disponível para me ajudar ao longo deste percurso. Obrigada por sempre teres tido paciência para responder às minhas questões.

À Carolina, pela companhia, esclarecimentos, e conselhos. Obrigada pelas inúmeras discussões científicas que tanto me ajudaram a evoluir.

À Joana Guerreiro, por tudo o que me ensinou, e por tantas vezes me ter ajudado sempre que precisei.

À Maria João, por todos os conhecimentos transmitidos e sugestões, e também pela disponibilidade para ajudar. Muito obrigada.

Agradeço também à Joana Poejo, que apesar de já não pertencer ao grupo, sempre se mostrou disponível para esclarecer as minhas dúvidas.

Estou grata à Doutora Maria do Rosário Bronze, pela enorme ajuda na parte da química analítica, e pela sua disponibilidade e compreensão.

Agradeço à Andreia Bento da Silva pela ajuda na realização da análise por HPLC e pela disponibilidade para esclarecer as minhas dúvidas.

Não posso deixar de agradecer aos amigos. Aos de Lisboa, de Coimbra, e aos de sempre:

Agradeço à Marcela, à Constança e à Marta pelo apoio, pelos bons momentos, e por terem tornado estes dois anos mais felizes.

Agradeço à Maria Inês, à Ana Tomé, à Inês Fonseca, à Cátia, à Sara, à Adriana, à Inês Guerra, ao Hugo, e à Ana Rita. Agradeço ao Miguel Sousa, ao DD, e ao Diogo Pacheco, às minhas Marianas (Poupado, Sotero e Inês), à Carlota, à Marta Leal e à Ana Afonso. Obrigada pela vossa amizade e por todo o apoio. Não seria tão fácil sem vocês.

Quero deixar um agradecimento especial ao André, por ser a melhor parte da minha semana, por todo o apoio e compreensão.

Agradeço à minha família: aos meus pais, irmãos e sobrinhos, por sempre terem acreditado e investido em mim. Saber que vos tenho a vocês é o melhor do mundo. Agradeço em especial aos meus irmãos por serem tão bons exemplos, e à minha mãe por toda a força, motivação, segurança e otimismo. Sem ela, nada disto seria possível. Um “obrigado” não chega!

Por fim, gostaria de agradecer a todas as pessoas que, direta ou indiretamente, contribuíram para a realização deste trabalho.

Muito obrigada a todos!

Abstract

Phenolic compounds present in grapes have been widely explored as cosmetic principles, because of their renowned antioxidant activity and proven ability to directly inhibit certain enzymes relevant for skin ageing.

The winemaking process generates large amounts of waste streams, thus recovery of phenolic bioactive compounds from residues and further incorporation in cosmetic products represents a promising market opportunity for wine producers, and may contribute to a sustainable development of the sector.

In the present work, extracts obtained from different winemaking waste streams (grape marc and wine lees), by different extraction procedures, were screened for bioactivity in several biological endpoints related to skin ageing. For this purpose, all samples were characterized in terms of antioxidant activity in chemical assays (ORAC/HOSC/HORAC) and cell-based assays in keratinocytes (HaCaT) and fibroblasts (HFF). Inhibitory capacity towards specific enzymes, namely tyrosinase, elastase and MMP-1, was evaluated. Phytochemical characterization was also carried out by colorimetric assays and HPLC-DAD-MS, in order to identify the main compounds responsible for the bioactivity of the extracts.

Red table wine lees extracts presented the highest antioxidant capacity, and were the most effective inhibitors of tyrosinase, elastase and MMP-1. The extract presenting the most promising results in all experiments was also the one with the highest phenolic content. Flavonoids, such as flavonols and anthocyanins, were identified as compounds playing significant roles in the bioactive response of samples.

Formulations of a grape marc extract sample with three different carriers (maltodextrin, whey protein isolate, and pea protein isolate) were evaluated, and results show that encapsulation of the extract contributed to the preservation of its phenolic constituents, and enhanced antioxidant activity relative to the non-formulated extract.

In conclusion, this work proves that winemaking waste streams are a valuable source of natural ingredients with potential for application in cosmetic products for skin whitening and anti-ageing purposes.

Keywords: Phenolic compounds; antioxidant activity; anti-ageing; skin whitening; tyrosinase; elastase; MMP-1; formulation; HaCaT; HFF

Resumo

A aplicação de compostos fenólicos provenientes das uvas em cosméticos tem sido explorada, dada a sua atividade antioxidante e capacidade para inibir enzimas relacionadas com o envelhecimento cutâneo.

O processo de produção de vinho gera grandes quantidades de resíduos, pelo que a recuperação de compostos fenólicos a partir dos mesmos, e a sua incorporação em cosméticos, representa uma promissora oportunidade de negócio para a indústria do vinho, podendo vir a contribuir para o desenvolvimento sustentável deste setor.

No presente trabalho, foi avaliada a bioatividade de extratos de resíduos de produção de vinho (bagaço e borras), obtidos por diferentes processos de extração, relativamente a vários alvos biológicos envolvidos no envelhecimento cutâneo. As amostras foram caracterizadas em termos de atividade antioxidante em ensaios químicos (ORAC/HOSC/HORAC) e celulares, em queratinócitos (HaCaT) e fibroblastos (HFF). Foi também examinada a capacidade para inibir enzimas específicas, nomeadamente tirosinase, elastase e MMP-1. A caracterização fitoquímica dos extratos foi realizada através de ensaios colorimétricos e HPLC-DAD-MS, com o intuito de identificar os principais compostos responsáveis pela bioatividade.

Os extratos de borras de vinho tinto de mesa evidenciaram uma maior atividade antioxidante, e capacidade para inibir a atividade das enzimas tirosinase, elastase e MMP-1. O extrato que revelou os resultados mais promissores foi também o que apresentou uma maior quantidade de compostos fenólicos. Verificou-se, ainda, que os flavonóides, entre os quais flavonóis e antocianinas, parecem ser relevantes na bioatividade das amostras.

Foram avaliadas formulações de um extrato de bagaço com maltodextrina, proteína de soro de leite, e proteína de ervilha, tendo-se concluído que o encapsulamento do extrato contribuiu para a preservação dos constituintes fenólicos, e aumentou a atividade antioxidante.

Resumindo, este trabalho permite concluir que resíduos de produção de vinho constituem uma valiosa fonte de ingredientes naturais com potencial para aplicação em produtos cosméticos com efeitos anti-manchas e anti-envelhecimento.

Palavras-chave: Compostos fenólicos; atividade antioxidante; anti-envelhecimento; anti-manchas; tirosinase; elastase; MMP-1; formulação; HaCaT; HFF

1. Table of Contents

List of figures

List of tables

Table 3.10. Summary of the results obtained for the selected extracts in cell-based assays, in terms of prevention of H_2O_2-induced ROS and intrinsic ROS generation, and protection against H_2O_2-induced cytotoxicity. For each assay, the extracts (at a concentration of 0.25 mg extract/mL) were rated by comparison with the untreated control. For prevention of ROS generation (fluorescence percentages relative to the untreated control): +++++ for <70%; ++++ for 70–75%; +++ for 75–80%; ++ for 80–85%; + for 85–90%; - for 90–95%; - - for 95–100%. For protection against H_2O_2-induced cytotoxicity (cell viability percentage): + for <50%; ++ for 50–60%; +++ for 60–70%; ++++ for 70–80%; +++++ for 80–90%. Results for HaCaT are represented in green, whereas results for HFF are represented in red.

List of abbreviations, acronyms and symbols

Short Form	Full Form
AAAPVN	N-succinyl-Ala-Ala-Ala-*p*-nitroanilide
AAPH	2,2'-azobis(2-methylpropionamidine)dihydrochloride
ADME	Absorption, Distribution, Metabolism, Excretion
AP-1	Activator Protein 1
CAT	Catalase
CAE	Caffeic Acid Equivalents
CCD-1112Sk	Human Foreskin Fibroblasts Cell Line
ChC	Collagenase from *Clostridium histolyticum*
DAD	Diode Array Detector
DB	Dry Basis
DCF	2',7'-Dichlorofluorescein
DCFH	2',7'-Dichlorofluorescin
DCFH-DA	2',7'-Dichlorofluorescin Diacetate
DE	Dextrose Equivalents
DMEM	Dulbecco's Modified Eagle Medium
DMSO	Dimethyl Sulfoxide
DNA	Deoxyribonucleic Acid
ECM	Extracellular Matrix
FBS	Fetal Bovine Serum
FC	*Folin Ciocalteu*
FIR	Far-IR
FL	Fluorescein Sodium Salt
GAE	Gallic Acid Equivalents
GAGs	Glycosaminoglycans
GPx	Glutathione Peroxidase
GR	Glutathione Reductase
GSH	Reduced form of Glutathione
GSSG	Oxidized form of Glutathione
HA	Hyaluronic Acid/ Hyaluronan
HaCaT	Spontaneously Immortalized Human Keratinocyte Cell Line
HFF	Human Foreskin Fibroblasts
HORAC	Hydroxyl Radical Averting Capacity
HOSC	Hydroxyl Radical Scavenging Capacity
HPLC	High Performance Liquid Chromatography

IC_{50}	Half Maximal Inhibitory Concentration
IκB	Inhibitor of κB
IMDM	Iscove's Modified Dulbecco's Medium
IR	Infrared
ISC	Intersystem Crossing
ISO	International Organization for Standardization
L-DOPA	3,4-Dihydroxy-L-phenylalanine
Malv-3-O-gl	Malvidin-3-O-glucoside
MAPK	Mitogen-associated Protein Kinases
MD	Maltodextrin
MIR	Middle-IR
MMP	Matrix Metalloproteinase
mRNA	Messenger RNA (Ribonucleic Acid)
MS	Mass Spectrometry
Mt-DNA	Mitochondrial DNA
MT-MMP	Membrane-Type MMP
MTS	5-(3-carboxymethoxyphenyl)-2-(4,5-dimethylthiazoly)-3-(4-sulfophenyl)tetrazolium, inner salt
MW	Microwave
NE	Neutrophil Elastase
NF-κB	Nuclear Factor kappa-light-chain-enhancer of activated B cells
NIR	Near-IR
NMF	Natural Moisturizing Factor
ORAC	Oxygen Radical Absorbance Capacity
PBS	Phosphate-Buffered Saline
PE	Pancreatic Elastases
PPE	Porcine Pancreatic Elastase
PPI	Pea Protein Isolate
PS	Photosensitizer
P-S	Penicillin-Streptomycin
ROS	Reactive Oxygen Species
S-L	Solid-Liquid
SOD	Superoxide Dismutase
SPB	Sodium Phosphate Buffer
TAC	Total Anthocyanin Content
TE	Trolox Equivalents
TGF-β	Transforming Growth Factor β

TIMPs	Tissue Inhibitors of MMP
TPC	Total Phenolic Content
Trolox	(+/-)-6-hydroxy-2,5,7,8-tetramethylchroman-2-carboxylic acid
TSP	Thrombospondin
USDA	United States Department of Agriculture
UV	Ultraviolet
vdW	Van der Waals forces
VEGF	Vascular Endothelial Growth Factor
WPI	Whey Protein Isolate

1. Introduction

1.1. Skin

The skin is the most extensive organ in the body, making up to about 16% of body weight [1], and several functions can be listed: protection against mechanical, chemical and physical agents, temperature regulation, synthesis of important substances and elimination of undesired ones, first line of defense against pathogens, and sensitivity, all aiming at keeping the internal body systems intact. [2]

Skin is a stratified structure where three different layers of tissue can be identified: the outermost layer is the epidermis, the middle layer is the dermis, and the innermost layer is the hypodermis. [2]

The epidermis is divided into an inner layer composed of viable cells (keratinocytes, melanocytes, Langerhans cells, and Merkel cells), which can be subdivided into the basal cell layer (*stratum basale*), the prickle cell layer (*stratum spinosum*), and the granular cell layer (*stratum granulosum*); and an outer horny layer composed of anucleated cells (corneocytes) named *stratum corneum*. The most abundant cells in the epidermis are the keratinocytes, and the four abovementioned layers result from a gradual process of keratinocyte differentiation that reflects the stages of maturation of keratin, an important structural protein responsible for mechanical resistance and impermeability of the skin. [1–3]

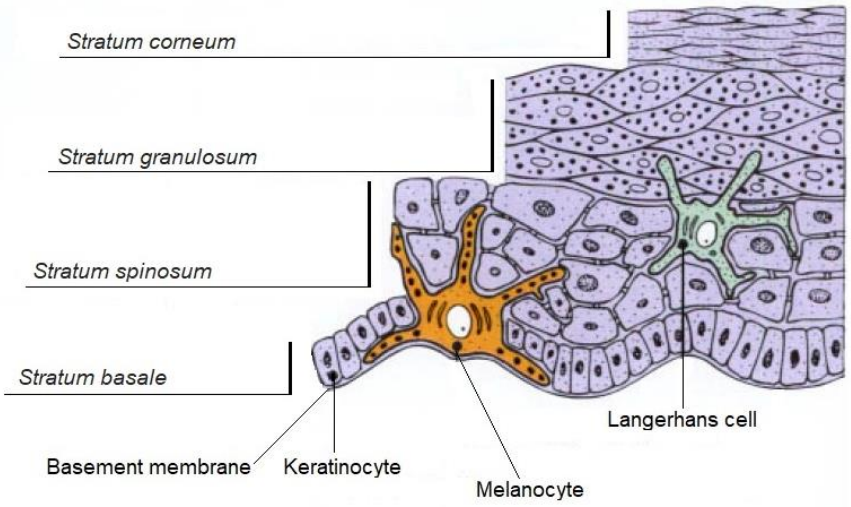

Figure 1.1. Layers of the epidermis. Adapted from *Dermatology – An Illustrated Colour Text, 3rd Edition* [1]

The *stratum basale* is composed of a single layer of continuously dividing and highly metabolically active keratinocytes with a cylindrical shape, which are anchored to the basal membrane by hemidesmosomes. As they rise to the surface, keratinocytes gradually lose water and start to flatten, resulting in several layers of polyhedral shaped cells that form the *stratum spinosum*, where production of keratin tonofilaments and keratohyalin, a keratin precursor, begins. Langerhans cells, dendritic cells with immunological functions, are mostly found in this layer. Flattening of

keratinocytes continues as they reach the *stratum granulosum*, where keratohyalin granules found in the cytoplasm of keratinocytes mature and are converted into keratin. At this point, keratinocytes begin to lose their nuclei and organelles, accumulating large amounts of keratin in their cytoplasm along with other granules containing specific proteins and lipids that will contribute to cell adhesion in the *stratum corneum*. Finally, in the top layer, the *stratum corneum*, keratinocytes are already flattened cells without nuclei or organelles (and therefore no metabolic activity) that take the name of corneocytes. Corneocytes have a thick cell envelope covered with lipids, and the cytoplasm is replaced by keratin tonofiblrils in a matrix formed from keratohyalin granules. The *stratum corneum* consists of a resistant layer of superimposed cells tightly stuck together, with variable thickness depending on the part of the body. In the more external layers of the *stratum corneum*, corneocytes are less tightly packed and are continuously lost by skin shedding, balancing the proliferation of cells at the basal cell layer. This process, from the moment keratinocytes are formed in the basal layer until they are lost in the surface layer, lasts about 28 days. In certain areas of the body, where skin is thicker, there is an additional layer, the *stratum lucidum*, where keratinocytes are already depleted of nuclei and organelles, and contain in their cytoplasm an homogeneous substance called eleidin. [1–3]

Among the proteins produced by keratinocytes, profilaggrin is one of the most important. It is a component of keratohyalin granules and once hydrolyzed to filaggrin during terminal differentiation of keratinocytes, it is crucial for aggregation of keratin tonofilaments. At the surface of the corneocyte layer, filaggrin is degraded to free aminoacid units among other substances, which are highly hygroscopic and are the main constituents of the *Natural Mosturizing Factor* (NMF), responsible for epidermal hydration. These aminoacids also contribute to skin barrier function, by playing a role in acidification of the *stratum corneum*, which is a prerequisite for the functioning of enzymes responsible for the formation of ceramides, the most important class of lipids present in the intercellular matrix of the *stratum corneum*, that help retaining water within the epidermis and constitute a barrier against the entry of external substances. [4,5]

Another major player in skin's hydration and emollience is the hydrolipidic film, composed of sebum, keratinocyte cell waste, bacterial substances (resulting from bacteria normally present in the skin), water from sweating and transpiration, and exogenous substances (cosmetic products and dirt). [2]

Distributed between the keratinocytes of the basal cell layer, there can be found Merkel cells and melanocytes. Merkel cells are mechanoreceptors responsible for tactile sensation, given that they are associated to sensory nerve endings. These cells are mainly located in highly sensitive skin areas, such as fingertips or lips. [2]

Melanocytes are responsible for the synthesis of melanin, the pigment that confers color to the skin. The amount of melanocytes makes up to 5-10% of the basal cell population, although this may vary depending on body area. When skin is exposed to UV radiation, melanin production begins, and cytoplasmic bodies called melanosomes are formed and accumulate in granules.

Melanocytes possess cytoplasmic extensions, called dendrites, which infiltrate between the keratinocytes of the basal and spinous layers, allowing for the transfer of melanosomes to adjacent keratinocytes by phagocytosis. Each melanocyte provides melanosomes to a group of approximately 36 neighboring keratinocytes. Once inside the keratinocytes, melanosomes arrange themselves around the nuclei conferring protection against UV radiation. In corneocytes, melanosomes are uniformly distributed inside the cell and act as a natural sunscreen, avoiding UV radiation penetrating the skin, and as a free radical scavenger. [1–3]

There are two types of melanin: the more common form, eumelanin, which confers a brown to black colour; and the less common phaeomelanin, which confers a yellow to red colour. Both types derive from synthetic pathways that depend on the catalytic activity of the enzyme tyrosinase. After being synthesized, tyrosinase accumulates in vesicles in the presence of a protein matrix. The aminoacid tyrosine is primarily oxidized to 3,4-dihydroxyphenylalanine (DOPA), which in turn is oxidized to dopaquinone. These first two steps are catalyzed by tyrosinase. In the presence of cysteine, phaeomelanin is produced, whereas in the eumelanin pathway, dopaquinone undergoes a cyclization reaction resulting in dopachrome and then 5,6-dihydroxyindole, which is oxidized to indole-5,6-quinone by tyrosinase, giving rise to eumelanin. These synthetic pathways are depicted in Figure 1.2. Differences in skin color among individuals does not depend on the number of melanocytes, but rather on the amount, size and distribution of melanosomes, as well as the ratio between different types of melanin. [1–3]

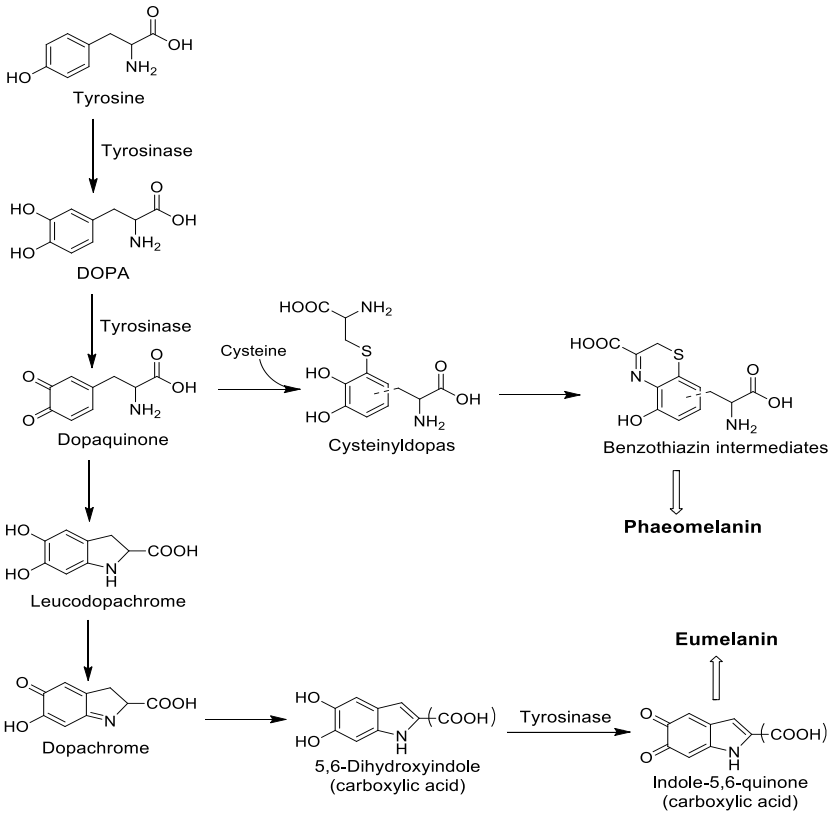

Figure 1.2. Eumelanin and phaeomelanin synthetic pathways.

The skin layer found beneath the epidermis is the dermis, which is intimately connected with the former, through the dermal-epidermal junction. In this junction, a structure called *rete ridges* can be found, consisting of epidermal projections into the dermis and *vice-versa*. It increases the contact surface area between the epidermis and the dermis, enhancing the adhesion between these two layers. [6]

The dermis is a matrix of connective tissue, with variable thickness depending on body area, that provides support to skin and its annexes. This skin layer is composed of cells, fibrous proteins and ground substance, and, as opposed to the epidermis, is richly innervated and vascularized. The resident cells in the dermis are predominantly fibroblasts, although mastocytes, lynphocytes, macrophages and dendritic cells are also present. Fibroblasts are responsible for the synthesis of both the fibers and the ground substance that form the extracellular matrix (ECM) of the dermis, while other cell types therein are mainly related to immunological functions. [1–3]

The dermis can be divided into two layers: the papillary dermis and the reticular dermis. The papillary dermis is the dermal portion closest to the epidermis. It interdigitates with the epidermal *rete ridges* and has a rich capillary network responsible for the nutrient supply of the epidermal layer and skin annexes. Protein fibers are arranged in a loose and irregular manner and the ground substance is abundant. The reticular dermis is found below the papillary dermis and is thicker, providing greater support to the skin structure. It is composed of coarser bundles of protein fibers displayed in a parallel orientation towards all skin layers. Other constituents of the dermis, namely cells, ground substance and blood vessels, are less abundant in the reticular layer than in the papillary dermis. [1,2] Collagen fibers are the predominant fibers found in the dermis, and their main function is to provide mechanical resistance and structural strength to the skin, preventing overstretching and tearing. There are several types of collagen, four of which can be found in skin: type I in the reticular dermis; type III in the papillary dermis; and types IV and VII in the basement membrane. [1] Types I and III are fibrillar collagens, while types IV and VII are non-fibrillar collagens. Types I and III collagens are the most widely occurring in skin. [7,8] Each collagen molecule is composed of three polypeptide chains, called α chains, intertwined to form a triple-helical structure. There are different types of α chains, differing slightly in amino acid composition, and collagens can be homo- or heterotrimeric, depending on wether they have the same or different α chains in their structure, respectively. Fibrillar collagens are synthesized and secreted into the ECM as soluble precursor molecules, called procollagens, with N- and C-terminal propeptide domains. Once in the ECM, these domains are cleaved by proteinases, triggering spontaneous self-assembly into fibrils and then fibers, which are stabilized by covalent cross-links initiated by enzymes from the lysyl oxidase family. Reticular collagens have no precursor forms, and their N- and C- terminals are intimately involved in the assembly of the collagen molecules, through different molecular interactions. [7,9]

Elastic fibers are also important constituents of the dermis, since they confer elasticity to the skin, maintaining skin tension, flexibility and resilience. These fibers are displayed mainly in the

reticular dermis forming a loose weave [1], and are mainly composed of elastin (90%) [8], but also microfibrils where elastin is deposited. Elastin has a very high durability, with a half-life of approximately 70 years, and once it is deposited during neonatal period, its synthesis ceases and there is very little turnover during adulthood, unless the elastic fibers are submitted to injury. Microfibrils, whose main components are fibrilin-1, fibrilin-2, and microfibril-associated glycoprotein-1, appear in the ECM and act as a scaffold for assembly and deposition of tropoelastin monomers. Once secreted, hydrosoluble tropoelastin molecules (precursors of elastin) are deposited in microfibrils in the ECM, where crosslinks between fibrilin and tropoelastin stabilize the association. At this point, two sequential processes are responsible for incorporating the tropoelastin monomers in the growing elastic fiber: coacervation and crosslinking. Coacervation is an entropically driven process, in which the entropy of the system rises when hydrophobic regions of tropoelastin monomers interact, due to release of water molecules that were oriented in those regions. This process is adjusted to the physiological conditions found in the ECM. Following coacervation, crosslinking of the deposited tropoelastin molecules occurs through the action of enzymes from the lysyl oxidase family. [10] Thereafter, elastic fibers are composed of an amorphous central core of insoluble elastin surrounded by an envelope of microfibrils. A supposition that elastogenesis begins in the upper dermal layer and proceeds deeper into the dermis is supported by the fact that the most superficial fibers of the dermis consist only of the fibrotubular component (vertical thin oxytalan fibers), whereas deeper in the dermis, horizontal thick and mature elastic fibers can be found. Ascending from the lower level of the papillary dermis to the dermal-epidermal junction, there are elaunin fibers, consisting of an intermediate form, with characteristics from both oxytalan fibers and elastic fibers. Oxytalan fibers arise from the terminals of elaunin fibers. [11]

The ground substance of the dermis is a semi-solid matrix, mainly composed of glycosaminoglycans (GAGs), and proteoglycans, secreted directly into the ECM. GAGs are linear polysaccharides composed of repeating disaccharide units, consisting of an N-acetylated or N-sulphated hexosamine, and either an uronic acid (glucuronic or iduronic) or galactose. Proteoglycans are high-molecular weight structures, composed of a protein core and one or more covalently bound glycosaminoglycan chains. These substances have the main function of retaining water, producing an amorphous hydrated gel capable of absorbing compressive forces, regulating permeability, cell migration, proliferation and differentiation. In the dermis, chondroitin sulfate, dermatan sulfates, and hyaluronan are the predominant GAGs. Hyaluronan, commonly referred to as hyaluronic acid (HA), is a well-known GAG that does not occur in the form of proteoglycan [1,12] but plays an important role in water homeostasis and lubrication (due to its viscoelastic properties when hydrated) [13], and has space-filling as well as shock-absorbing functions [14]. HA exists both in the dermis (particularly in the papillary dermis) and the epidermis, although dermal fibroblasts have a much higher production rate than epidermal keratinocytes. [14]

The deepest layer in the skin is the hypodermis, located below the dermis. It comprises mainly adipocytes (cells containing large amounts of lipids in their cytoplasm) grouped into lobes

separated by connective tissue, and is of variable thickness depending on the individual and body area. This layer is infiltrated by blood vessels that ensure nutrition of the tissue. [2]

1.2. Skin Ageing

Skin ageing is mainly characterized by wrinkling, sagging, loss of elasticity and volume, and pigmentation disorders. These features are undesirable not only for cosmetic reasons and appearance, but also because aged skin is known to have a compromised barrier function [15], resulting in a dry appearance and susceptibility to environmental aggressors, and therefore an enhanced risk for skin disorders. In aged skin, the main alterations occur at the level of the dermal connective tissue, and are translated in qualitative and quantitative changes in collagen and elastic fibers, as well as glycosaminoglycans and proteoglycans. These alterations result in a diminished tensile strength and elasticity, an increased frailty of the skin and a reduced capacity for wound healing. [8]

1.2.1. Intrinsic and Extrinsic Ageing

Ageing is caused by both endogenous and exogenous factors and it can be divided into intrinsic and extrinsic ageing, respectively. Intrinsically aged skin manifestations include a thinned but smooth epidermis, fine wrinkles, loss of underlying adipose tissue, and dryness. On the other hand, extrinsically aged skin is characterized by deep wrinkles, uneven pigmentation (with hyperpigmented regions), teleangiectasias, roughness and a leathery appearance. [14,16]

Intrinsic ageing is a physiological process caused by factors that are inherent to the organism itself, resulting from the fulfilment of biological functions and from the natural degeneration of these functions over time (chronological effect). The main biological events associated with intrinsic ageing are the production of reactive oxygen species (ROS) from cellular respiration (aerobic metabolism), the loss of replicative ability of cells because of telomeres shortening, and an increased degradation of the extracellular matrix (ECM). All these processes are normal and occur naturally with ageing. [17] Also, some genetic factors must be considered, such as epigenetic modifications or certain genetic polymorphisms which can influence skin ageing rate. [16]

ROS produced during cell respiration are a consequence of an incomplete reduction of molecular oxygen, caused by leakage of electrons from the electron transport chain. [18] Although equipped with antioxidant defenses, mitochondria may suffer DNA damage due to continuous ROS production. Over time, this damage accumulates specially due to a lack of DNA repair systems in the mitochondria, as opposed to the nucleus, which may affect mitochondrial ability to generate energy, hence leading to an impaired functionality of cells, or even cause apoptosis. Moreover, a deficient oxidative phosphorylation is likely to enhance ROS generation. [19]

All dividing cells have a limited lifespan, becoming senescent after a certain number of divisions. With each division a cell undergoes, a small fragment of a structure named telomere is

lost. Telomeres are repetitive segments of non-coding DNA that are present on the edges of coding DNA to maintain the stability of genetic material, by avoiding loss of coding segments during the replicative process. Since each time a cell divides, a part of the telomere is lost, there is a point in time when the telomere becomes critically short and the DNA is no longer stable, being more susceptible to loss of coding fragments. Since this could affect somatic cell function, at this point the cell is unable to undergo further division and apoptosis is induced. In skin, cellular senescence affects mainly keratinocytes, fibroblasts and melanocytes. [17] Apart from loss of replicative ability of existing cells, senescence is also characterized by a decreased number of cells in the tissue. [16] The onset of senescence in ageing skin occurs in cells from both dermal and epidermal layers. [8]

The increased degradation of the cutaneous extracellular matrix observed in aged skin is a consequence of two things: increased levels of ECM-degrading enzymes, and an altered expression of dermal ECM components, due to gradual oxidative damage caused during life to genes coding for these components. [17]

Extrinsic ageing is caused by environmental factors, whose impact in skin ageing depends on the duration, frequency and intensity of exposure. It is mainly driven by the continuous production of reactive oxygen species (ROS) upon exposure to solar radiation, cigarette smoke, and pollutants. Exposure to solar radiation is the main contributor to skin ageing, in a process referred to as photoageing (further discussed in section 1.2.5.). [17]

Extrinsic and intrinsic ageing effects are cumulative and are believed to share certain underlying mechanisms, particularly in what concerns to an increased generation of ROS in skin. Moreover, the normally occurring pro-oxidant environment in intrinsically aged skin can be even more heightened by external oxidant agents. [20]

1.2.2. Reactive Oxygen Species and Antioxidant Defense

Reactive oxygen species (ROS) are chemically unstable species with a transitory existence, which react with surrounding molecules in order to achieve their steady state. The term ROS refers to all reactive molecules containing oxygen in their composition, including both free radical species, such as superoxide anion ($O_2^{-\bullet}$), hydroxyl ($^{\bullet}OH$), or peroxyl ($ROO^{\bullet}$); and non-radical species, such as hydrogen peroxide (H_2O_2) and singlet oxygen ($^1O_2$), among others. [16]

ROS can be from endogenous or exogenous origin. Exogenous sources include cigarette smoke, radiation, pollution, while the most relevant endogenous source is cellular respiration. ROS are generated as by-products of aerobic metabolism, because electrons leak from the electron transport chain and partially reduce oxygen, forming the superoxide anion radical ($O_2^{-\bullet}$), which subsequently gives rise to other ROS. [18]

ROS are capable of inducing damage to biomolecules, including DNA oxidation leading to mutations, protein oxidation leading to loss or reduced function, and membrane lipid oxidation leading to impaired transmembrane transport and altered transmembrane signaling [21]; hence, to counteract their effect, there are natural antioxidant defenses of enzymatic and non-enzymatic

origin present in the organism with the function of neutralizing ROS, maintaining them within physiologically acceptable levels. The most important non-enzymatic antioxidants include vitamin A (retinol) vitamin C (ascorbic acid), vitamin E (α-tocopherol), and glutathione (GSH). The lead enzymatic antioxidant defense consists of superoxide dismutase (SOD), catalase (CAT), and glutathione peroxidase (GPx). Non-enzymatic antioxidants are depleted much more easily than enzymatic antioxidant defenses. [2]

Retinoic acid, the active form of vitamin A, acts by scavenging radicals intracellularly, while vitamic C acts as a radical scavenger both intracellularly and extracellularly. Vitamin E is a lipid-soluble antioxidant found in the hydrophobic interior of membranes, providing antioxidant defense against membrane damage through lipid peroxidation. Glutathione (GSH) is a tripeptide (glutamic acid-cysteine-glycine) of great importance found in all cell compartments. The ratio between its reduced and oxidized states (GSH/GSSG) is a reliable indicator of the oxidation state of a system. GSH is a co-factor for glutathione peroxidase, participating in the enzymatic antioxidant defense. [18]

Superoxide dismutases (SOD) have the ability to convert superoxide anion radical ($O_2^{-\bullet}$) to hydrogen peroxide (H_2O_2), and can be divided in subclasses: SOD-1 is found in the cytosol, SOD-2 is located in the mitochondria, and SOD-3 is an enzyme found in the extracellular matrix. [2] The resulting H_2O_2 has a high diffusion rate across membranes, and the ability to rapidly permeate cell membranes and inflict damage elsewhere. Moreover, it can react with iron and other transition metal ions to form the highly reactive hydroxyl radical ($^{\bullet}OH$), through Fenton-like reactions: $Metal^{2+} + H_2O_2 \rightarrow Metal^{3+} + {}^{\bullet}OH + OH^-$. The superoxide anion radical can also contribute to generation of the hydroxyl radical, by reducing metal (III) to metal (II), making it available for the Fenton-like reaction. This step is called Haber-Weiss reaction: $Metal^{3+} + O_2^{-\bullet} \rightarrow Metal^{2+} + O_2$. The hydroxyl radical is highly reactive and is able to oxidize numerous biomolecules, including membrane lipids by initiating lipid peroxidation through abstraction of hydrogen atoms from unsaturated fatty acids, which results in the generation of peroxyl radicals ($ROO^{\bullet}$). [18]

H_2O_2 can be detoxified to water (H_2O) by either catalase (CAT) or glutathione peroxidase (GPx). Catalase is a highly efficient detoxifying enzyme, although it is only found in the peroxisome. On the other hand, glutathione peroxidase is located both in the mitochondria and in the cytosol. GPx relies on GSH as a cofactor and catalyzes its oxidation to GSSG, which in turn is restored by glutathione reductase (GR). [22] The GPx-GSH system also has a protective role of the cell membrane by reducing lipid hydroperoxides (products of lipid peroxidation) to their corresponding alcohols. Subclass GPx-1 is the most common and is found in the cytoplasm of most mammalian cells, having the ability to reduce both H_2O_2 and fatty-acid peroxides; GPx-4 is a membrane-bound enzyme and is able to reduce esterified peroxyl lipids; subclass GPx-3 can be found in the extracellular compartment. [18]

Despite numerous antioxidant defense systems, a fraction of formed ROS recurrently evades this antioxidant control, which results in an accumulation of ROS. Furthermore, the shift

towards an oxidant state is worsened with ageing, given the decline in efficiency of these systems. When the balance between ROS and antioxidants is disrupted, due to an excess of ROS or to a depletion of antioxidants, a state of oxidative stress is established. [2]

1.2.3. Enzymes enrolled in skin ageing processes

As already mentioned, skin ageing is a complex process in which the major damage is observed in the dermal connective tissue, primarily due to loss of mature collagen, alterations in elastic fibers, and increased expression of ECM-degrading enzymes. Another feature of aged skin is the mottled appearance due to hyperpigmentation disorders.

Matrix metalloproteinases (MMPs) are endopeptidases with a zinc ion (Zn^{2+}), a three-histidine zinc-binding motif and a conserved methionine in their active site. These enzymes are translated as zymogens (inactive pro-enzymes), with a signal sequence peptide that determines if their activity will be performed intracellularly, anchored to the cell membrane, or in the extracellular matrix (ECM). Pro-MMPs are kept inactive by an interaction between a cysteine residue present in the pro-domain and Zn^{2+}, and activation requires a disruption of this interaction, which may happen by direct cleavage of the pro-domain by other proteinases, reaction with oxidant species (ROS, for instance), or allosteric perturbations caused by interaction with non-substrate molecules. MMPs are responsible for the turnover and degradation of ECM components, such as all types of collagen, laminins, integrins, elastin, proteoglycans, fibronectin, and many others. Despite the wide specificity overlap between different MMP substrates, these enzymes can be divided into subgroups: collagenases (MMP-1, -8 and -13), gelatinases (MMP-2 and -9), stromelysins (MMP-3, -10 and -11), matrilysins (MMP-7 and -26), and membrane-type (MT)-MMPs (MMP-14, -15, -16, -17, -24 and -25). MMPs have a role in homeostasis and numerous physiological processes, such as tissue repair and remodeling, cell migration and differentiation, etc., and both their expression levels and activity are tightly regulated at the level of transcription, activation and inhibition. However, overexpression of active MMPs is the driving cause of several pathological conditions, including accelerated skin ageing. [23–25] The most relevant MMPs participating in the connective tissue degradation observed in ageing skin are MMP-1, MMP-3, and MMP-9, produced by keratinocytes and fibroblasts, and MMP-8 or neutrophil collagenase, liberated by infiltrating neutrophils. Stromelysin MMP-3 and gelatinase MMP-9 can only digest collagen after triple helix degradation initiated by a collagenase, which makes MMP-1 the most significant enzyme enrolled in the skin ageing process, given it has substrate specificity for both types I and III collagen. Specific tissue inhibitors of MMPs (TIMPs), which are present both in intracellular and extracellular compartments, and play an important role in the regulation of MMP activity, are found to be inefficient in counteracting the increased amount of active MMPs observed in ageing skin [2,23], due to inactivation by ROS or insufficient expression [20].

Elastolytic enzymes, defined as elastases or elastase-type proteases, can be released by pancreatic cells, neutrophils, macrophages, fibroblasts and keratinocytes. Elastases belong to a

class of broadly specific endopeptidases with the ability to not only solubilize insoluble elastin thus contributing to degradation of elastic fibers, but also to cleave other ECM proteins such as collagen or fibronectin. [26] There are two subclasses of elastase-type proteases: chymotrypsin serine proteases, such as neutrophil elastase (NE) and pancreatic elastases (PE); and metalloelastases, such as macrophage elastase (MMP-12) and skin fibroblast elastase. [27–29]

Serine proteases are a family of enzymes with a conserved catalytic triad (histidine-serine-aspartate) in their active site, of which serine serves as a nucleophile in the catalytic process. These proteases are synthesized as inactive zymogens: PE are secreted to the digestive tract in their inactive form, where they suffer activation from trypsin; NE zymogen is activated by cathepsin C and is stored in neutrophilic granules already in its active form. [30,31]

Neutrophil elastase (NE) is able to degrade elastic fibers at all stages of development (oxytalan, elaunin and mature elastic fibers) [32], and it further contributes to degradation of ECM connective tissue by inducing an increase in active MMP-1 and MMP-2 levels [33], as well as degradation of TIMPs [34]. Macrophage elastase (MMP-12) is the most active MMP against elastin despite having a broad specificity, being also able to degrade a number of other ECM components. Although the liberation of this enzyme by macrophages contributes to degradation of elastic fibers in the cutaneous ECM, it is crucial for the migration of these cells in tissues. Moreover, MMP-12 degrades the main inhibitor of NE, which enhances elastolytic activity. [25,35,36] Both macrophages and neutrophils are immunologically active cells that infiltrate tissues during inflammatory processes, thereby playing an important role in skin ageing following those responses.

Skin fibroblast elastase is a membrane-bound metalloprotease expressed, as its name states, in skin fibroblasts. This protease cleaves the immature oxytalan and elaunin fibers, but has a limited proteolytic activity towards mature elastic fibers. Skin fibroblast elastase is believed to contribute to connective tissue degradation even in the absence of an inflammatory response. [32,37]

Pancreatic elastase-1, despite its designation, is not expressed in the pancreas, yet it is found to be expressed in keratinocytes from skin basal cell layer (*stratum basale*). On the other hand, other PE isozymes are only expressed in pancreatic cells. [38]

Although necessary for physiological purposes, such as cell migration, wound healing, or tissue repair, an exacerbated amount of elastase-type proteases in tissues leads to several pathologies as well as skin ageing. [29,32,36,39] Moreover, elastolytic activity may enter a vicious cycle because elastin peptides liberated in a certain elastolytic site chemotactically attract leucocytes, which in turn lead to an increased release of elastase-type proteases. [40]

Hyaluronidases belong to a complex family of enzymes that degrade hyaluronic acid (HA), and therefore contribute to loss of ground substance from the cutaneous ECM observed in aged skin. These enzymes can be categorized according to substrate specificity and generated end-products. [41]

Tyrosinase is a copper-containing enzyme with a critical role in the production of melanin. It is the rate-limiting enzyme of melanin synthesis and catalyzes the first two steps of the process: hydroxylation of tyrosine to DOPA (monophenolase activity) and the oxidation of DOPA to dopaquinone (diphenolase activity). [42,43] Dysregulation in tyrosinase expression or activity may lead to pigmentation disorders such as hyperpigmentation mottles.

1.2.4. Alterations observed in aged skin

Aged skin reveals notable structural and biochemical alterations in all its layers. At the surface level, a disturbed barrier function can be noticed. A flattening of the *rete ridges* in the dermal-epidermal junction occurs, leading to a lowering of contact surface area between dermis and epidermis, and therefore a decreased number of basal keratinocytes as well as a higher susceptibility to epidermal shearing. Epidermal cell turnover, meaning the process of ascending differentiation of keratinocytes from the basal layer until they reach the *stratum corneum*, has also been shown to decline with age. [8]

Apart from the reduced number of fibroblasts encountered in the dermis, dermal atrophy is mainly driven by alterations in connective tissue constituents (collagen, elastin and GAGs). Thinning of collagen bundles and an increased space between fibers are observed. These phenomena are probably caused by the augmented levels of MMPs and reduced amounts of types I and III procollagen detected in both intrinsically and extrinsically aged skin. On the other hand, changes in the elastic network of aged skin are complex and variable, with depletion of oxytalan fibers in the papillary dermis, and an increase in thickness and number of elaunin and elastic fibers in the reticular dermis. In addition, intrinsically aged skin reveals a decreased amount of GAGs forming the ground substance, resulting in a reduced support provided to the connective tissue fibers and a structural collapse of the dermis. [8] On the other hand, extrinsically aged skin reveals an increased deposition of ground substance, including GAGs and proteoglycans, as opposed to the observed depletion of collagen fibers. [19]

The dry appearance of intrinsically aged skin may be due to the reduced ground substance, which leads to a lower capacity of skin to retain water, and to the decreased number of total keratinocytes, which are known to contribute to the formation of the natural moisturizing factor (NMF).

The number of enzymatically active melanocytes is also found to be decreased in both intrinsically and extrinsically aged skin. However, an enhanced pigmentation (although uneven) is observed in aged skin, particularly in sun-exposed areas, which seems contradictory. This can be explained by the fact that, although a generalized decrease in the number of melanocytes occurs in all skin areas (sun-exposed and sun-protected), melanocytes in chronically sun-exposed areas possess an increased capacity for melanin production, and, due to their scarce and uneven distribution, hyperpigmented areas appear. [44]

1.2.5. Photoageing

Solar radiation is the main contributor to skin ageing, in a process defined as photoageing. Ultraviolet (UV) radiation reaching the earth's surface comprises UV-A (320 – 400 nm) and UV-B (290 – 320 nm). UV-B has a much more significant impact on skin than UV-A, because of the more energetic wavelength, however, UV-A effects are more relevant, given the much higher amount of this radiation traversing the atmospheric layer without being absorbed. Moreover, UV-A penetrates more deeply in the skin, reaching the dermis, while UV-B is mainly retained in the epidermis and absorbed by molecules therein. [17] UV radiation interacts with endogenous cromophores in skin, such as nucleic acids, urocanic acid, aromatic aminoacids, melanins and their precursors, porphyrins, flavins, among others, resulting in either free radical formation by direct photoionization, or in excitation of molecules. When in their excited state, cromophores can either dissipate the absorbed radiative energy by converting it into heat or light (fluorescence); or, providing their excited state is long-lived enough, they can initiate photochemical reactions that result in the generation of ROS. When the excited state of a cromophore is long-lived enough, which happens in the case of photosensitizer (PS) molecules, intersystem crossing (ISC) may take place. ISC consists of a transition between an excited singlet state of a PS to its excited triplet state, which can either return to the ground state by light emission (phosphorescence) or it can undergo photochemical reactions. Type-I photochemical reactions involve the transfer of electrons or protons to oxygen or other adjacent molecules, generating ionic radicals (including superoxide anion radical, which is further converted to hydrogen peroxide by enzymatic means). Type-II photochemical reactions happen when there is an energy transfer between the excited triplet state of a PS and the triplet ground state of molecular oxygen, giving rise to the very reactive singlet oxygen ($^1O_2$). [45] Singlet oxygen, as well as hydroxyl radical, can react with and damage nucleic acids, proteins, lipids and sterols [46], and singlet oxygen is known to cause the "common deletion" of mtDNA (deletion of a characteristic portion of mtDNA observed in several cell types of aged individuals) [19,20].

Infrared (IR) radiation can be divided into three regions: IR-A (760 – 1400 nm), also defined as near infrared (NIR); IR-B (1400 – 3000 nm), also defined as middle infrared (MIR); and IR-C (3000 – 1000000 nm), also defined as far infrared (FIR). IR radiation accounts for about 40% of the solar radiation reaching earth's surface, therefore its effects on skin ageing must not be ignored. While IR-A can penetrate through the epidermis and dermis, reaching even subcutaneous tissue without significantly raising skin temperature, IR-B and IR-C are essentially absorbed in the epidermis, where they contribute to a significant increase in temperature of the skin to about 40ºC. [47] Furthermore, IR radiation is also emitted by numerous sources, such as stoves, furnaces, or electronical devices, which increases daily exposure.

Heat shock, meaning submitting cells to a higher than the ideal temperature, was seen to induce production of ROS, particularly H_2O_2 and $O_2^{-\bullet}$, in keratinocytes, through the action of a number of enzymes, including an enzymatic complex of the electron transport chain in the

mitochondria. [48] These ROS may further generate additional ones, by initiating the already described Fenton reaction.

ROS generated following solar radiation absorption by endogenous molecules are the driving force of photoageing mechanisms.

1.2.6. Mechanisms involved in skin ageing

Regardless of their origin (UV, IR or endogenous), ROS have the ability to cause damage to several biomolecules, including connective tissue proteins through fragmentation of the peptide chain, crosslinking, oxidation of specific aminoacids, and alteration of net electrical charge, which renders them more vulnerable to degradation by proteases. [18] Apart from that, ROS may cause connective tissue damage and decline by inducing certain cytoplasmic signal transduction pathways through activation of specific receptors on the surface of keratinocytes and fibroblasts. This effect is mediated by inhibition of protein-tyrosine phosphatase-κ, whose function is to keep the membrane receptors inactive (in a hypophosphorylated state). Inactivation of protein-tyrosine phosphatase-κ leads to activation of growth factor and cytokine membrane receptors with consequent intracellular signaling through stimulation of the mitogen-associated protein kinases (MAPK) pathway, leading to the activation of the transcription factor complex AP-1 (activator protein 1), which in turn induces the transcription of MMP genes (-1, -3 and -9) in both fibroblasts and keratinocytes, and down-regulates the transcription of TGF-β (transforming growth factor β – a major pro-fibrotic cytokine) receptors as well as types I and III procollagen genes in fibroblasts. [19,21] ROS can also activate transcription factor NF-κB (nuclear factor kappa-light-chain-enhancer of activated B cells), through activation of kinases that phosphorylate IκB (inhibitor of κB), freeing NF-κB. This transcription factor induces the expression of several pro-inflammatory cytokines and adhesion molecules, contributing to the recruitment of inflammatory cells [18,19], such as macrophages and neutrophils, which further exacerbate ECM damage by liberating specific ECM-degrading proteins, like macrophage elastase (MMP-12), neutrophil elastase and neutrophil collagenase (MMP-8). [19,29,33] In fact, is has been reported that both UV and IR/heat induce several MMPs, by activating signaling cascades or by promoting inflammatory cellular infiltration. [20,47,49]

As ROS induce MMP-1, -3, and -9, and decrease procollagen synthesis, collagen is the most affected ECM component during skin ageing. Furthermore, there is evidence that a matrix of degraded collagen fibers may negatively affect fibroblasts in terms of proliferative capacity and type I procollagen synthesis, which hinders collagen recovery and exacerbates the accumulation of damage. [50]

Vascular changes observed in photodamaged skin include teleangiectasias (dilated blood vessels), vascular hyperpermeability, and pronounced angiogenesis. Angiogenesis comprises an enhanced permeability of blood vessels and breakdown of ECM, leading to infiltration of cells from the blood stream (namely inflammatory cells, like neutrophils or macrophages) into tissues, which

causes further damage to the ECM. Angiogenesis is known to occur in inflammatory processes, following acute and chronic UV-B radiation exposure. This may be due to an up-regulation of the angiogenic promoter VEGF (vascular endothelial growth factor) whereas the angiogenic inhibitor TSP-1 (thrombospondin 1) appears down-regulated, in both keratinocytes and fibroblasts. [51] NIR exposure was also shown to induce angiogenesis, with up-regulation of VEGF and down-regulation of TSP-2. [52] This imbalance, observed after exposure to UV-B or NIR radiation, is probably caused by action of generated ROS in specific proteins related to the transcription of these factors.

As previously mentioned, there is a complexity to the alterations in elastic fiber network observed in aged skin. In intrinsically aged skin, there is a reduction in elastin amount and disintegration of elastic fibers in the papillary dermis, particularly in what concerns to oxytalan and elaunin fibers. [8] On the other hand, photoaged skin reveals an accelerated degradation of these fibers, along with an accumulation of thick and dense elastotic material disposed in a disorganized fashion along the reticular dermis. [20,32,35] This accumulation of elastotic material, often referred to as solar elastosis, may be correlated with the increased expression of tropoelastin in both keratinocytes and fibroblasts, after acute or chronical exposure to UV-B radiation, suggesting that in photodamaged skin, epidermis is an additional source of elastic material. [53] The same is observed in IR exposed skin, as heat increases the amount of tropoelastin mRNA in keratinocytes as well as in fibroblasts, through the action of generated ROS. As opposed to the observations on the levels of tropoelastin, heat, which is a direct effect of IR irradiation, decreased fibrillin-1 (important component of microfibrils) expression in the dermis. These consequences of IR-generated heat may contribute to the decline of oxytalan fibers in the papillary dermis [35], and to an excessive deposition of tropoelastin in the existing fibers, rendering them thicker, which contributes to the accumulation of elastotic material. The concomitant increase in production of tropoelastin and induction of elastase-degrading enzymes in photodamaged skin, including MMP-12, NE, and skin fibroblast elastase, leads to degradation of newly synthesized tropoelastin and pre-existing elastic fibers, causing deposition of dystrophic and abnormal elastin which is unable to assemble into functional elastic fibers. [32,33,35]

Regarding pigmentation disorders, it has been established that the effect of UV radiation on melanocytes is not related to an acceleration of the ageing process, but is rather associated with activation or proliferation of these cells. This explains the higher number of enzymatically active melanocytes encountered in sun-exposed skin areas when compared to sun-protected skin. Several types of pigmented lesions may occur in photoaged skin, which are related to localized increases in number of melanocytes, melanocytes size, or number of melanosomes. [54]

1.3. Phytochemicals

Phytochemicals are plant secondary metabolites, that is, non-nutrient compounds that are not directly necessary for plant growth and development. Their function is to provide protection against adverse environmental factors, and the ability of plants to synthesize these compounds

determined natural selection throughout the course of evolution. Therefore, production of phytochemicals results from an adaptive response of plants to encountered challenges, and the accumulation of such compounds is a sign that plants were submitted to stress conditions. These challenges include pathogens, herbivore predators or insects, as well as UV and visible radiation, extreme temperature conditions, water stress, and nutrient deficiency. This broad variety of stress factors led to a wide diversity of chemical structures among phytochemicals, in order to respond to the various functions required for plant survival. [55]

In this work, the focus was laid on a specific group of phytochemicals: phenolics or phenolic compounds. Phenolic compounds are characterized by the presence of at least one aromatic ring with one or more hydroxyl groups, and can be divided into several classes and subclasses, as described schematically in Figure 1.3.

Phenolic acids are simple phenolics (one phenolic ring) but often occur in the bound form forming complex structures, whereas flavonoids are most frequently found in a glycosylated form, although aglycones may also occur. Flavonoids present a characteristic structure composed of two aromatic rings connected by an oxygenated heterocycle ring. Subclasses of flavonoids are determined by structural derivatizations and oxidation state of the heterocycle ring (pyran). [56] Generic structures of the several classes of phenolic compounds are depicted in Figure 1.4. It is worthy of note that the represented structures correspond to the characteristic core of each type of phenolic, and are depleted of the aromatic-linked hydroxyl groups that are typical of phenolic compounds.

Tannins are a group of polymeric phenolics resulting from the coupling of monomers from other classes of phenolic compounds, particularly phenolic acids and flavonoids, and therefore comprise a large variety of compounds. [57]

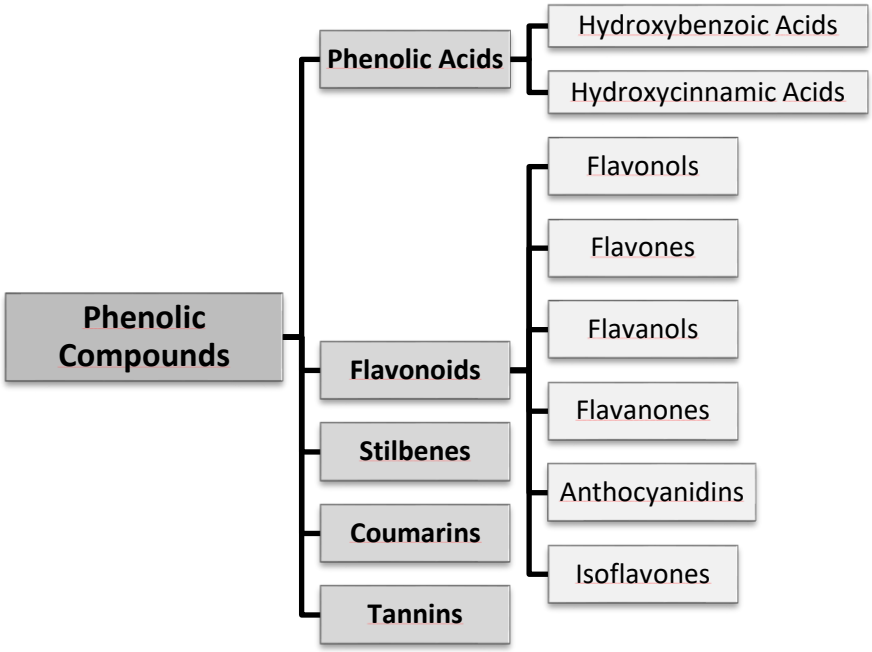

Figure 1.3. Hierarchical classification of phenolic compounds. Adapted from *Potential Sinergy of Phytochemicals in Cancer Prevention: Mechanism of Action* [56]

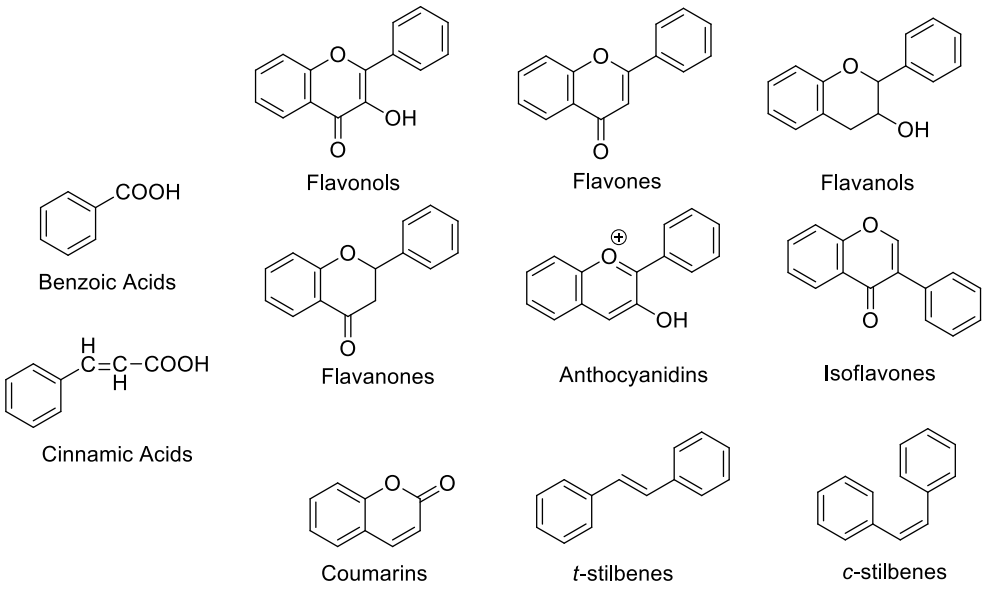

Figure 1.4. Generic core structure of different types of phenolic compounds.

1.3.1. Role of phenolics in skin

Although skin is equipped with endogenous antioxidant defenses, a decline in the functioning ability of these systems with ageing is evident. Along with this decrease in self-protection capacity, there is an increasing need for exogenous antioxidant provisions, through diet or cosmetic products, in order to compensate for the lack of antioxidant defenses and fight oxidative stress.

Phenolic compounds are well-known for improving the ageing skin phenotype, which is achieved not only through their antioxidant capacity, but also by their ability to exert other actions independent of any antioxidant activity. These include inhibition of the activity and expression of certain proteins, such as ECM-degrading enzymes or pro-inflammatory cytokines; interference with intracellular signaling cascades through interaction with membrane receptors or MAPK pathway; and protection of detoxifying enzymes (catalase, GPx, SOD).

Additionally, phenolics are known to have UV radiation absorbing capacity due to their structural features, thus having a potential for use as sunscreen agents, which can prevent UV-derived damage, including inflammation, oxidative stress and DNA damage. [58] Also because of structural characteristics, several phenolics not only combat ROS by neutralizing them, but also by indirectly inhibiting their production through chelation of transition metal ions (such as Fe^{2+}, which takes part in the $^{\bullet}OH$-generating Fenton chemistry), yielding further antioxidant effects. In fact, many phenolics possess more than one mechanism of action contributing to their overall antioxidant capacity. [59,60] Hence, antioxidant capacity of phenolics is driven by free radical scavenging, deactivation of singlet oxygen, and transition metal ion chelation. Free radicals can be neutralized by being provided with an electron or a hydrogen atom, or by forming an adduct with another molecule. In the case of singlet oxygen, quenching may occur by chemical mechanisms (reaction of $^1O_2$ with a molecule giving rise to an oxidized product) or physical processes (energy or charge transfer). [61] Antioxidant effects of phenolic compounds are closely related to their structural arrangement, and depend primarily on the stability of intermediate species formed as a consequence of ROS neutralization. The main structural features required for antioxidant capacity, and those responsible for stabilization of the intermediate forms of the antioxidant, are: planarity of the structure; ability to form intramolecular hydrogen bonds; presence of aromatic hydroxyl groups in favorable positions; and presence of “iron-binding motifs”. [59,62]

Some examples of the effects of phenolic antioxidants or phenolic-rich natural extracts in several biological endpoints related to skin ageing are discriminated in Table 1.1.. This overview of phenolic effects corroborates the importance of phenolics in prevention and treatment of skin ageing.

Table 1.1. Skin-related effects of several phenolic compounds and phenolic-rich natural extracts.

Compound/Source	Biological Effects	References
Resveratrol	Inhibition of oxidative-induced apoptosis in fibroblasts (3T3); anti-inflammatory activity through NF-κB inhibition; inhibition of AP-1 in several cell lines, including epithelial HeLa cells; inhibition and down-regulation of MMP-2 and MMP-9 in multiple myeloma cells (KM3); inhibition of tyrosinase activity	[63–66]
Quercetin	Inhibition and down-regulation of MMP-1, through inactivation of AP-1 and inhibition of MAPK pathways in human dermal fibroblasts (HDF); inhibition of neutrophil elastase activity; protection of endogenous enzymatic antioxidant defense (GPx, GR, SOD, catalase) upon exposure of rat skin to UV radiation	[67–69]
Kaempferol	Inhibition and down-regulation of MMP-1 induction, through inactivation of AP-1 and inhibition of MAPK pathways in human dermal fibroblasts (HDF)	[68]
Catechin	Suppression of oxidant-inducible VEGF expression in human keratinocytes (HaCaT)	[70]
Epigallocatechin-gallate (EGCG)	Inhibition of neutrophil elastase activity and UV-induced leukocyte infiltration in human skin; inhibition of MMP-2 and MMP-9; inhibition of heat-shock-induced MMP-1 expression, reduction of AP-1 DNA binding activity and inhibition of MAPK pathways in HDF	[69,71,72]
Epigallocatechin (EGC)	Inhibition of MMP-2 and MMP-9	[69]
Myricetin	Inhibition of neutrophil elastase, MMP-2 and MMP-9; inhibition and down-regulation of MMP-1 in HDF	[69,73]
Pelargonidin	Inhibition of neutrophil elastase; inhibition of MMP-2	[69]
Delphinidin	Inhibition of neutrophil elastase; inhibition of MMP-2 and MMP-9; protection of UV-irradiated HaCaT cells against apoptosis	[69,74]
Cyanidin-3-O-glucoside	Inhibition of MMP-2 and NFκB, and increased expression of TIMP-2, in human lung cancer cells (A549)	[75]
Rutin	Suppression of oxidant-inducible VEGF expression in HaCaT cells	[70]
Caffeic acid	Down-regulation and inhibition of the induction of MMP-1 activity, up-regulation of glutathione (GSH), glutathione peroxidase (GPx) and catalase in UV-irradiated HaCaT cells	[76]
Ferulic Acid	Suppression of VEGF expression in oxidant-induced HaCaT cells; down-regulation and inhibition of the induction of MMP-1 activity, up-regulation of GSH, GPx and catalase in UV-irradiated HaCaT cells	[70,76]

Table 1.1. (continued)

Compound/Source	Biological Effects	References
Ellagic Acid	Facilitation of normal secretion of tropoelastin and assembly into elastic fibers, by binding to elastin and protecting it from proteolytic degradation through direct inhibition of elastolytic enzymes including serine proteases and MMP-2 in dermal fibroblasts	[77]
Tannic Acid	Facilitation of normal secretion of tropoelastin and assembly into elastic fibers, by binding to elastin and protecting it from proteolytic degradation through direct inhibition of elastolytic enzymes including serine proteases and MMP-2 in dermal fibroblasts	[77]
Phenolics with a catechol group	Inhibition of neutrophil elastase	[78]
Extracts from edible berries	Suppression of oxidant-inducible VEGF expression in HaCaT cells; and NF-κB inhibition in hemangioendothelioma cells (EOMA)	[70,79]
Emblica officinalis extract	Stimulation of cell proliferation, induction of the expression of type-I procollagen, decreased production of MMP-1, and increased TIMP-1 expression in human skin fibroblasts	[80]
Grape pomace extract	Inhibition of *C. histolyticum collagenase* (ChC) and porcine pancreatic elastase (PPE)	[26]
White tea extract	Inhibition of ChC and PPE	[39]
Green tea extract	Inhibition of ChC and PPE	[39]
Pomegranate extract	Inhibition of ChC and PPE; inhibition of UV-induced expression of MMP-1, MMP-2, MMP-7 and MMP-9; inhibition of UV-induced decrease in TIMP-1; inhibition of MAPK pathways in HaCaT; induction of NHEK proliferation; stimulation of type-I procollagen synthesis and inhibition of MMP-1 production in dermal fibroblasts	[39,81,82]
Coffea Arabica extract	Increase of type-I procollagen expression, inhibition of MMP-1, MMP-3 and MMP-9 expression, and inhibition of MAPK pathways in human foreskin fibroblasts (Hs68)	[83]
Sorghum brans extract	Inhibition of hyaluronidase activity	[84]
Cocoa pod extract	Inhibition of neutrophil elastase, MMP-1 and tyrosinase (even higher inhibition than kojic acid)	[85]
Grape seed proanthocyanidins	Up-regulation of GPx; inhibition of oxidant-induced NF-κB and MAPK pathways activation in normal human epidermal keratinocytes (NHEK)	[86]

1.3.2. Grapes and red wine phenolics

Phenolic compounds are the most important phytochemicals found in grapes, and are distributed throughout the stem, leaves, seeds, flesh and skins, with a higher phenolic abundance in seeds and a bigger scarcity of these compounds in the flesh. [87]

Phenolics encountered in grapes greatly depend on the cultivar/variety, in terms of both qualitative and quantitative composition. Anthocyanins are more prevalent in red grape varieties, being responsible for grape skin pigmentation. [88]

Differences can be pointed out between grapes and wine in what concerns to qualitative and quantitative phenolic composition. Wine is richer in terms of phenolics when compared to regular grape juice due to the winemaking process, which allows an extraction of phenolics from grape skin and seeds that does not occur in the process of making juice. Moreover, fermentation and chemical reactions taking place during the winemaking process lead to generation of phenolic conjugates, such as tannins. [89] Thus, wine might be a more promising source of phenolic compounds than grapes and more effective at exerting certain biological effects.

1.4. Wine industry

Europe is responsible for the largest share of wine production globally, accounting for more than 60% of the world's entire production, according to the *Wine Annual Report and Statistics 2015* from the United States Department of Agriculture (USDA) [90], backed up by data from the *International Organisation of Vine and Wine* (Figure 1.5.).

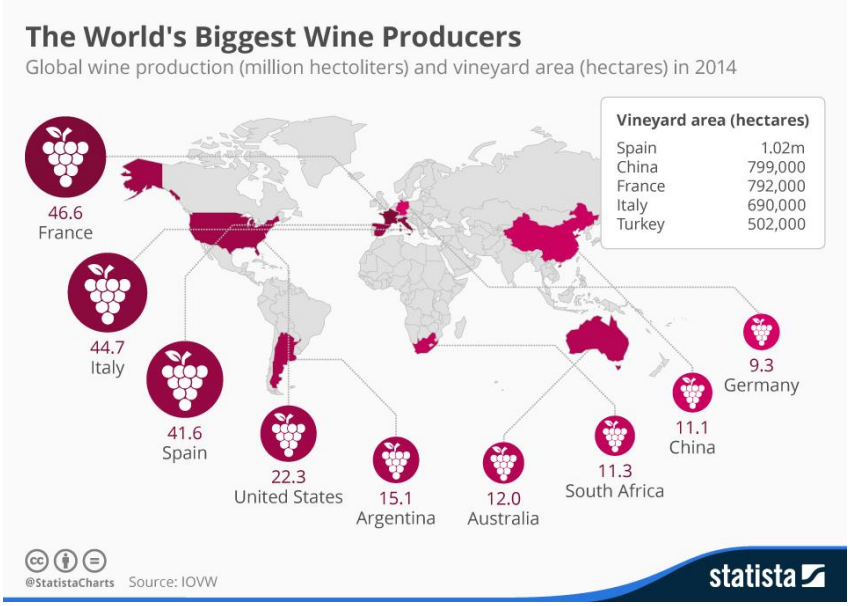

Figure 1.5. Worldwide production of wine: main countries contributing to winemaking industry. Figure taken from *The Statistics Portal (statista)* [91].

The winemaking process comprises several phases, yielding large amounts of organic waste. In short, after being destemmed, grapes are crushed resulting in a mixture of pulp, skins and seeds, called must. Yeast strains naturally present in the must are responsible for the alcoholic

fermentation (1st fermentation), in which sugar content of grapes is converted into ethanol with liberation of carbon dioxide and heat. For red wine production, the 1st fermentation is initiated without separation of the skins and seeds from the must, allowing extraction of aromas and coloring compounds, such as anthocyanins, from the skins. The skin-contact time will determine the color and composition of the resulting wine, therefore the moment of separation of the solid fraction of the must from its liquid fraction must be carefully chosen. The resulting pressed solid fraction consists of grape marc. When all the sugar is converted into ethanol, the 1st fermentation is finished, and the solid deposit left at the bottom of the fermentation vat consists of wine lees. Wine lees obtained from the 1st fermentation step are mainly composed of dead yeast and bacteria. The following step is the malolactic fermentation (2nd fermentation), in which malic acid is transformed into lactic acid by lactic bacteria (present in or added to the wine). From the 2nd fermentation step, wine lees are also obtained. To terminate any remaining microbiological processes, sulfites are added to the wine. The wine is then matured for variable periods of time prior to consumption. [92–94]

The main difference between the winemaking process of red table wine and Port wine is that, in Port wine, the alcoholic fermentation is interrupted by the addition of wine brandy, which explains the sweetness and high alcoholic content of Port wine. [95]

It is estimated that in Europe alone, about 14.5 million tons of solid waste, including stems, grape marc and wine lees, are generated annually in the winemaking process. [96] Since the wine industry is considered an important sector of the European economy, and considering the large amounts of waste resulting from the winemaking process, the recovery of bioactive compounds from these residues and further incorporation in nutraceutical, pharmaceutical or cosmetic products represents a promising market opportunity for wine producers, and might contribute to a sustainable development of the sector.

Furthermore, there is nowadays an increasing interest in cosmetics based on active principles obtained from natural sources, both from cosmetic companies, justified by the need for alternative ingredients due to legal restrictions and stringent regulations concerning the use of synthetic ingredients in cosmetic products, and from the consuming society due to a rise in consumer health consciousness.

1.5. Aim and Structure of the Thesis

In this thesis, selected samples obtained from winemaking waste streams through different extraction and formulation processes were screened for bioactivity in several biological endpoints, in order to explore their applicability in cosmetic products for anti-ageing and skin whitening purposes. The present thesis falls within the scope of the European project “Research on extraction and formulation intensification processes for natural actives of wine” (acronym “WineSense”), FP7-PEOPLE-2013-IAPP (612208). This project has the main goal of contributing to a sustainable development of wine industry through valorization of winemaking waste streams for alternative commercial applications, including cosmetics.

To achieve this goal, the work was divided in three parts:

- Part 1 – Phytochemical and antioxidant activity characterization of wine lees and grape marc extracts. In this part, red grape marc and wine lees extracts from the 1st fermentation step of red table wine and Port wine were evaluated in terms of phenolic and anthocyanin content, by colorimetric assays as well as HPLC-DAD-MS. Furthermore, antioxidant capacity of the extracts was determined by three complementary chemical assays (ORAC, HOSC and HORAC).
- Part 2 – Screening of the cosmetic potential of wine lees and grape marc extracts. Extracts were tested for inhibitory activity towards three of the main enzymes responsible for skin ageing signs, namely tyrosinase, elastase and MMP-1. Also, cell-based assays were performed in human keratinocytes and skin fibroblasts. Cytotoxicity was evaluated, and capacity of samples to inhibit ROS production in cells, as well as their ability to prevent oxidant-induced cytotoxicity, was assessed.
- Part 3 – Impact of formulation process on the stability and antioxidant activity of conventional grape marc extract. Formulations of conventional grape marc extract with different carrier materials (maltodextrin, whey protein isolate and pea protein isolate) were evaluated in terms of phytochemical composition by colorimetric assays, and antioxidant activity by chemical and cell-based assays.

2. Experimental Section

2.1. Chemicals

Reagents used for phytochemical characterization of the samples, namely total phenolic content and monomeric anthocyanin pigment content, were gallic acid ($C_7H_6O_5$) from Fluka (Switzerland), sodium carbonate (Na_2CO_3) and *Folin-Ciocalteu* reagent, both from Panreac (Barcelona, Spain), potassium chloride (KCl) from Sigma-Aldrich (St. Louis, Missouri, USA), and sodium acetate trihydrate ($C_2H_3NaO_2$•$3H_2O$), also from Sigma-Aldrich (Steinheim, Germany). For HPLC analyses, acetonitrile (CH_3CN) from Panreac (Barcelona, Spain) and formic acid (CH_2O_2) from VWR-CHEM (Radnor, Pennsylvania, USA) were used.

For antioxidant activity assays, fluorescein sodium salt ($C_{20}H_{10}Na_2O_5$), 2,2'-azobis(2-methylpropionamidine)dihydrochloride (AAPH), cobalt (II) fluoride tetrahydrate (CoF_2•$4H_2O$) were purchased from Sigma-Aldrich (St. Louis, Missouri, USA), (+/-)-6-hydroxy-2,5,7,8-tetramethylchroman-2-carboxylic acid (Trolox) was acquired from Fluka (Germany), 2-picolinic acid ($C_6H_5NO_2$) and caffeic acid ($C_9H_8O_4$) were from Sigma-Aldrich (China), hydrogen peroxide 30 wt. % in water (H_2O_2) and iron chloride ($FeCl_3$) were from Sigma-Aldrich (Steinheim, Germany), and acetone (C_3H_6O) from Sigma-Aldrich (Poland). For the preparation of phosphate-buffered saline (PBS) 75 mM pH 7.40, chemicals used were potassium phosphate monobasic anhydrous (KH_2PO_4) from Amresco (Solon, Ohio, USA), sodium phosphate dibasic dihydrate (Na_2HPO_4•$2H_2O$) from Sigma-Aldrich (Steinheim, Germany), potassium chloride (KCl) and sodium chloride (NaCl), both from Sigma-Aldrich (St. Louis, Missouri, USA). Sodium phosphate dibasic dihydrate (Na_2HPO_4•$2H_2O$) and sodium phosphate monobasic monohydrate (NaH_2PO_4•H_2O) from Sigma-Aldrich (Steinheim, Germany) were used to prepare sodium phosphate buffer solution (SPB) 75 mM pH 7.40.

Assessment of tyrosinase inhibition was performed using 3,4-Dihydroxy-L-phenylalanine (L-DOPA) (Sigma-Aldrich, China), mushroom tyrosinase (Sigma-Aldrich, St. Louis, Missouri, USA), and kojic acid as a positive control (Sigma-Aldrich, UK); elastase inhibition was assayed with porcine pancreatic elastase (PPE) type III and N-succinyl-Ala-Ala-Ala-*p*-nitroanilide (AAAPVN), both from Sigma-Aldrich (St. Louis, Missouri, USA), as well as recombinant (expressed in *E.* coli) Matrix metalloproteinase-1 (MMP-1) used for the MMP-1 inhibition assay; MMP fluorogenic substrate was obtained from Enzo Life Sciences (Farmingdale, New York, USA). Tyrosinase assay buffer (SPB 0.1 M, pH 6.8) was prepared with sodium phosphate dibasic dihydrate and sodium phosphate monobasic monohydrate; Tris base from Sigma-Aldrich (St. Louis, Missouri, USA) and hydrochloric acid (HCl) 37% (w/w) from Honeywell Riedel-de-Häen (Hanover, Germany) were used to prepare elastase assay buffer (Tris-HCl 0.1 M, pH 8); buffer used in MMP-1 assay (0.05 M Tris-HCl, pH 7.5) was prepared with Tris-HCl from Fluka (USA), calcium chloride dihydrate ($CaCl_2$•$2H_2O$) from Riedel-de Haën (Switzerland), sodium azide (NaN_3) from Sigma-Aldrich (Steinheim, Germany), Brij

35 from Fisher Scientific (Geel, Belgium), zinc sulfate heptahydrate ($ZnSO_4 \cdot 7H_2O$) from Merck (Darmstadt, Germany), and sodium chloride.

Extracts were dissolved in dimethyl sulfoxide (DMSO) from Carlo Erba Reagents (Val de Reuil, Paris, France), and formulations were dissolved in a mixture of ethanol, also from Carlo Erba Reagents, and water acidified with sulfuric acid (H_2SO_4) from Sigma-Aldrich (Steinheim, Germany).

High glucose Dulbecco's modified eagle medium (DMEM), used to culture HaCaT cell line, and Iscove's Modified Dulbecco's Medium (IMDM – GlutaMAX™), used in CCD-1112Sk cell line cultures, were both from Gibco (Thermo Fisher Scientific, USA). Cells were subcultured after treatment with 0.25% trypsin-EDTA, also from Gibco (Thermo Fisher Scientific, USA).

Sodium bicarbonate ($NaHCO_3$) from Sigma-Aldrich (Steinheim, Germany) was added to DMEM. Both DMEM and IMDM were supplemented with fetal bovine serum (FBS) from Biowest (Nuaillé, France), and Penicillin-Streptomycin from Gibco (Thermo Fisher Scientific, USA). CellTiter 96® AQ_{ueous} One Solution Cell Proliferation Assay (MTS/5-(3-carboxymethoxyphenyl)-2-(4,5-dimethylthiazoly)-3-(4-sulfophenyl)tetrazolium, inner salt), from Promega (Madison, Wisconsin, USA), was used to assess cell viability. For cellular antioxidant activity assays, 2',7'-dichlorofluorescin diacetate (DCFH-DA) from Sigma-Aldrich (Israel) was used as a fluorescent probe. Oenin chloride (≥95% purity) from Extrasynthese (Genay Cedex, France) and Quercetin (≥95% purity) from Sigma-Aldrich (India) were used as standards.

2.2. Samples

All samples, both extracts and formulations, were provided by the High Pressure Processes Group from the Department of Chemical Engineering and Environmental Technology, University of Valladolid, under the scope of the project "Research on extraction and formulation intensification processes for natural actives of wine" (acronym "WineSense"), FP7-PEOPLE-2013-IAPP (612208).

Samples were obtained from three different winemaking waste stream matrices, namely grape marc and wine lees from the 1st fermentation step of red table wine, both provided by Matarromera winery, and wine lees from the 1st fermentation step of Port wine, provided by Sogrape winery.

All samples, their respective origin, and extraction/formulation processes are briefly discriminated in Table 2.1.. A more detailed description is provided in sections 2.2.1. and 2.2.2.. From this point on, samples are referred to as discriminated in the following table, by their sample ID.

Table 2.1. Discrimination of the samples under study in this work.

	Sample ID	Raw Material	Extraction/Formulation Process
Wine Lees Extracts	**Mt**	Matarromera wine lees from 1st fermentation step – red table wine	Solid-liquid extraction (25ºC)
	MW Mt		Solid-liquid extraction (25ºC) after MW pretreatment
	Port	Sogrape wine lees from 1st fermentation step – Port wine	Solid-liquid extraction (25ºC)
	MW Port		Solid-liquid extraction (25ºC) after MW pretreatment
Grape Marc Extracts	**GM**	Grape marc	Solid-liquid extraction (60ºC)
	MW80 GM		Solid-liquid extraction (80ºC) after MW pretreatment
	MW100 GM		Solid-liquid extraction (100ºC) after MW pretreatment
Formulations (GM)	**GM:MD**	Grape Marc (GM) extract formulated with maltodextrin (MD)	Spray-drying (T_{inlet}=140ºC; T_{outlet}=81ºC) at an extract:carrier ratio of 1:1
	GM:WPI	Grape Marc (GM) extract formulated with whey protein isolate (WPI)	
	GM:PPI	Grape Marc (GM) extract formulated with pea protein isolate (PPI)	

2.2.1. Extraction Process

Different extraction processes were applied to the mentioned waste stream matrices, and the effect of microwave (MW) pretreatment on conventional solid-liquid (S-L) extraction was explored. Grape marc extracts and wine lees extracts from the 1st fermentation step of Port wine and of red table wine were obtained by conventional solid-liquid extraction preceded or not by MW treatment. MW pretreatments were carried out in a CEM Discover Microwave (CEM Corporation, North Carolina, USA) with a maximum power of 300W, using a 100 mL QianCap (Q Labtech, USA) safe glass pressure reactor. All the solid-liquid extractions were performed with an agitation of 300 rpm.

S-L extraction of grape marc was carried out with 50:50 (%V/V) EtOH:H_2O (water acidified to pH 1 with sulfuric acid), with an extraction temperature of 60ºC. For MW-pretreated grape marc, S-L extraction was performed at 80ºC or 100ºC, with the same extraction solvent. Extraction at

80ºC was preceded by a 60 second MW treatment, while extraction at 100ºC was preceded by MW treatment until the pressure mark reached 2 bar.

S-L extractions of wine lees matrices were performed at 25ºC with 50:50 (%V/V) EtOH:H_2O (water acidified to pH 2.6 with sulfuric acid). For MW-pretreated wine lees, S-L extraction was performed at 25ºC with 63:37 (%V/V) EtOH:H_2O. Pretreated matrices were subjected to MW for 90 seconds prior the extraction.

2.2.2. Formulation Process

Grape marc conventional extract was formulated as described in the literature. [97] The samples were spray dried with different carriers, namely maltodextrin DE18, whey protein isolate and pea protein isolate (Myprotein, Northwich, UK), in a GEA Mobile Minor ™ spray dryer model MM Basic (Düsseldorf, Germany) equipped with a rotary atomizer. The pressure was kept at 0.6 MPa, and the air flow rate was 40 kg/h. The feed mixture was pumped into the equipment using a peristaltic pump (Watson Marlow 520S), with a mass flow rate of 19.9 g/min. The inlet temperature was 140ºC while the outlet temperature was 81ºC. Carrier/extract ratio was of 1:1. Maltodextrin with a DE of 18%, whey protein isolate and pea protein isolate were used as carriers.

2.2.3. Sample Handling

For phytochemical characterization, namely determination of total phenolic content (TPC) and total anthocyanin content (TAC), extracts were tested in their original extraction solvent. As for all the remaining studies, samples were dryed in aliquotes in a CentriVap Concentrator (Labconco, Missouri, USA) and then stored at -20ºC. Later on, concentrated solutions were prepared in DMSO. This procedure can be justified by two factors: (1) the original extraction solvents affected the results of the biological assays and did not allow for bioactivity screening, given their toxicity towards the biological material in extract concentrations required for evident bioactivity; (2) the extracts were highly susceptible to degradation when stored in their extraction solvents (possibly because they were highly diluted and due to an anti-solvent effect of the extracted compounds).

In what concerns to the three formulations prepared from grape marc conventional extract, samples were handled differently from the extracts, and according to the literature. [97] In order to disassemble the particles obtained by spray drying, 20 mg of each sample were dissolved in a mixture of 50:50 (%V/V) EtOH:H_2O (water acidified to pH 1 with sulfuric acid), and then sonicated for approximately 20 minutes. This solution was then used for phytochemical characterization (TPC and TAC) and antioxidant activity determination (ORAC, HORAC and HOSC).

For cell-based assays, extracts were dissolved in DMSO and diluted in culture medium or PBS, depending on the assay. DMSO concentrated solutions of the extracts were not filtered, as DMSO inhibits microorganism growth even when used in small percentages. [98] Formulations were sterilized using a protocol already described by other authors with some modifications. [99] In

brief, formulations were put in contact with UV radiation for 1h at room temperature in a Biological Safety Cabinet (Nuaire, USA).

2.3. Phytochemical Characterization

2.3.1. Total Phenolic Content (TPC)

The Folin-Ciocalteu method is a colorimetric assay that allows for quantification of total phenolic content in samples of interest. It relies on the transfer of electrons from phenolic compounds to phosphomolybdic/phosphotungstic acid complexes in alkaline medium, resulting in the formation of blue complexes which can be determined spectroscopically at 765 nm. [100]

This assay was based on previous work [101] and adapted to a Spark 10M (Tecan Group Ltd., Männedorf, Zürich, Switzerland) spectrophotometer microplate reader. Briefly, 237 µL of distilled water, 3 µL of sample dilution, 15 µL of FC reagent and 45 µL of sodium carbonate (Na_2CO_3) saturated solution were added to each inner well of a 96-well transparent microplate, and distilled water was added to the outer wells to prevent evaporation from the inner wells. All plates were agitated before going on a 30 minute incubation at 37ºC. Subsequently, absorbance was measured at 765 nm in the spectrophotometer microplate reader. At least four dilutions were prepared for each sample and all samples were tested at least in three independent assays and in duplicates. All sample and standard dilutions were prepared in distilled water, which was also used as the blank.

Gallic acid was used as control standard and a calibration curve with seven points (0, 50, 100, 200, 400, 600, 800 mg/L), calculated from the blank-corrected A_{765} of gallic acid solutions, was used to calculate the phenolic content of the samples from their blank-corrected A_{765}. These calculations took under consideration the effect of the dilution factors on phenolic determination. [102] The results were expressed in micromoles of Gallic Acid Equivalents per gram of raw material or dry extract (or per gram of dry product in the case of formulations) (µmol GAE/g dry basis), and were calculated as follows:

$$TPC\ (\mu M\ GAE/g\ raw\ material) = \frac{St * \frac{1}{S} * \frac{V}{W}}{MW} * 10^3 \qquad (1)$$

$$TPC\ (\mu M\ GAE/g\ dry\ basis) = \frac{\frac{St * \frac{1}{S}}{db}}{MW} * 10^3 \qquad (2)$$

St – Phenolic content calculated from the standard regression equation, in mg/L

S – Phenolic content calculated from the sample regression equation, in mg/L

V – Volume of solvent used to make the extract, in L

W – Weight of the raw material used to make the extract, in g

db – Dry basis (extract or formulation product), in g/L

MW – Molecular weight (170.12 g/mol for gallic acid)

10^3 – Conversion factor to µM

2.3.2. Total Anthocyanin Content (TAC)

Total monomeric anthocyanin pigment content was assessed by a pH differential method approved by the Association of Official Agricultural Chemists (AOAC), according to the protocol described in the AOAC Official Method 2005.02. [103]

This method relies on the color dependency on the pH of the monomeric anthocyanin pigments. Briefly, three appropriate dilutions of each sample were prepared in two buffers with different pH values (0.025 M Potassium Chloride, KCl – pH 1; 0.4 M Sodium Acetate, $C_2H_3NaO_2$ – pH 4.5). Both buffers were prepared using previously boiled distilled water. Then, 200 µL of each dilution were added at least in duplicates to a 96-well transparent microplate and absorbance was measured at 520 nm, and 700 nm to correct for haze. Samples were tested in at least three independent assays.

Since malvidin-3-O-glucoside is a major compound in the extracts under study, results were expressed in micromoles of malvidin-3-O-glucoside equivalents per gram of raw material or dry extract (or per gram of dry product in the case of formulations) (µmol malv-3-O-gl/g dry basis), and were calculated as follows:

$$TAC\ (\mu M\ malv-3-O-\frac{gl}{g} raw\ material) = \frac{\frac{A*MW*DF*10^3}{\varepsilon*l}*\frac{V}{W}*1.81}{MW} * 10^3 \quad (3)$$

$$TAC\ (\mu M\ malv-3-O-\frac{gl}{g} dry\ basis) = \frac{\frac{\frac{A*MW*DF*10^3}{\varepsilon*l}}{db}1.81}{MW} * 10^3 \quad (4)$$

A – $(A_{520nm} - A_{700nm})_{pH\ 1.0} - (A_{520nm} - A_{700nm})_{pH\ 4.5}$

MW – Molecular Weight (493.43 g/mol for malvidin-3-glucoside)

DF – Dilution Factor

l – Optical pathlength, in cm

ε – Molar Extinction Coefficient (28000 $L.mol^{-1}.cm^{-1}$ for malvidin-3-glucoside) [104]

10^3 – Conversion factor to mg and to µM

V – Volume of solvent used to make the extract, in L

W – Weight of the raw material used to make the extract, in g

1.81 – Optical pathlength correction factor

db – Dry basis (extract or formulation product), in g/L

2.3.3. High Performance Liquid Chromatography

2.3.3.1. Separation of Anthocyanins

Anthocyanins present in the extracts were analyzed by HPLC-DAD using a LaChrom Elite (VWR, Hitachi) apparatus, equipped with a quaternary pump, an autosampler and a column oven, and coupled to a photodiode array detector (DAD) L-2455. Data were acquired and processed with Agilent EZChrom Elite software. Separation was performed using a reversed-phase LiChrospher® 100 RP-18 5µm LiChroCART® 250-4 (Merck Millipore, Massachusetts, USA) column, operated at 25ºC in a thermostated oven. The analysis method followed was adapted from a method already described in the literature. [105] The mobile phase consisted of ultrapure water:formic acid (90:10, V/V) (eluent A) and ultrapure water:acetonitrile:formic acid (60:30:10, V/V) (eluent B), and the gradient program used was from 80:20 A:B to 15:85 A:B in 69 min, from 15:85 A:B to 0:100 A:B in 1 min, from 0:100 A:B to 80:20 A:B in 10 min, and 80:20 A:B for 10 min, with a flowrate of 1 mL/min, and an injection volume of 20 µL. Total run time was 90 min. Absorption spectra were recorded from 200 to 600 nm, using a photodiode array detector, and anthocyanins were monitored at a wavelength of 520 nm.

Total anthocyanin content was obtained using a calibration curve with the main anthocyanin present in the samples, malvidin-3-O-glucoside, and results were expressed as micromoles of malvidin-3-O-glucoside equivalents per gram of dry extract. Results were compared with those obtained by the colorimetric assay (section 3.1.1.).

2.3.3.2. Separation and Identification of Phenolics

The following analyses were performed by the *Food Functionality and Bioactives Laboratory* from iBET/ITQB (Instituto de Biologia Experimental e Tecnológica/Instituto de Tecnologia Química e Biológica).

Samples were analyzed by HPLC-DAD-MS, using a Waters Alliance 2695 Separation Module (Waters, Ireland) system equipped with a quaternary pump, a degasser, an autosampler and a column oven. The liquid chromatography system was coupled to a photodiode array detector 996 PDA (Waters, Ireland), and to a mass spectrometer MicroMass Quattromicro® API (Waters, Ireland). All data were acquired and processed by MassLynx® 4.1 software.

Chromatographic separation of compounds was carried out in a reversed-phase LiChrospher® 100 RP-18 5µm LiChroCART® 250-4 column inside a thermostated oven at 35ºC. The mobile phase consisted of formic acid (0.5% V/V in ultrapure water) (eluent A) and acetonitrile (eluent B). The gradient program used was 99:1 A:B for 5 min, from 99:1 A:B to 40:60 A:B in 40 min, from 40:60 A:B to 10:90 A:B in 45 min, held isocratically (90% B) for 10 min, from 10:90 A:B to 99:1 A:B in 10 min, and finally held isocratically (99:1 A:B) for 10 min, at a flowrate of 0.3 mL/min, with an injection volume of 20 µL. Total run time was 120 min. Absorption spectra were acquired

from 210 to 600 nm by a photodiode array detector. Anthocyanins were monitored at 520 nm, flavonols at 360 nm, phenolic acids at 320 nm, and phenolic compounds in general at 280 nm.

Mass spectrometry was performed using an electrospray ion source in negative ion mode (ESI^-). The ion source temperature was 120ºC, the capillary voltage was 2.5 kV, and the source voltage was 30 V. Compounds separated by HPLC were ionized and the mass spectra were recorded in a full scan mode, with m/Z range between 100 and 1500. High purity nitrogen was used as drying and nebulizing gas, and ultrahigh purity argon was used as collision gas.

2.4. Antioxidant Activity

2.4.1. Oxygen Radical Absorbance Capacity (ORAC)

This method evaluates the capacity of the tested samples to prevent the oxidation of a fluorescent probe (fluorescein sodium salt - FL) by peroxyl radicals ($ROO^•$) generated during thermal decomposition of AAPH. The presence of antioxidant species capable of reducing the radicals translates into a delay in the loss of FL fluorescence.

This assay was carried out as previously described [106], taking into account subsequent modifications introduced for the FL800 microplate fluorescence reader (Bio-Tek Instruments, Winooski, VT, USA). [107] Briefly, in a 96-well black microplate, 25 µL of the sample dilution and 150 µL of FL (3×10^{-4} mM) were added to each of the 60 inner wells, and distilled water was added to the 36 outer wells to prevent evaporation from the inner wells. The microplate was then submitted to a 10 minute incubation period at 37ºC inside the fluorescent microplate reader. After this period, the reaction began with the addition of 25 µL of AAPH (153 mM) to each inner well through an injector. Fluorescence emitted by the reduced form of FL was recorded over time (every minute for a period of 40 minutes), under the control of Gen5 software. Fluorescence filters for an excitation wavelength of 485±20 nm and an emission wavelength of 528±20 nm were used.

At least four dilutions were prepared for each sample, and all samples were tested at least in three independent assays and in triplicates. The solvent in which the extracts were dissolved (DMSO) did not present any ORAC antioxidant activity in the concentrations tested. The solvent used for dissolution of the formulations (50% (V/V) EtOH:H_2O, water acidified to pH 1 with sulfuric acid), was tested in the same concentrations as the samples and its effect was subtracted from that of the formulations, because ethanol can present some antioxidant activity itself. [108]

AAPH, FL, Trolox, samples and standard solutions, were all prepared in a phosphate-buffered saline (PBS), 75 mM, pH 7.4, which was also used as the blank. Trolox solutions of 0, 5, 10, 20, 30, 40 µM were used as control standards and a regression equation, calculated from the blank-corrected net AUC (area under the FL decay curve) values, allowed determination of the samples' ORAC values. These calculations were made taking into account the effect of the dilution factor on antioxidant capacity. [102] Results were expressed as micromoles of trolox equivalents

per gram of extract (or per gram of dry product in the case of formulations) (µmol TE/g dry basis), or per micromole of GAE (µmol TE/µmol GAE), and calculated as follows:

$$ORAC\ (\mu M\ TE/g\ dry\ basis) = \frac{St * \frac{1}{S}}{db} \quad (5)$$

St – Trolox equivalents calculated from the standard regression equation, in µM

S – Trolox equivalents calculated from the sample regression equation, in µM

db – Dry basis (extract or formulation product), in g/L

$$ORAC\ (\mu M\ TE/\mu M\ GAE) = \frac{ORAC\ (\mu M\ TE/g\ dry\ basis)}{TPC\ (\mu M\ GAE/g\ dry\ basis)} \quad (6)$$

2.4.2. Hydroxyl Radical Scavenging Capacity (HOSC)

This method evaluates the capacity of the tested samples to scavenge hydroxyl radicals (•OH), by measuring their capacity to prevent fluorescein oxidation by hydroxyl radicals generated from a Fe(III)-driven Fenton-like reaction. The presence of antioxidant species capable of scavenging the radicals translates into a delay in the loss of FL fluorescence.

The assay was performed according to a validated method described in the literature [109], adapted for the FLx800 fluorescence microplate reader (BioTek Instruments, Winooski, VT, USA). Briefly, in a 96-well black microplate, 170 µL of FL solution (9.96×10^{-8} M), 30 µL of the appropriate sample dilution, 40 µL of H_2O_2 solution (0.20 M), and 60 µL of $FeCl_3$ solution (3.42 mM) were added to each of the 60 inner wells, and distilled water was added to the 36 outer wells to prevent evaporation from the inner wells. Fluorescence emitted by the reduced form of FL was recorded over time (every minute for a period of 60 minutes), at 37°C, under the control of Gen5 software. Fluorescence filters for an excitation wavelength of 485±20 nm and an emission wavelength of 528±20 nm were used.

At least four dilutions were prepared for each sample, and all samples were tested at least in three independent assays and in triplicates. The influence of the solvent in which the samples were dissolved (DMSO in the case of extracts and ethanol in the case of formulations) in the antioxidant activity was taken under consideration.

FL solution was prepared in a Sodium Phosphate Buffer (SPB), 75 mM, pH 7.4. $FeCl_3$ and H_2O_2 solutions were prepared in MilliQ water, while trolox and sample dilutions were made in Acetone:MilliQ water 50% (V/V). Trolox solutions of 0, 5, 10, 15, 20, 30 µM were used as control standards and a regression equation, calculated from the blank-corrected net AUC (area under the FL decay curve) values, allowed for determination of the samples' HOSC values, which were expressed as micromoles of trolox equivalents per gram of extract (or per gram of dry product in the case of formulations) (µmol TE/g dry basis), or per micromole of GAE (µmol TE/µmol GAE). Calculations were made according to equations (5) and (6), and took into account the dilution effect on antioxidant capacity. [102]

2.4.3. Hydroxyl Radical Averting Capacity (HORAC)

This assay aims to evaluate the capacity of a given sample to prevent generation of hydroxyl radicals (•OH) by a Co(II)-mediated Fenton-like reaction, using FL as the probe. In the presence of species capable of deactivating the metal thus preventing the generation of the radical, a delay in the decay of the FL fluorescence curve will be observed.

The procedure was performed based on the method described in the literature [110], with some modifications for the FLx800 fluorescence microplate reader (BioTek Instruments, Winooski, VT, USA). Briefly, in a 96-well black microplate, 170 µL of FL solution (9.96×10^{-8} M), 30 µL of the appropriate sample dilution, 40 µL of H_2O_2 solution (0.21 M), and 60 µL of CoF_2 solution (2.03 mM) were added to each of the 60 inner wells, and distilled water was added to the 36 outer wells to prevent evaporation from the inner wells. Fluorescence emitted by the reduced form of FL was recorded over time (every minute for a period of 60 minutes), at 37ºC, under the control of Gen5 software. Fluorescence filters for an excitation wavelength of 485±20 nm and an emission wavelength of 528±20 nm were used.

At least four dilutions were prepared for each sample, and all samples were tested at least in three independent assays and in triplicates. The influence of the solvent in which the samples were dissolved (DMSO in the case of extracts and ethanol in the case of formulations) in the antioxidant activity was taken under consideration.

FL solution was prepared in a Sodium Phosphate Buffer (SPB), 75 mM, pH 7.4. CoF_2 and H_2O_2 solutions were prepared in MilliQ water, while caffeic acid and sample dilutions were made in Acetone:MilliQ water 50% (V/V). Caffeic acid solutions of 0, 50, 100, 150, 200, 250 µM were used as control standards and a regression equation, calculated from the blank-corrected net AUC (area under the FL decay curve) values, allowed for determination of the samples' HORAC values, which were expressed as micromoles of caffeic acid equivalents per gram of extract (or per gram of dry product in the case of formulations) (µmol CAE/g dry basis), or per micromole of GAE (µmol TE/µmol GAE). Results were calculated according to equations (5) and (6), and, consistent with the ORAC and HOSC assays, the calculations took under consideration the dilution effect on antioxidant capacity. [102]

2.5. Enzymatic Assays

2.5.1. Inhibition of Tyrosinase

Tyrosinase inhibitory activity of samples was determined spectrophotometrically, using mushroom tyrosinase and L-DOPA as the substrate, as previously reported. [111] Tyrosinase converts L-DOPA to Dopaquinone, which in turn cyclizes to form Dopachrome. Dopachrome formation can be monitored by measuring the absorbance at 475 nm (ε_{475}=3700 $M^{-1}cm^{-1}$). [112]

Shortly, 80 µL of sodium phosphate buffer (SPB) (0.1 M; pH 6.8), 40 µL of sample dilution, 40 µL of tyrosinase working solution (30 U/mL) and 40 µL of L-DOPA (2.5 mM) were added to each

well of a 96-well transparent microplate. After an incubation period of 30 minutes at 37°C, absorbance was measured at 475 nm in a multimode microplate reader (Spark 10M, Tecan Group Ltd., Männedorf, Zürich, Switzerland). All samples were tested in triplicates and accompanied by a blank with all components except the substrate. Calculations were made in comparison to a control containing DMSO in place of the sample, and the percentage inhibition of the enzyme was calculated as follows:

$$\%\ inhibition = \frac{(Acontrol - Asample)}{Acontrol} * 100 \qquad (7)$$

Tyrosinase was dissolved in potassium phosphate buffer (50 mM; pH 6.5) at a concentration of 1000 U/mL and stored in aliquots at -20°C. Right before the assay, aliquots were diluted to a working solution in SPB (0.1 M; pH 6.8) and L-DOPA was dissolved in the same buffer. Samples were dissolved in DMSO and diluted in SPB (0.1 M; pH 6.8).

Results were obtained from at least three independent experiments. The inhibitory potential of the extracts was evaluated with increasing concentrations, in order to establish dose-dependent relationships and determine the IC_{50} value.

2.5.2. Inhibition of Elastase

Elastase inhibitory activity of samples was determined through a colorimetric assay, using porcine pancreatic elastase (PPE) and N-succinyl-Ala-Ala-Ala-p-nitroanilide (AAAPVN) as the substrate. Formation of *p*-nitroaniline through cleavage of the substrate can be monitored by measuring the absorbance at 410 nm ($\varepsilon_{410\ nm}$ = 8 800 $M^{-1}cm^{-1}$). [113]

Briefly, in a 96-well transparent microplate, 100 µL of Tris-HCl buffer (0.1 M; pH 8), 30 µL of sample dilution, and 10 µL of elastase working solution (0.5 U/mL) were added to each well. After equilibrating the temperature to 25°C for 20 minutes, 40 µL of AAAPVN (0.25 mg/mL) were added to the reaction mixture. Then, absorbance at 410 nm was recorded for 20 minutes in a multimode microplate reader (Spark 10M, Tecan Group Ltd., Männedorf, Zürich, Switzerland).

Elastase was dissolved in buffer at a concentration of 4 U/mL and stored in aliquots at -20°C. Right before the assay, aliquots were diluted to a working solution in Tris-HCl buffer (0.1 M; pH 8). AAAPVN was dissolved in DMSO at 25 mg/mL and then diluted in the same buffer. Samples were dissolved in DMSO and diluted in the buffer.

All samples were tested in triplicates and accompanied by a blank with all components except the substrate. Calculations were made in comparison to a control containing DMSO in place of the sample, and the percentage inhibition of the enzyme was calculated according to equation (7).

Results were obtained from at least two independent experiments. The inhibitory potential of the extracts was evaluated with increasing concentrations, in order to establish dose-dependent relationships and determine the IC_{50} value.

2.5.3. Inhibition of MMP-1

Matrix metalloproteinase-1 (MMP-1) inhibitory capacity of samples was assayed using human recombinant MMP-1, and a peptidic fluorogenic MMP substrate highly fluorescent once cleaved by the enzyme, with and excitation wavelength of 340 nm and an emission wavelength of 440 nm.

Briefly, in a 96-well black microplate, 88 µL of assay buffer, 5 µL of sample dilution, 2 µL of MMP-1 working solution (0.01 mg/mL) and 5 µL of fluorogenic substrate solution (0.02 mM) were added to each well. Reaction was allowed to occur for 20h at 37ºC, and then fluorescence was measured (Ex/Em=340 nm/440 nm) in a multimode microplate reader (Spark 10M, Tecan Group Ltd., Männedorf, Zürich, Switzerland).

MMP-1 was stored at -20ºC in aliquots diluted in water containing 0.1% BSA (bovine serum albumin) at a concentration of 0.5 mg/mL. Before the assay, aliquots were diluted in buffer to a concentration of 0.01 mg/mL. MMP fluorogenic substrate was dissolved in DMSO to a concentration of 16.7 mM and stored in aliquots at -20ºC. Before the assay, aliquots were diluted in buffer to a concentration of 0.02 mM.

Buffer used in the assays was Tris-HCl 50 mM, pH 7.5, with 10 mM $CaCl_2$, 150mM NaCl, 0.02% (w/V) NaN_3, 0.05% (w/V) Brij 35 and 0.05 mM $ZnSO_4$, as described in the literature. [114]

All samples were tested in triplicates and accompanied by a blank with all components except the enzyme. Calculations were made in comparison to a control containing DMSO in place of the sample, and the percentage inhibition of the enzyme was calculated according to equation (7).

Results were obtained from at least two independent experiments. The inhibitory potential of the extracts was evaluated with increasing concentrations, in order to establish dose-dependent relationships and determine the IC_{50} value.

2.6. Cell-based Assays

2.6.1. Cell culture

Human immortalized non-tumorigenic keratinocyte cell line HaCaT (Ethnicity: Caucasian; Age: 62 years; Gender: male; Tissue: skin) was supplied by CLS (Cell Lines Service, Germany). HaCaT cells were cultured using high glucose, high pyruvate, Dulbecco's modified eagle medium (DMEM), supplemented with 10% heat-inactivated fetal bovine serum (FBS), 100 units/mL penicillin and 100 µg/mL streptomycin (1% P-S V/V).

Human foreskin fibroblasts (HFF) cell line CCD-1112Sk (ATCC® CRL-2429) (Ethnicity: Caucasian; Age: newborn; Gender: male; Tissue: foreskin) was obtained from the American Type Cell Culture collection (ATCC, USA). HFF were cultured with Glutamax™ Iscove's Modified Dulbecco's Medium (IMDM), supplemented with 10% (V/V) heat-inactivated fetal bovine serum (FBS), 100 units/mL penicillin and 100 µg/mL streptomycin (1% P-S V/V).

Both cell lines were maintained in a humidified atmosphere at 37 ^{o}C with 5% CO_2 during growth, and cells were subcultured following trypsinization when approximately 80-90% confluence was reached. HaCaT cells were passaged at a density of $2x10^4$ cells per cm^2, while HFF cells were passaged at a density of $1x10^4$ cells per cm^2.

Keratinocytes were used between passages 47 and 52, and fibroblasts were used between passages 8 and 13.

Cells were maintained in their respective culture medium supplemented with 10% FBS and 1% P-S, but all experiments were performed in culture medium supplemented only with 0.5% FBS and no antibiotic. For every assay, cells were seeded in 96-well TC (tissue culture)-treated microplates at a density of $1.4x10^5$ cells per cm^2 (HaCaT) or $3.1x10^4$ cells per cm^2 (HFF) and allowed to reach confluence (three days for HaCaT and one day for HFF).

2.6.2. Cytotoxicity Evaluation

After reaching confluence, growth medium was removed and cells were exposed to several concentrations of samples (100 µL) dissolved in culture medium (supplemented with 0.5 % V/V FBS and no antibiotic) and incubated at 37^{o}C and 5 % CO_2 for 24 or 48 hours. After these incubation periods, well content was removed and cells were washed with PBS at least twice. Then, 100 µL of MTS solution (1.6% V/V in medium supplemented with 0.5% FBS) were added to each well, and the cells were incubated at 37^{o}C, 5% CO_2 for 3 hours. Absorbance was then measured at 490 nm in a multimode microplate reader (Spark 10M, Tecan Group Ltd., Männedorf, Zürich, Switzerland), and cell viability was determined as a percentage of control, after blank subtraction. The MTS assay is based on the reduction of a tetrazolium salt by viable cells to generate a colored, aqueous soluble formazan product, of which the absorbance can be measured at 490 nm. The amount of formazan produced is directly proportional to the number of viable cells. [13,14]

Two standards, malvidin-3-O-glucoside and quercetin, were also tested. Concentrated stock solutions of quercetin and malvidin-3-O-glucoside were prepared in DMSO and EtOH:H_2O (2:1), respectively.

Concentrations of solvent used in the tested concentration range of the extracts and standards did not affect cell viability.

2.6.3. Inhibition of ROS Generation at Cellular Level

The capacity of the extracts to inhibit ROS production in cells was evaluated using two different approaches: pre-incubation and co-incubation. In both cases, 2',7'-dichlorofluorescin diacetate (DCFH-DA) was used as a fluorescent probe. Non-fluorescent DCFH-DA readily diffuses through the cell membrane and once in the intracellular medium, the diacetate moiety is cleaved by cellular esterases giving rise to the more polar 2',7'-dichlorodidhydrofluorescein ($DCFH_2$) which remains trapped within the cell. ROS from intrinsic oxidative stress or generated by an oxidative stress inducer easily diffuse into the cell, where they oxidize $DCFH_2$ to its fluorescent form, DCF.

Accumulation of DCF in cells may be measured by an increase in fluorescence at 538 nm (with excitation at 485 nm), which is assumed to be proportional to the amount of ROS. [22,117]

In the pre-incubation approach, cells were treated with selected non-toxic concentrations of the samples diluted in culture medium (0.5% FBS) for different periods, washed twice with PBS, and then incubated with 25 µM DCFH-DA in PBS for 1 hour. Fluorescence was measured at this point in order to assess the antioxidant effect of the samples towards intrinsic ROS. DCFH-DA was then removed and a concentration of H_2O_2 insufficient to be considered cytotoxic (0.04 mM for keratinocytes and 0.6 mM for fibroblasts) was added to the cells in PBS. After 1 hour, fluorescence was measured.

In the co-incubation approach, cells were incubated with 25 µM DCFH-DA for 1 hour in PBS, and then the chosen concentrations of stress inducer and extract were added to the cells at the same time, in PBS. After 1 hour, fluorescence was measured. Any remaining colour of the reaction mixture caused no interference in the fluorescence readings, as was seen by the measurement of fluorescence at time point zero.

Formulations were only tested in the pre-incubation approach, with slight modifications. In particular, cells were incubated with formulations and the respective non-formulated extract for 1, 4 and 24h at a fixed concentration of phenolics. After 1 and 4h incubations, cells were washed twice and fresh medium (without any sample) was added until the 24h mark was reached. From this point on, the procedure was the same as with the extracts.

All results were presented as a fluorescence percentage relative to the untreated control, where the same amount of stress was induced.

Fluorescence measurements were performed in a FL800 microplate fluorescence reader (Bio-Tek Instruments, Winooski, VT, USA), and fluorescence filters for an excitation wavelength of 485±20 nm and an emission wavelength of 528±20 nm were used.

2.6.4. Protection against H_2O_2-induced cytotoxicity

To assess the potential of the samples to prevent cytotoxicity induced by H_2O_2, cells were incubated with selected non-toxic concentrations of samples for 24 hours. After this period, cells were washed twice with PBS and incubated for 1 hour with H_2O_2 in culture medium (0.5% FBS) at a concentration capable of inducing at least 50% of cell death, and then cell viability was measured using the already described MTS method.

1 mM was the concentration of H_2O_2 chosen for the keratinocytes cell line, leading to a decrease in cell viability of approximately 50%, while 1.25 mM was the concentration of H_2O_2 chosen for the fibroblasts cell line and led to a drop of 60–70% in cell viability. These concentrations were chosen after a cytotoxicity screening of H_2O_2 towards both cell lines.

2.7. Statistical Analysis

All results are expressed as mean ± standard deviation (SD). Statistical analysis of the results was performed using GraphPad Prism 6 software (GrapghPad Software, Inc., La Jolla, CA). When homogeneous variance was confirmed, results were analysed by one-way analysis of variance (ANOVA), followed by the Tukey test for multiple comparisons. In the case of heterogeneous variances, an appropriate student t-test was performed in order to determine whether means were significantly different. A $p\text{-value}<0.05$ was accepted as statistically significant in all cases.

3. Results and Discussion

3.1. Phytochemical and Antioxidant Activity Characterization of Wine Lees and Grape Marc Extracts

3.1.1. Phytochemical Composition of the Extracts

Phenolic compounds are the main phytochemicals encountered in grapes and wine, hence total phenolic content (TPC) of the extracts was evaluated by the commonly used *Folin-Ciocalteu* method. Since the extracts studied in this work were obtained from red grape marc and red wine lees, and given anthocyanins are known to be the main compounds responsible for pigmentation of red grape skin and red wine, total anthocyanin content (TAC) was also evaluated. Gallic acid is a representative phenolic found in grapes and wine, hence TPC results were expressed in gallic acid equivalents. On the other hand, malvidin-3-O-glucoside had already been identified as the main anthocyanin present in the studied samples.

The first approach was to assess the efficiency of the different extraction processes applied to winemaking waste stream matrices, expressed as TPC and TAC per gram of raw material. Currently, MW radiation is widely used to assist extraction of several compounds from plants, because it generally increases extraction yields when compared to conventional extraction. This is because water molecules present in the matrix absorb MW energy and lead to a rapid increase in temperature, which in turn causes disruption of plant cell membrane-limited compartments enhancing the availability of compounds to be extracted. [118]

In both wine lees extracts, higher values of TPC and TAC are observed in the case of MW-pretreated matrices (Figure 3.1.), suggesting that MW treatment prior to extraction positively influences extraction efficiency. This finding is in agreement with the abovementioned principle of MW-assisted extraction, and similar results have been reported in the literature. For instance, MW increased the extraction yield of several phenolic compounds from cherries [119] and enhanced TPC of peanut skin extracts. [120] However, grape marc conventional extract (GM) presents higher TPC yield (64.8 µmol GAE/g raw material) when compared to grape marc extracts obtained from MW-pretreated matrices (34.6 µmol GAE/g raw material for MW80 GM and 34.4 µmol GAE/g raw material for MW100 GM). This might be explained by a possible temperature-driven degradation of certain phenolics present in this raw material, as already stated in the literature. [119,121] On the other hand, TAC value in MW80 GM (0.38 µmol malv-3-O-gl/g raw material) is significantly higher than that in GM (0.26 µmol malv-3-O-gl/g raw material). This tendency might mean that MW-pretreatment actually enhances anthocyanin extraction, given that anthocyanidins are generally found in the glycosylated form inside plant cell vacuoles [55], which suffer rupture upon MW treatment. A similar effect was observed in the extraction of anthocyanins from purple corn cob, in which MW-assisted extraction increased TAC relative to conventional methods. [122] In what concerns MW100 GM extract, the same is not observed. In fact, MW100 GM extract presents the

same amount of total anthocyanins as GM (0.27 *vs*. 0.26 µmol malv-3-O-gl/g raw material), and less than MW80 GM, which might be due to degradation caused by the higher extraction temperature used for preparation of MW100 GM (100ºC) when compared to the other two extracts.

Nevertheless, all three grape marc extracts reveal much lower extraction efficiency when it comes to TPC and TAC than any of the wine lees extracts. A possible explanation for this is the fact that grape marc has a larger granulometry than wine lees, *i.e.*, grape marc particles are larger than wine lees particles, which results in a smaller contact surface area of the former with the extraction solvent, leading to a less efficient extraction.

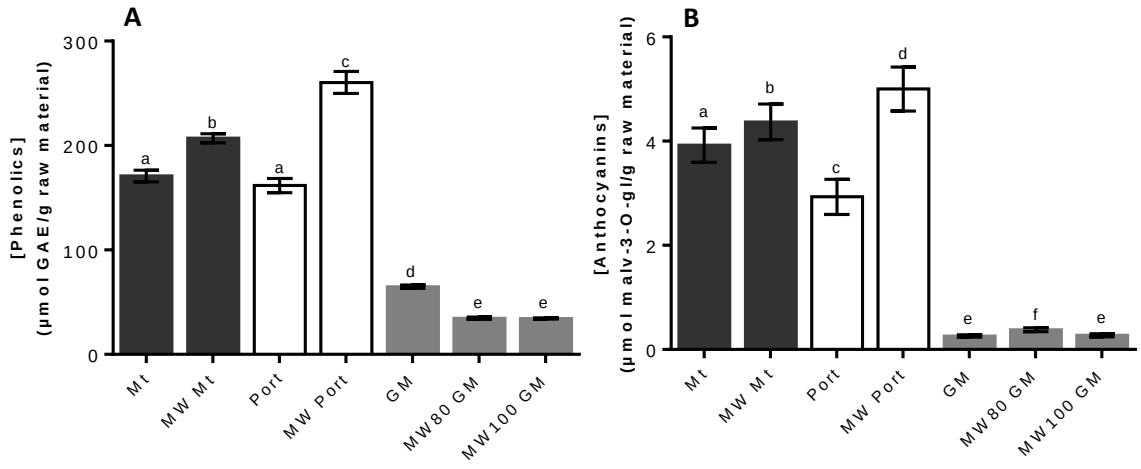

Figure 3.1. Extraction efficiency in terms of (A) TPC and (B) TAC, obtained by colorimetric assays. Results identified with different letters are significantly different (p-value<0.05), whereas coincident letters indicate that results are statistically equal. Results were obtained from at least three independent experiments.

Similar to what is observed for TPC and TAC of the extracts as a function of raw material, MW-pretreated wine lees extracts tend to present higher TPC and TAC values per gram of dry extract, whereas the same is not observed in grape marc extracts. The most relevant conclusion that can be drawn from Table 3.1. is the fact that red table wine lees extracts, both with and without MW pretreatment (MW Mt and Mt, respectively), are the richest of the studied extracts in terms of TPC and TAC. In particular, TPC values of red table wine lees extracts are at least two-fold higher than those of Port wine lees extracts, and three-fold higher than those of grape marc extracts, whereas TAC values of red table wine lees extracts are at least two-fold higher than those of Port wine lees extracts and ten-fold higher than those of grape marc extracts. Although TPC values are comparable among Port wine lees extracts and grape marc extracts due to the same orders of magnitude, TAC results show a clear disparity between extracts obtained from these two matrices. Port wine lees extracts possess higher content of anthocyanins (12.32 and 23.41 µmol malv-3-O-gl/g extract, for Port and MW Port) when compared to grape marc extracts (ranging from 3.54 to 5.41 µmol malv-3-O-gl/g extract). The discrepancies in TPC and TAC observed between Port wine lees and grape marc extracts can result from two possible events: higher amounts of “impurities”

(non-phenolic compounds, such as sugars) interfering in TPC determination of grape marc extract and leading to an overestimation of TPC [88]; and higher availability of anthocyanins in wine lees extracts due to the winemaking process. [89]

Table 3.1. Phytochemical composition of the extracts in terms of Total Phenolic Content (TPC) and Total Anthocyanin Content (TAC), obtained by colorimetric assays. Results identified with different letters are significantly different (p-value<0.05), whereas coincident letters indicate that results are statistically equal (lowercase letters for TPC; uppercase letters for TAC). Results were obtained from at least three independent experiments.

	Extract	TPC (µmol GAE/g extract)	TAC (µmol malv-3-O-gl/g extract)
Wine Lees	Mt	1395 ± 46 (a)	57.9 ± 4.9 (A)
	MW Mt	1564 ± 33 (b)	59.8 ± 4.7 (A)
	Port	376 ± 16 (c)	12.3 ± 1.4 (B)
	MW Port	673 ± 27 (d)	23.4 ± 2.0 (C)
Grape Marc	GM	493 ± 12 (e)	3.54 ± 0.28 (D)
	MW80 GM	269.5 ± 8.7 (f)	5.41 ± 0.52 (E)
	MW100 GM	266.1 ± 5.6 (f)	3.75 ± 0.39 (D)

TPC values found in the literature for grape marc are widely variable, ranging from 174 to 12473 µmol GAE/g sample; TAC values were also variable, ranging from 4 to 23 µmol malv-3-O-gl/g sample. [123–126] In the case of wine lees, results found in the literature were very scarce and yet highly variable. TPC ranged from 288 to 3127 µmol GAE/g sample, whereas TAC values, found in one research paper, were 11.2 and 13.6 µmol malv-3-O-gl/g sample, depending on the extraction method. [127,128] Nevertheless, anthocyanin content found in wines and lees differed depending on yeast strain. [129] TPC and TAC results obtained for the samples under study in this thesis were also variable depending on the raw material and extraction procedure. Comparison with the literature is not easy, because TPC and TAC determinations greatly depend on grape variety, maturation stage, environmental conditions during grape growth, vinification parameters, extraction procedure and extraction solvent.

Results described so far were obtained by colorimetric assays, based on light absorption by reaction mixtures. These methods are fast, easy to use, and less expensive; however, there are some downsides to them, such as low selectivity, low sensitivity, and considerable susceptibility to interferences from contaminants. Therefore, HPLC analyses of the samples were performed.

Primarily, a specific HPLC method for anthocyanin separation (method 1), coupled to a diode array detector (DAD), was used to assess TAC of the samples as malvidin-3-O-glucoside equivalents, using a calibration curve of this standard. TAC results obtained by HPLC-DAD (Table

3.2.) were consistent with those obtained by the colorimetric assay (Table 3.1.), and a correlation factor (R^2) of 0.9915 was calculated from comparison of the two methods. Although relative amounts of anthocyanins correlated well, HPLC results showed slightly higher TAC values for all the samples when compared to the colorimetric assay, which could be justified by the higher sensitivity of the HPLC method. [130] However, these discrepancies do not seem relevant as the results obtained by the two methods belong to the same order of magnitude.

In addition, HPLC method 1 allowed for quantification of malvidin-3-O-glucoside from the respective regression equation calculated for five concentration plots. As can be seen in Table 3.2., malvidin-3-O-glucoside contributes significantly to the total amount of anthocyanins in all samples.

Table 3.2. TAC values and quantification of malvidin-3-O-glucoside obtained by HPLC method 1.

	TAC (µmol malv-3-O-gl/g extract)	[Malv-3-O-gl] (µmol/g extract)	% Malv-3-O-gl relative to TAC
Mt	70.10	25.71	37
MW Mt	68.14	24.77	36
Port	13.45	5.40	40
MW Port	33.62	14.29	43
GM	3.55	1.63	46
MW80 GM	7.89	3.30	42
MW100 GM	5.22	2.29	44

A different HPLC method was used to separate phenolics in general (method 2), and in this case HPLC was coupled to a diode array detector (DAD) and a mass spectrometer (MS). From this method, several conclusions could be drawn in what concerns to total phenolic, phenolic acid, flavonol and anthocyanin contents, by monitoring the chromatograms at 280, 320, 360 and 520 nm, respectively. Results obtained for TPC by this method were consistent with those obtained by *Folin-Ciocalteu*, in terms of relative quantification: MW Mt>Mt>MW Port>GM>Port>MW80 GM≈MW100 GM. In all cases, extracts obtained from the same matrix by different extraction procedures had the same qualitative composition, differing only in quantitative composition, which suggests that MW pretreatment led to a higher extraction yield of the same phenolic compounds. An example of this observation is presented in Figure 3.2. for Mt and MW Mt. Different waste stream matrices possess differences in qualitative composition in what concerns anthocyanins, flavonols, phenolic acids, and phenolics in general. Chromatographic profiles of one extract sample from each raw material, at 520, 360, 320 and 280 nm can be seen in appendix A.

In Port wine lees extracts (Port and MW Port), anthocyanins were apparently more prevalent than flavonols; in red table wine lees extracts (Mt and MW Mt) the amount of flavonols seemed higher than that of anthocyanins, and the same was observed for grape marc conventional extract (GM). In MW80 GM and MW100 GM, the amount of anthocyanins appears to be higher than that of flavonols. In addition, an estimate of the relative amount of flavonols between extracts was

obtained by calculating the total peak area of the chromatograms at 360 nm. It was found that the order of flavonol content is: Mt>MW Mt>MW Port>Port>MW80 GM>MW100 GM>GM.

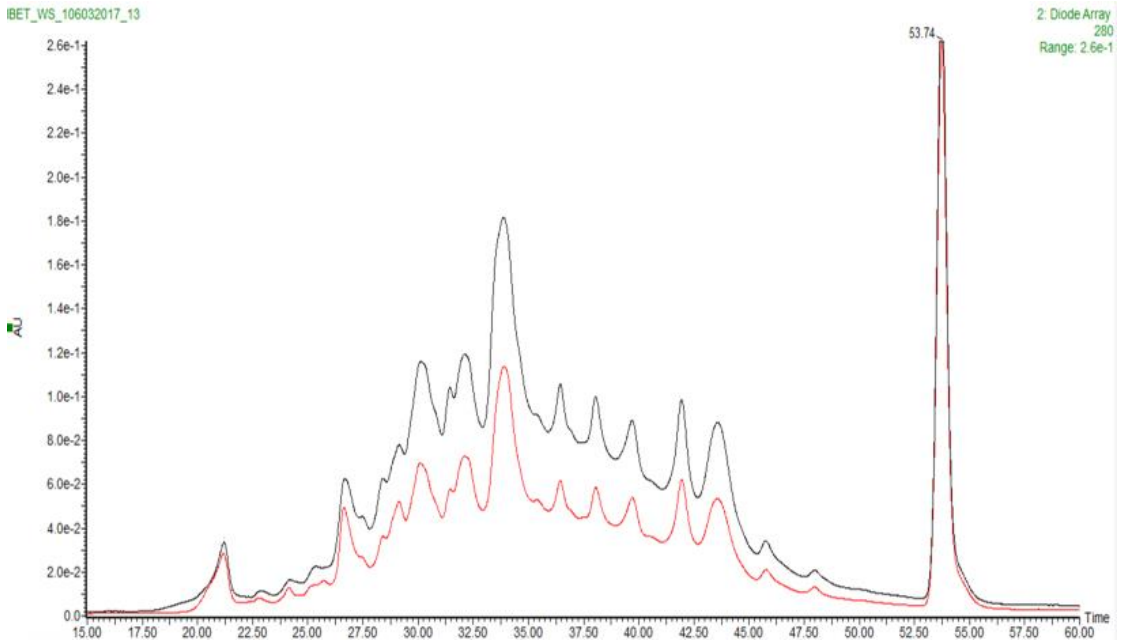

Figure 3.2. Chromatograms at 280 nm of Mt (red) and MW Mt (black), as obtained by the HPLC method 2.

Putative identification of some compounds was performed by HPLC-MS (Table 3.3.), taking under consideration the relative absorption of the compounds present in the peaks at four wavelengths (280, 320, 360 and 520 nm), the respective m/Z peaks found in mass spectra, comparison of chromatographic profiles with those of standard compounds, databanks [131,132], and studies already reported in the literature for comparable matrices. [88,133–142] Some of the identifications remain to be confirmed by tandem MS or comparison with standard compounds. Since the chromatographic profiles of extracts obtained from the same waste stream matrices are qualitatively identical, identifications presented in Table 3.3. are organized by raw materials.

Table 3.3. Putative identification of phenolic compounds present in the three raw materials, as obtained by HPLC-DAD-MS. m/Z values between parenthesis correspond to fragments of the molecular ion found in mass spectra; values separated by "/" indicate different compounds that co-eluted in the chromatographic separation. Retention times are rounded to the whole number. Identified peaks are numbered and the correspondent chromatograms are presented in Appendix A.

	Peak	Putative compound	Phenolic subclass	Mass (g/mol)	Retention time (min)	$[M-H]^-$	Red table wine lees	Port wine lees	Grape marc
520 nm	1	Delphinidin-3-O-glucoside	Anthocyanin	465.39	30	463	✓	✗	✓
	6	Vitisin A (10-carboxypyranomalvidin-3-O-glucoside)	Pyranoanthocyanin	561.46	32	559	✗	✓	✗
	2	Malvidin-3-O-glucoside	Anthocyanin	493.43	34	491 (329)	✓	✓	✓
	3	Delphinidin derivative	Anthocyanin	611	40	609 (301)	✓	✗	✗
	4	Petunidin 3-O-(6''-p-coumaroyl-glucoside)	Anthocyanin	625.55	42	623	✓	✗	✗
	5	Malvidin 3-O-(6''-p-coumaroyl-glucoside)	Anthocyanin	639.59	44	637	✓	✓	✓
360 nm	7	Myricetin-3-O-glucoside	Flavonol	480.38	32	479 (317)	✓	✗	✓
	8	Quercetin-3-O-glucuronide/Quercetin-3-O-glucoside	Flavonol	478.37/464.37	34	477/463 (301)	✓	✗	✓
	9	Syringetin-3-O-glucoside	Flavonol	508.43	36	507 (345)	✓	✓	✓
	10	Myricetin	Flavonol	318.24	38	317	✓	✓	✓
	11	Quercetin	Flavonol	302.24	42	301	✓	✓	✓
	12	Kaempferol	Flavonol	286.23	46	285	✓	✗	✓

Table 3.3. (continued)

360 nm	13	Rhamnetin	Flavonol	316.26	46	315	✗	✓	✗
320 nm	16	2-S-glutathionyl-caftaric acid	Hydroxycinnamic acid	617.54	26	616 (311)	✗	✗	✓
	14	Caftaric acid	Hydroxycinnamic acid	312.23	27	311 (179,149)	✓	✓	✓
	15	Procyanidin trimer/dimer/catechin/epicatechin; Coutaric acid	Flavanols; Hydroxycinnamic acid	866.77/578.52/ 290.26; 296.23	29	865/577/289; 295 (163,149)	✓	Catechin; Coutaric acid	✓
280 nm	17	Gallic acid	Hydroxybenzoic acid	170.12	21	169	✓	✓	✓

3.1.2. Antioxidant Activity of the Extracts

Phenolics are well known for their antioxidant activity, which is an important feature that determines the relevance of these compounds for cosmetic applications, given that ROS are the driving cause of skin ageing. Therefore, the extracts under study were submitted to three complementary antioxidant assays, aiming at assessing antioxidant capacities of the samples towards different biologically relevant radical species. As described in section 2.4., the ORAC assay measures the capacity of samples to scavenge peroxyl radicals (ROO•), HOSC measures the ability to scavenge hydroxyl radicals (•OH), and HORAC evaluates the capacity of samples to prevent hydroxyl radical formation, through metal chelating abilities. Trolox was chosen as a standard in ORAC and HOSC assays, given its ability to scavenge free radicals, such as ROO• and •OH, whereas caffeic acid was the standard used in HORAC assays, due to its metal-chelating ability.

As expected, results obtained for each antioxidant assay were quite different from one another. Nevertheless, ORAC, HOSC and HORAC values correlated well with TPC values in all cases, with R^2 values of 0.9644, 0.9769 and 0.9728, respectively. This makes sense because the higher the TPC, the more promising are the extracts in terms of antioxidant activity. In all three assays, antioxidant activity correlated slightly better with TPC than with TAC, which suggests that apart from anthocyanins, other phenolic compounds are contributing to the overall antioxidant activity of the extracts. Furthermore, antioxidant activity results show that in all extracts there are phenolics exerting the three types of antioxidant activity: peroxyl and hydroxyl radicals scavenging, and transition metal ion chelation. In fact, it has been reported that certain phenolics, such as the flavonol quercetin, have the ability to scavenge free radicals and to chelate transition metal ions, exerting their effects by these two different mechanisms of action. [59]

Taking a close look at antioxidant activity results as expressed per gram of extract (Table 3.4.), it can be stated that red table wine lees extracts (Mt and MW Mt) presented significantly better results than all the other extracts in all the three assays, with antioxidant capacity >3000 µmol TE/g extract in ORAC and HOSC, and HORAC values >1900 µmol CAE/g extract. In the case of Port wine lees extracts, MW Port had significantly higher potential for hydroxyl radical scavenging, presenting an HOSC value of 1285 µmol TE/g extract as opposed to Port, with an HOSC value of 837 µmol TE/g extract. The same tendency was observed in the HORAC assay, in which MW Port revealed a better capacity for metal chelation than Port (HORAC values of 776 and 458 µmol CAE/g extract for MW Port and Port, respectively). In what concerns to peroxyl radical scavenging capacity (ORAC), MW Port was also more effective than Port, with ORAC values of 716 and 451 µmol TE/g extract, respectively. Among grape marc extracts, MW80 GM and MW100 GM showed lower antioxidant capacity than GM in all the three assays, MW80 GM showing significantly higher antioxidant capacities than MW100 GM in ORAC and HORAC assays. Once again, consistent to what has been observed for TPC and TAC, antioxidant values (ORAC) found in the literature for grape pomace and wine lees were variable for the same reasons. ORAC values for grape marc samples ranged from 245 to 2337 µmol TE/g sample [143,144], while ORAC values for wine lees,

found in one research paper, were 6250 and 6100 µmol TE/g sample, depending on extraction methodology. [128] Comparison of the results obtained for the extracts studied herein with those found in the literature is difficult, since different grape varieties and extraction procedures lead to different qualitative and quantitative phenolic contents, and therefore to different antioxidant activities. Representative results for HORAC and HOSC assays were not found in the literature.

Table 3.4. Antioxidant activity of the extracts as obtained by different chemical assays, Results are expressed as antioxidant activity per gram of extract. Results identified with different letters are significantly different (p-value<0.05), whereas coincident letters indicate that results are statistically equal (lowercase letters for ORAC; uppercase letters for HOSC; underlined lowercase letters for HORAC). Results were obtained from at least three independent experiments.

	Extract	ORAC (µmol TE/g extract)	HOSC (µmol TE/g extract)	HORAC (µmol CAE/g extract)
Wine Lees	Mt	3167 ± 189 (a)	3680 ± 163 (A)	1932 ± 130 (a)
	MW Mt	3500 ± 223 (a)	4776 ± 268 (B)	2625 ± 135 (b)
	Port	451 ± 26 (b)	837 ± 49 (C)	458 ± 29 (c)
	MW Port	716 ± 41 (c)	1285 ± 95 (D)	776 ± 49 (d)
Grape Marc	GM	481 ± 30 (b,d)	746 ± 49 (C)	305 ± 28 (e)
	MW80 GM	448 ± 31 (b,d)	441 ± 34 (E)	198 ± 19 (f)
	MW100 GM	320 ± 29 (e)	478 ± 35 (E)	133 ± 10 (g)

Antioxidant values expressed per mass of extract do not clarify wether the antioxidant effect is due to the total amount of phenolics or to the presence and reactivity of specific compounds. In order to better understand the quality of the antioxidants present in the extracts, results were normalized to antioxidant capacity per micromole of gallic acid equivalents (GAE) (Table 3.5.). In this way, results are not biased by TPC, but instead it is possible to get a clearer idea about the actual quality of the extracts. Red table wine lees extracts (Mt and MW Mt) presented the highest antioxidant capacity per micromole of GAE in all the three assays, with ORAC values of 2.24–2.27 µmol TE/µmol GAE, HOSC values of 2.64–3.05 µmol TE/µmol GAE, and HORAC values of 1.38–1.68 µmol CAE/µmol GAE. On the other hand, grape marc extracts (GM, MW80 GM and MW100 GM) revealed the lowest antioxidant capacity per micromole of GAE, particularly in HOSC, with values of 1.51–1.80 µmol TE/µmol GAE, and HORAC, with values of 0.50–0.73 µmol CAE/µmol GAE. These results suggest that the phenolic families present in red table wine lees are more effective in scavenging $^{\bullet}$OH and ROO$^{\bullet}$ radicals as well as chelating transition metal ions than those encountered in Port wine lees and grape marc. In red table wine lees and grape marc extracts, MW pretreatment either enhanced or had no significant impact on the antioxidant quality of the extracts, except in the case of MW100 GM, which presented an HORAC value (0.50 µmol CAE/µmol GAE)

significantly lower than that of GM (0.62 µmol CAE/µmol GAE). This might be explained by the general tendency of MW to increase phenolic extraction yield, leading to stronger antioxidant capacity of samples. However, in the case of Port wine lees, the conventional extract presented an enhanced antioxidant capacity when compared with the extract obtained from the MW-pretreated matrix, in both ORAC (1.20 *vs.* 1.06 µmol TE/µmol GAE), HOSC (2.23 *vs.* 1.91 µmol TE/µmol GAE) and HORAC (1.22 *vs.* 1.15 µmol CAE/µmol GAE). A possible explanation for this observation is that MW pretreatment may lead to degradation of certain compounds that might also be relevant for antioxidant activity. Additionally, there are cases in which relative results of the extracts in each antioxidant assay are different. For instance, MW Mt presented better results than Mt in both HOSC (3.05 *vs.* 2.64 µmol TE/µmol GAE) and HORAC (1.68 *vs.* 1.38 µmol CAE/µmol GAE) assays but, in the ORAC assay, differences between the results obtained for the two samples were not statistically significant (2.27 *vs.* 2.24 µmol TE/µmol GAE). This observation supports the claim that different extracts may be richer in certain phenolic families than others, having different activities towards distinct oxidant sources. These findings make sense if we consider the great variety of phenolic structures found in plants, presenting different redox potentials, antioxidant stoichiometry, solubility and mechanisms of action. [8,145] For instance, flavonoids are more capable of inactivating peroxyl radicals than small phenolic antioxidants, whereas monohydroxybenzoic acids are very effective in the inactivation of hydroxyl radicals. [60] Moreover, antioxidant activity depends not only on TPC, but also on interactions taking place between antioxidant molecules, causing synergistic or antagonistic effects. [146]

Table 3.5. Antioxidant activity of the extracts as obtained by different chemical assays. Results are expressed as antioxidant activity per micromole of GAE. Results identified with different letters are significantly different (p-value<0.05), whereas coincident letters indicate that results are statistically equal (lowercase letters for ORAC; uppercase letters for HOSC; underlined lowercase letters for HORAC). Results were obtained from at least three independent experiments.

	Extract	ORAC (µmol TE/µmol GAE)	HOSC (µmol TE/µmol GAE)	HORAC (µmol CAE/ µmol GAE)
Wine Lees	Mt	2.27 ± 0.14 (a)	2.64 ± 0.12 (A)	1.38 ± 0.09 (a)
	MW Mt	2.24 ± 0.14 (a)	3.05 ± 0.17 (B)	1.68 ± 0.09 (b)
	Port	1.20 ± 0.07 (b)	2.23 ± 0.13 (C)	1.22 ± 0.08 (a,c)
	MW Port	1.06 ± 0.06 (c,d)	1.91 ± 0.14 (D)	1.15 ± 0.07 (c)
Grape Marc	GM	0.97 ± 0.06 (c)	1.51 ± 0.10 (E)	0.62 ± 0.06 (d)
	MW80 GM	1.66 ± 0.12 (e)	1.64 ± 0.13 (E,F)	0.73 ± 0.07 (d)
	MW100 GM	1.20 ± 0.11 (b,d)	1.80 ± 0.13 (D,F)	0.50 ± 0.04 (e)

In short, all the studied extracts are promising sources of antioxidant compounds (with ability to scavenge free radicals as well as to prevent their formation) that can be used for cosmetic applications.

3.2. Screening of the Cosmetic Potential of Wine Lees and Grape Marc Extracts

3.2.1. Anti-Hyperpigmentation Activity

Along with ageing, pigmentation disorders tend to appear in skin, particularly hyperpigmented regions, which are more common in sun-exposed areas. This issue has attracted the attention of cosmetic industries and led the quest to find compounds with anti-hyperpigmentation potential. As described in section 1.2., these pigmentation lesions are caused by alterations resulting in accumulation of melanin. Thus, inhibition of melanin production is the most explored approach in this field. Because tyrosinase is the rate-limiting enzyme in melanin synthesis, it is a promising target for development of skin whitening cosmetic products. [2]

3.2.1.1. Inhibition of Tyrosinase

Phenolic compounds, due to their aromatic structural features, bear some similarities to tyrosine, the substrate of tyrosinase that initiates the synthesis of melanin. Hence, phenolics are potential analogs of tyrosine that can interact with the enzyme instead, functioning as a competitive inhibitor. In addition, tyrosinase contains a copper ion in its active site and, as it has already been pointed out, certain phenolics have the ability to chelate transition metal ions, which further stresses the potential of these phytochemicals as tyrosinase inhibitors. [147]

Considering that grape marc and wine lees extracts are rich in phenolic compounds, being a great source of potential tyrosinase inhibitors, they were assessed for inhibition capacity towards diphenolase activity of tyrosinase, using DOPA as substrate. For this purpose, mushroom tyrosinase was used, which is highly homologous with mammalian tyrosinases and contains a conserved copper-binding domain in the active site, common to all tyrosinases. Moreover, the commercial availability of mushroom tyrosinase is much higher, due to a lack of purified form of the human enzyme. [43]

All tested extracts showed a dose-dependent inhibiting effect on mushroom tyrosinase, which allowed for determination of IC_{50} values (Table 3.6.). Wine lees extracts have lower IC_{50} values (≤ 1.06 mg extract/mL) than grape marc extracts (≥ 4 mg extract/mL), which means that the former are more potent inhibitors of tyrosinase than the latter. In other words, a smaller amount of wine lees extracts is needed to reduce the activity of the enzyme to 50%. Amongst wine lees matrices, red table wine lees (Mt and MW Mt) showed the best results, with the highest potential for tyrosinase inhibition (IC_{50} ≤ 0.2 mg extract/mL). These results suggest that the capacity of the extracts to inhibit tyrosinase is related to phenolic composition.

Correlation of IC_{50} values for tyrosinase with TPC and TAC of extracts was examined. R^2 values for correlations with TPC and TAC were, respectively, 0.5561 and 0.6399. IC_{50} values

apparently correlate better with TAC than with TPC, suggesting that anthocyanins may play an important role in tyrosinase inhibition, which is in accordance to the fact that flavonoids (a family of phenolics in which anthocyanins are included) are able to chelate transition metal ions, such as Cu^{2+} [148], which is present in tyrosinase active site. Nevertheless, both correlation values are considerably low, because the plots would be better adjusted to a decreasing exponential function model than to a linear regression (graphs not shown). To address this issue, correlations of TPC and TAC with IC_{50} results obtained for wine lees and grape marc were examined separately. It was found that wine lees extracts correlated with TPC with R^2=0.9526 and with TAC with R^2=0.9429, whereas grape marc extracts had very low correlation factors with both TPC and TAC (R^2=0.2458 and 0.1806, respectively). These findings suggest that for wine lees extracts (higher TPC and TAC values), the amount of phenolics and anthocyanins determines the inhibitory activity of tyrosinase, whereas for grape marc extracts (lower TPC and TAC values), the capacity to inhibit tyrosinase probably relies more on the amount of specific phenolic compounds rather than the overall amount of phenolics. Nevertheless, MW100 GM revealed the highest IC_{50} (5.4 mg extract/mL) among grape marc extracts, suggesting that the extraction conditions applied in this case may be causing loss of certain compounds related to tyrosinase inhibition.

Table 3.6. IC_{50} values of the extracts towards tyrosinase. Results were obtained from at least three independent experiments.

	Extract	IC_{50} Tyrosinase (mg extract/mL)
Wine Lees	Mt	0.20 ± 0.01
	MW Mt	0.14 ± 0.01
	Port	1.06 ± 0.07
	MW Port	0.62 ± 0.04
Grape Marc	GM	4.03 ± 0.14
	MW80 GM	4.00 ± 0.14
	MW100 GM	5.40 ± 0.18
	Kojic Acid	0.030 ± 0.001 mg/mL

Kojic acid is a well-studied inhibitor of tyrosinase that is widely used as a reference for comparison with novel potential inhibitors of the enzyme. This inhibitor of tyrosinase is currently used as a part of cosmetic skin whitening formulations, and its high efficacy is due to its ability to inhibit both monophenolase and diphenolase activities of tyrosinase. Kojic acid is an effective inhibitor of tyrosinase because it is able to chelate copper at the active site and because it has

structural features characteristic of an intermediate between DOPA and dopaquinone, namely hydroxyl and oxo groups in *ortho* position [43,149] (confront Figures 1.2. and 3.3.).

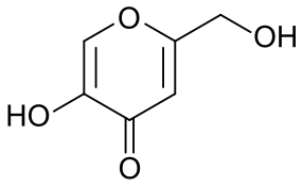

Figure 3.3. Kojic acid structure.

Kojic acid inhibitory activity towards mushroom tyrosinase was assessed in the same conditions as the extracts, yielding the lowest IC_{50}. None of the tested samples was as effective as kojic acid. However, red table wine lees extracts came remarkably close, particularly MW Mt, presenting an IC_{50} value only about five-fold higher than that of kojic acid.

The flavonoid structure is compatible with the role of tyrosinase inhibitors, and flavonoids possess metal-binding properties due to the presence of metal-binding motifs in their structure. [43,59] Hence, it is possible to assume that phenolics belonging to the flavonoid family of compounds may play a significant role in tyrosinase inhibition. Among flavonoids, flavonols and anthocyanins can be found. Anthocyanidins are highly unstable and thus are more commonly found in cells in the more stable glycosylated form (anthocyanins). [55] Yet, it has been reported that substitution of the 3-OH group of flavonoids decreases tyrosinase inhibitory activity [150], suggesting that non-glycosylated flavonols may be more promising tyrosinase inhibitors than anthocyanins.

Quercetin, myricetin and kaempferol are three of the most relevant tyrosinase inhibitors [43], and have been identified in both red table wine lees extracts and grape marc extracts. In Port wine lees extracts, only two of these three flavonols were identified: quercetin and myricetin. IC_{50} values of these flavonols towards tyrosinase reported in the literature are variable due to different assay conditions used in their determination. IC_{50} for quercetin ranged from 50 to 165 µM [151–154], values for myricetin were found to be >50 µM [152], and for kaempferol IC_{50} values ranged from 50 to 230 µM. [153–155]

Because of the limited amount of time available to develop this research project, quantification of the phenolics identified in the extracts by HPLC method 2 could not be performed. Hence, an approach considering relative amounts of quercetin, myricetin and kaempferol between samples was used. For this purpose, the areas of the peaks corresponding to myricetin, quercetin and kaempferol, in chromatograms obtained by HPLC method 2, were calculated for each sample, and relative amounts of these compounds were compared (Figure 3.4.).

The summed area of the peaks corresponding to myricetin, quercetin and kaempferol is much higher in wine lees extracts, ranging from 96011 to 671489 a.u., than in grape marc extracts, with summed areas of 6741–13482 a.u..

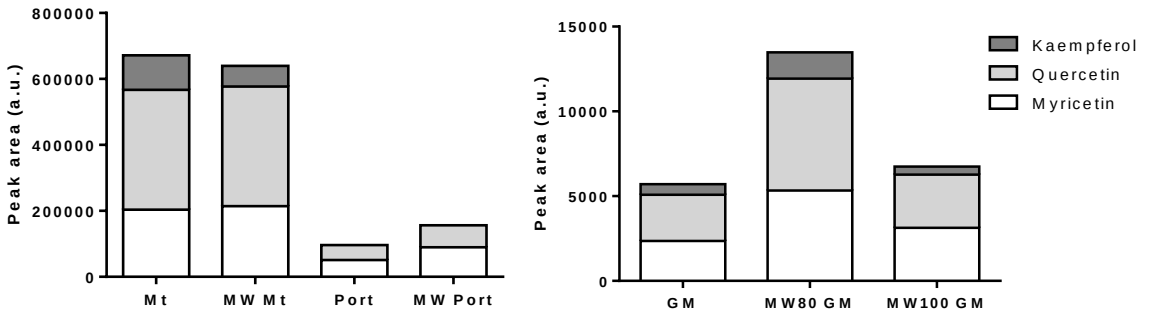

Figure 3.4. Sum of the peak areas corresponding to myricetin, quercetin and kaempferol. Values are expressed in arbitrary units (a.u.) of area.

Considering that the three abovementioned flavonols have already been recognized as tyrosinase inhibitors, it makes sense that the most promising of the tested extracts are those with the highest sum percentage of these compounds (Mt with 671489 and MW Mt with 639423 a.u.). Also, MW Port has a higher value of summed area than Port (156466 *vs.* 96011 a.u.), presenting a lower IC_{50} towards tyrosinase. However, in the case of grape marc extracts, the correlation between summed areas of the three flavonols is not straightforward, since sums of peak areas are 5701, 13482 and 6741 a.u. for GM, MW80 GM, and MW100 GM, respectively. In spite of having a larger amount of myricetin, quercetin and kaempferol than GM, MW100 GM presents a higher tyrosinase IC_{50} than the latter.

When comparing the order of flavonol content in the extracts (Mt>MW Mt>MW Port>Port>MW80 GM>MW100 GM>GM) (section 3.1.1.) with tyrosinase IC_{50} values, it seems that, although flavonols, including myricetin, quercetin and kaempferol, may play a relevant role in tyrosinase inhibition, there must be other phenolics contributing to the bioactivity of the extracts towards tyrosinase.

Anyhow, results obtained in tyrosinase inhibition assays prove that extracts obtained from both red table wine lees, Port wine lees, and grape marc may be a source of tyrosinase-inhibiting compounds, or mixtures of compounds, for application in cosmetics with skin whitening effects.

3.2.2. Anti-Ageing Activity

Skin ageing is mainly characterized by alterations in dermal connective tissue components, such as elastic fibers and collagen, resulting in loss of elasticity, tensile strength and volume, leading to skin laxity and wrinkle formation.

Several phenolic compounds have been found to inhibit ECM-degrading enzymes (Table 1.1.), hence the phenolic-rich extracts under study were assayed for their inhibitory capacity towards different ECM proteases.

3.2.2.1. Inhibition of Elastase

As it has been described in section 1.2., alterations in elastic fibers include two distinct events affecting elastin: reduced amount of elastin in intrinsically aged skin, and accumulation of degraded elastin in extrinsically aged skin. Elastases play a major role in both cases, leading to the skin ageing phenotype observed, because these proteases contribute to the diminished amounts of elastin in intrinsically aged skin, and degrade recently formed tropoelastin in extrinsically aged skin, hampering its correct assembly into normal elastic fibers. Moreover, elastases are broadly specific, also being able to degrade other ECM proteins besides elastin. This being said, and bearing in mind the fact that several phenolics have been demonstrated to have anti-elastase activity [26,28,69], assessment of elastase inhibitory capacity of the extracts under study seems relevant for validation of their anti-ageing potential.

In this work, elastase from porcine pancreas (PPE) was used. This enzyme belongs to the family of serine proteases, and presents a characteristic structure common to all members of this family, as well as the same catalytic mechanism. [31,156] Hence, PPE is a representative enzyme of the family of serine proteases, to which human neutrophil elastase (NE) and human pancreatic elastase-1 also belong, this being a reliable model to get first indications of the capacity of the extracts to inhibit these elastolytic enzymes which contribute to skin ageing (section 1.2.3.). Furthermore, PPE is much more commercially accessible.

All the extracts revealed a dose-dependent inhibition of PPE, allowing for determination of IC_{50} values (Table 3.7.). In agreement with what has been seen for tyrosinase, red table wine lees extracts presented the lowest IC_{50} values (≤ 0.17 mg extract/mL). However, results obtained for the other samples did not follow the same trend as for tyrosinase inhibition. MW Port (IC_{50}=0.83 mg extract/mL) and GM (IC_{50}=0.87 mg extract/mL) were stronger inhibitors of elastase than Port (IC_{50}=1.92 mg extract/mL), MW80 GM (IC_{50}=3.43 mg extract/mL), and MW100 GM (IC_{50}=3.31 mg extract/mL). Correlation of IC_{50} values for elastase with TPC and TAC of extracts, similarly to what has been observed for tyrosinase, was low, with R^2 of 0.6807 for TPC and 0.5774 for TAC. The low correlation factor with TPC can be explained, once again, by a wrong choice of adjustment function, given that the plots would better adjust to a decreasing exponential function model instead of a linear regression. On the other hand, there is no clear relationship between IC_{50} and TAC, suggesting that anthocyanins are not major players in the inhibition of elastase. In fact, although the relationship between IC_{50} and TPC is not linear, there is a direct correspondence between these two parameters, which reinforces the hypothesis that phenolics other than anthocyanins are responsible for the inhibitory capacity of the extracts, and the amount of phenolics determines this inhibition. These findings are in agreement with the literature, because the glycoside moiety of phenolics was found to hinder the inhibitory interaction with elastase [69,157], supporting that anthocyanins (glycosylated anthocyanidins) may not be relevant for elastase inhibition. Also, it has been reported that higher TPC values lead to stronger inhibition of elastase. [26] Regarding the flavonol content of the extracts (Mt>MW Mt>MW Port>Port>MW80 GM>MW100 GM>GM),

estimated from total peak area at 360 nm by HPLC method 2, it is clear that other compounds apart from flavonols are contributing to the elastase inhibitory capacity of extracts.

Table 3.7. IC_{50} values of the extracts towards elastase. Results were obtained from at least three independent experiments.

	Extract	IC_{50} Elastase (mg extract/mL)
Wine Lees	Mt	0.17 ± 0.01
	MW Mt	0.108 ± 0.002
	Port	1.92 ± 0.09
	MW Port	0.83 ± 0.04
Grape Marc	GM	0.87 ± 0.03
	MW80 GM	3.43 ± 0.11
	MW100 GM	3.31 ± 0.11

Phenolic compounds can interact with proteins through hydrogen bonds, hydrophobic interactions, ionic bonds, and covalent bonds. [158] Inhibition of elastase (serine protease) relies on van der Waals (vdW) interactions and hydrogen bonds between specific amino acid residues of the enzyme and structural motifs of the inhibitor, thus phenolics with a larger number of potential interaction sites, including aromatic rings for vdW interactions and hydroxyl groups for hydrogen bonding, are more likely to better inhibit elastase. It has been reported that inhibition of elastase can be achieved by several groups of compounds belonging to the two major classes of phenolics (phenolic acids and flavonoids), such as caffeic acid (IC_{50} of 93 µM towards NE) [159], catechins and procyanidins (1 mM catechin inhibits PPE to an extent of 12%, and the inhibitory potential increases with degree of polymerization) [26,28], myricetin (IC_{50} of 4 µM towards NE), quercetin (IC_{50} of 20 µM towards NE) [69], among others. Structural features playing an important part in the inhibitory capacity of phenolics towards elastase are the galloyl moiety, degree of polymerization in the case of procyanidins, hydroxylation of the structure, etc. [26,28,69,159]

Gallic acid has been identified in all winemaking waste stream matrices tested, as well as myricetin and quercetin, whereas procyanidins were only detected in red table wine lees and grape marc extracts. The presence of these compounds might explain the capacity of the extracts to inhibit elastase, and the differences observed in IC_{50} values are probably due to the different amounts of these phenolics encountered in each sample. A published study, also testing grape marc inhibitory capacity towards PPE, reported a lower IC_{50} value (14.7 µg extract/mL) than those obtained herein. [26] The differences may be explained by the different raw material (white grape

pomace), extraction procedure and assay conditions, leading to different compositions of the extracts when compared to those under study in this work.

3.2.2.2. Inhibition of MMP-1

Matrix metalloproteinase-1 (MMP-1), also known as interstitial collagenase, is one of the most important enzymes participating in the process of skin ageing through degradation of ECM components. Being a collagenase, MMP-1 has the ability to initiate degradation of fibrillar types of collagen, such as collagens I and III which are the predominant forms existing in skin, paving the way for further degradation by gelatinases and stromelysins. MMP-1 can also cleave non-fibrillar collagen and other ECM constituents. For these reasons, MMP-1 was the chosen MMP for inhibitory activity screening herein. As already described in section 1.2.3., MMPs have a conserved methionine and a zinc-binding motif in their active site, as well as a similar fold [36], thus inhibitory capacity of the extracts towards MMP-1 may provide an insight into their capacity to inhibit other enzymes from the MMP family.

Inhibition of collagenase can be achieved by either unspecific non-covalent interactions with amino acid side chains leading to conformational changes, interaction with the binding site, or complexation of the zinc ion (Zn^{2+}) present in the catalytic site. The most effective inhibitor would combine both metal ion chelation and interactions with the protein through vdW forces and hydrogen bonds. [26,39,160,161]

All the tested extracts revealed a dose-dependent inhibition of MMP-1, and IC_{50} values were determined (Table 3.8.). Similarly to previous enzymatic assays, red table wine lees presented the best results in terms of inhibitory capacity towards MMP-1 (IC_{50} ≤ 0.22 mg extract/mL). However, in this assay, MW Mt results were not better than Mt results, suggesting that, in this particular case, although MW-pretreatment enhanced overall phenolic content, it might not have increased the amount of certain phenolics contributing more to MMP-1 inhibition.

Correlation factors of IC_{50} values with TPC and TAC were 0.8768 and 0.9135, respectively. These correlations were much better than those encountered for the other studied enzymes, meaning that there is a considerably linear relationship of both TPC and TAC with IC_{50}. In addition, inhibitory capacity showed slightly better correlation with TAC than with TPC, suggesting that anthocyanins may play a part in MMP-1 inhibition. Considering that anthocyanins are flavonoids, thus having metal-binding capabilities, and that collagenase inhibition can be achieved by chelation of the Zn^{2+} ion at the active site, there is logic to this observation.

Given the lack of specificity involved in collagenase inhibition by phenolic compounds, it makes sense that a higher inhibition would be achieved by a higher amount of phenolics. Moreover, several compounds from different phenolic groups have been shown to inhibit collagenase and/or other MMPs. Among them, catechins (1 mM catechin inhibits the activity of a bacterial collagenase by more than 20%; 1 mM EGCG inhibits the activity of the protease by 60%) and procyanidins (1 mM inhibited a bacterial collagenase slightly more effectively than the correspondent monomer,

catechin), gallic acid (250 µM inhibited the activity of a bacterial collagenase by 42%), delphinidin (IC_{50} of 3 and 13 µM towards MMP-2 and MMP-9, respectively), myricetin (IC_{50} of 10 and 12 µM towards MMP-2 and MMP-9, respectively), quercetin, kaempferol, (both with IC_{50} > 125 µM), etc. [26,69]

Table 3.8. IC_{50} values of the extracts towards MMP-1. Results were obtained from at least three independent experiments.

	Extract	IC_{50} MMP-1 (mg extract/mL)
Wine Lees	Mt	0.22 ± 0.01
	MW Mt	0.21 ± 0.01
	Port	1.16 ± 0.03
	MW Port	0.57 ± 0.02
Grape Marc	GM	1.24 ± 0.10
	MW80 GM	1.15 ± 0.08
	MW100 GM	1.43 ± 0.04

Although certain glycosylated derivatives of flavonoids present collagenase inhibitory activity, they are reported to be less effective than non-glycosylated compounds. Indeed, glycosyl moieties are known to contribute to an enhanced steric hindrance, hampering the interaction between the phenolic and the enzyme. [26,69] Also, it has been reported that important structural features contributing to inhibition of MMPs include the presence of galloyl moieties, polyhydroxylation of the flavonoid backbone, planarity of the molecule, and presence of metal-binding motifs. [69,161] Therefore, it can be speculated that the compounds responsible for MMP-1 inhibitory capacity of the tested extracts may be gallic acid, procyanidins, catechin/epicatechin, and flavonol aglycones. The latter including myricetin, quercetin and kaempferol, which are not only capable of establishing vdW interactions and hydrogen bonds with the protein, but also have the ability to chelate transition metal ions, including Zn^{2+}. [59] The relative summed areas of myricetin, quercetin, and kaempferol (Figure 3.4.) between extracts is: MW Mt>Mt>MW Port>Port>MW80 GM>MW100 GM>GM. On the other hand, the order of MMP-1 IC_{50} is MW Mt>Mt>MW Port>Port>MW80 GM>GM>MW100 GM, supporting the hypothesis that these flavonol aglycones contribute to MMP-1 inhibition.

In a study using white grape marc extract [26], IC_{50} for collagenase (20.3 µg extract/mL) was lower than the values obtained herein, possibly due to the different raw material and extraction procedure, leading to different composition of the extract. In addition, those researchers tested

inhibitory capacity of the extract on collagenase from *Clostridium histolyticum*, which might also be contributing to the different results.

3.2.3. Cellular Antioxidant Activity

Selection of the most promising extracts was made in accordance to the results discussed above, namely phytochemical composition, antioxidant capacity, anti-hyperpigmentation effects, and anti-ageing potential. These results are summarized in Table 3.9., in which extracts are rated according to their performance in each assay. The extracts selected to proceed to cell-based assays were GM, MW80 GM, MW Port and MW Mt. It is of note that at least one sample from each waste stream matrix was selected, for comparison purposes in cell-based assays. MW Port and MW Mt were chosen because, in general, these samples showed better results than the equivalent conventional extracts, obtained from matrices that suffered no MW pretreatment, in all the previous experiments. In the case of grape marc extracts, GM was generally better than the equivalent extracts obtained after MW pretreatment, however, both GM and MW80 GM showed better results than MW100 GM. In addition, MW80 GM presented a higher TAC than GM. For these reasons, and in order to compare two extracts from the same waste stream matrix, obtained by different extraction procedures, both GM and MW80 GM were selected for cell-based assays.

Table 3.9. Summary of the results obtained for the extracts in chemical and enzymatic assays, in terms of antioxidant, anti-hyperpigmentation and anti-ageing activity. For each assay, the mean of the results was calculated, and extracts were rated based on their percentage relative to the mean. For antioxidant activity assays (percentages calculated from antioxidant capacities per gram of extract): - for 0–50%; + for 50–100%; ++ for 100–150%; +++ for 150–200%; ++++ for 200–250%; +++++ for >250%. For enzymatic assays: +++++ for 0–10%; ++++ for 10–25%; +++ for 25–50%; ++ for 50–100%; + for 100–200%; - for >200%.

		Antioxidant Activity			Anti-Hyperpigmentation Activity	Anti-Ageing Activity	
	Extract	ORAC	HOSC	HORAC	Tyrosinase	Elastase	MMP-1
Wine Lees	Mt	++++	++++	++++	+++++	++++	+++
	MW Mt	+++++	+++++	+++++	+++++	+++++	++++
	Port	-	-	+	+++	+	+
	MW Port	+	+	++	+++	++	++
Grape Marc	GM	-	-	-	+	++	+
	MW80 GM	-	-	-	+	-	+
	MW100 GM	-	-	-	-	-	+

Since keratinocytes and fibroblasts are the predominant cell types encountered in skin, representing the epidermal and dermal layers, respectively, cellular assays were based on keratinocyte and fibroblast cell lines. These cell types are those responsible for skin integrity, and, when affected by senescence or oxidative stress, they are leading players in the emergence of the aged skin phenotype.

3.2.3.1. Cytotoxicity evaluation

Potential cytotoxicity of the extracts was evaluated for incubation times of 24 and 48 hours, in both keratinocyte and fibroblast cell lines (HaCaT and HFF, respectively), in order to select non-toxic concentrations for further studies. Several concentrations of each extract were tested in terms of milligrams of extract per milliliter of solution in culture medium with 0.5% FBS. Results of these studies are depicted in Figure 3.5. for keratinocytes (HaCaT), and in Figure 3.6. for fibroblasts (HFF). The cytotoxicity profile of the extracts has been found to be very similar in the two cell lines, which is consistent with another study where the cytotoxicity of several substances was found to be identical between HaCaT and a fibroblast cell line from mouse (3T3). [162]

Extract concentrations were considered cytotoxic according to the definition of cytotoxicity proposed by the International Organization for Standardization (ISO 10993-5), which states that a reduction in cell viability by more than 30% is considered a cytotoxic effect. [163]

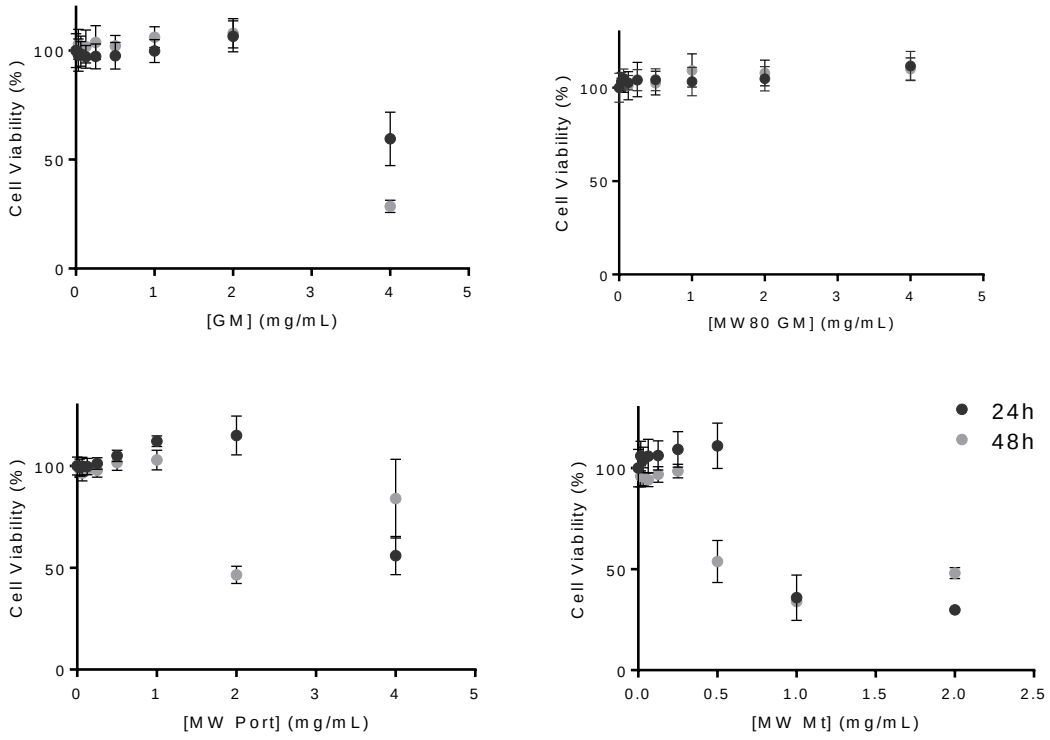

Figure 3.5. Cytotoxicity screening of the chosen extracts (24 and 48 hours of incubation) in HaCaT. Results were obtained from three independent experiments.

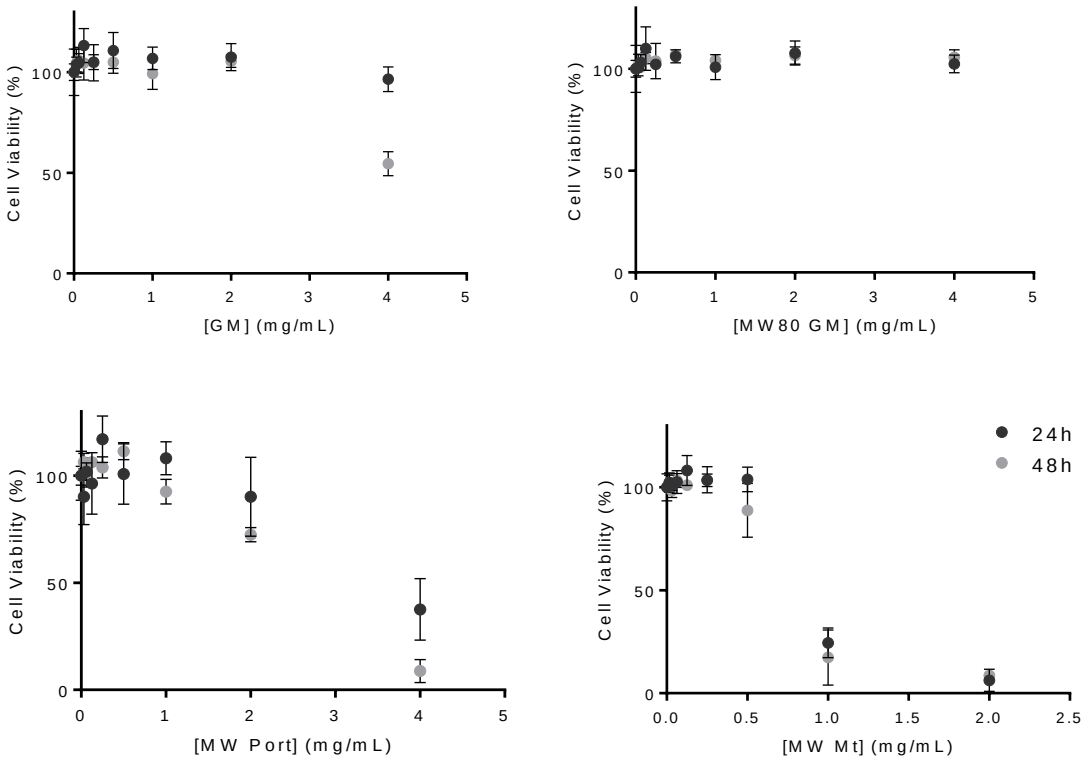

Figure 3.6. Cytotoxicity screening of the chosen extracts (24 and 48 hours of incubation) in HFF. Results were obtained from three independent experiments.

GM, MW80 GM and MW Port were tested between 0.03 and 4 mg extract/mL, whereas MW Mt was tested from 0.02 to 2 mg extract/mL. Considering incubation times of 48h in both HaCaT and HFF, it is possible to conclude that GM can be regarded as non-cytotoxic when used in concentrations below 2 mg extract/mL (0.99 µmol GAE/mL), whereas MW80 GM did not reveal any cytotoxicity even in the highest concentration tested (4 mg extract/mL; 1.08 µmol GAE/mL). MW Port does not reduce cell viability until the concentration of 1 mg extract/mL (0.67 µmol GAE/mL) is reached in both cell lines, and MW Mt was considered to be non-cytotoxic up to 0.25 mg extract/mL (0.39 µmol GAE/mL). A pattern can be noticed among these results, because the higher the phenolic content of the extract, the higher its potential for cytotoxicity. In other words, the ascending order of TPC is MW80 GM<GM<MW Port<MW Mt, which coincides with the ascending order of cytotoxic potential. This finding is legitimate if we consider the fact that phenolics may present deleterious effects when excessive concentrations are applied, acting either as pro-oxidants or disrupting the redox balance of cells. [164–166] Thus, to attain beneficial effects, a proper amount of extract or phenolics must be chosen.

It should be noted that in HaCaT cell viability was increased by the extracts (p-value<0.05), especially in the case of 24h incubation with MW Port and MW Mt, before actual cytotoxicity was exhibited. This has already been observed in HaCaT for phenolic compounds and natural extracts, as moderate concentrations of phenolics are likely to display a protective effect of cells against

intracellular ROS generation, lipid peroxidation and DNA damage. [167,168] Although this has already been observed for HFF as well [169], results herein do not show evident cytoprotective or proliferative effects of extracts on HFF, possibly because of the magnitude of the error (evident in the case of MW Port) or due to different extract-cell interactions in different cell lines.

Since keratinocytes and fibroblasts presented a relatively similar behavior in cytotoxicity screening of the extracts, it was possible to choose the same maximum extract concentrations for both cell lines to be used in subsequent experiments. The following maximum extract concentrations were used: 2 mg extract/mL GM, 2 mg extract/mL MW80 GM, 1 mg extract/mL MW Port, and 0.25 mg extract/mL MW Mt.

3.2.3.2. Protection against an Oxidative Stress Inducer – H_2O_2

Chemical antioxidant assays, such as ORAC, HOSC and HORAC, are useful tools for an initial antioxidant activity screening of compounds or natural extracts. However, these methods have considerable limitations concerning the prediction of the antioxidant activity of the tested samples in a biological environment. Parameters like bioavailability, cellular uptake, and metabolism are not taken under consideration in chemical assays given the simplicity of these systems. For instance, two compounds may have similar antioxidant activities as determined by chemical assays, yet one may be more promising than the other when applied in biological context because of its pharmacokinetic profile (ADME – Absortion, Distribution, Metabolism and Excretion). Cellular antioxidant assays comprise some of the complexity of biological systems, namely cellular uptake of the applied compounds, subcellular location, and metabolism. [117]

In order to better understand the rationale behind the potential protective effects of the extracts towards keratinocytes and fibroblasts, studies were performed using an oxidative stress inducer, H_2O_2. Exogenous H_2O_2 can cause harm to various biomolecules, including lipid peroxidation, protein carbonylation and DNA damage [168], probably because it takes part in the Fenton chemistry of cells.

Four concentrations of each extract were used in cellular antioxidant activity assays, more specifically, the chosen maximum concentration (section 3.2.3.1.) along with three subsequent dilutions.

The effect of the extracts in H_2O_2-induced ROS formation in cells was assessed in two different conditions: pre-incubation of the cells with the extracts prior to addition of the stressor (H_2O_2), and co-incubation of the extracts with the stressor. Pre-incubation may reflect a preventive action of the extracts, whereas co-incubation is more representative of a possible therapeutic approach.

Firstly, a concentration of H_2O_2 considered as non-toxic to the cells had to be determined. After a cytotoxicity screening (data not shown), the concentrations 0.04 mM and 0.6 mM were chosen for HaCaT and HFF, respectively. HaCaT revealed higher sensitivity to H_2O_2-induced stress than HFF. Comparative results for H_2O_2 sensitivity of fibroblasts and keratinocytes were not found in

the literature, however, HaCaT cell line was found to be more sensitive to H_2O_2-induced damage than other cell lines. [168,170,171]

As a primary approach, both cell lines were pre-incubated with four different concentrations of each extract for 24h prior stress induction with H_2O_2 for 1h (Figure 3.7. A and B). 24h incubation with the extracts was firstly assessed because it was expected to present more significant protective effects on the cells when compared to smaller incubation periods. Differences between the various extract concentrations and the untreated control, where stress had also been induced, seemed more significant in HFF. Nevertheless, results observed in the two cell lines were pretty similar. In HaCaT, all the extracts showed moderate improvements in ROS generation in at least two of the four tested concentrations (Figure 3.7. A), while in HFF all concentrations of the tested extracts had beneficial effects on suppressing ROS generation with significant differences relative to the non-treated control (Figure 3.7. B).

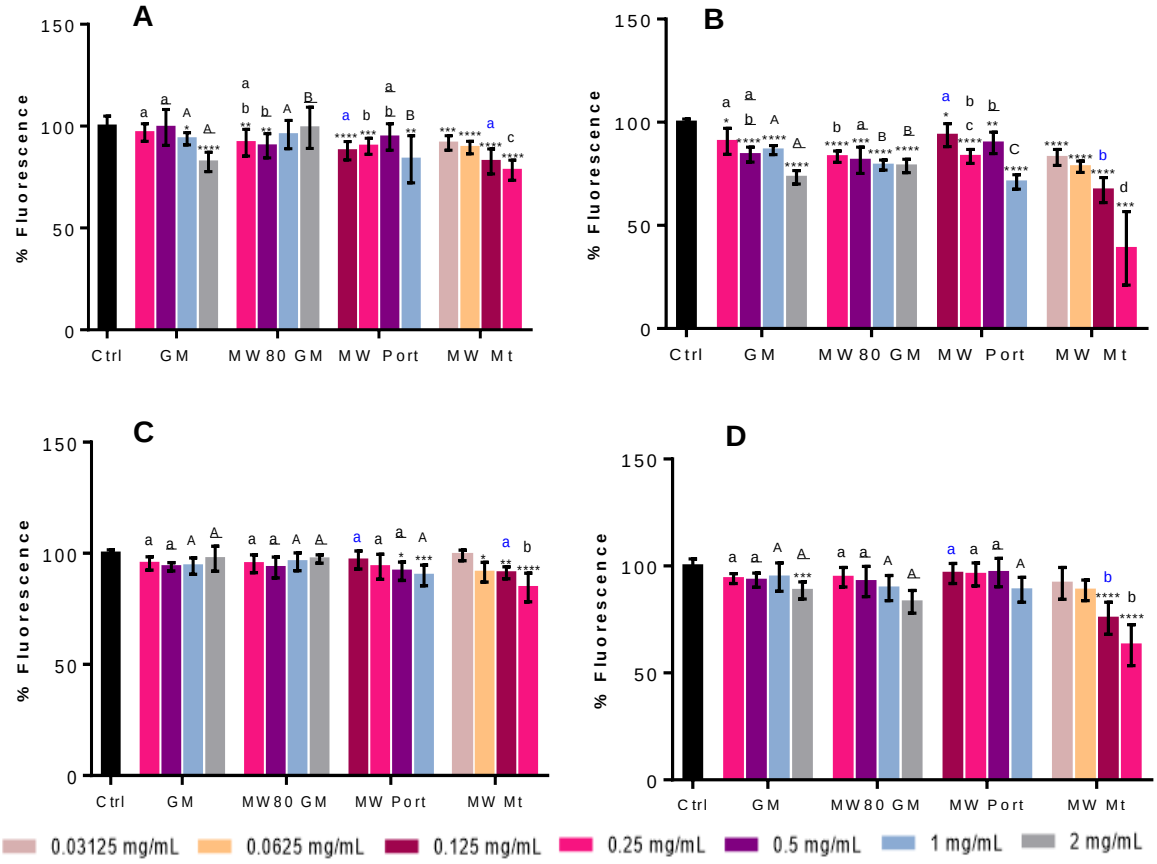

Figure 3.7. Pre-incubation of cells with the extracts for 24h and 1h prior to addition of H_2O_2 – effect on total ROS generation. (A) 24h in HaCaT; (B) 24h in HFF; (C) 1h in HaCaT; (D) 1h in HFF. The symbol * indicates significance relative to the control (* p-value<0.05; ** p-value<0.01, *** p-value<0.001, **** p-value<0.0001). The same concentrations of different extracts were compared (blue lowercase letters for 0.125 mg/mL; black lowercase letters for 0.25 mg/mL; underlined lowercase letters for 0.5 mg/mL; uppercase letters for 1 mg/mL; underlined uppercase letters for 2 mg/mL); statistically different results (p-value<0.5) are identified with different letters. Results were obtained from at least two independent experiments.

In both HaCaT and HFF, the highest concentration of MW Port (1 mg extract/mL) presented better results (84% fluorescence relative to the untreated control in HaCaT and 71% in HFF) than the correspondent concentrations of both grape marc extracts (94% fluorescence relative to the untreated control for GM and 96% for MW80 GM in HaCaT; 87% for GM and 79% for MW80 GM in HFF), stressing that the TPC of the extracts may be determinant in their capacity to inhibit ROS in cells (TPC: MW Port>GM>GM MW80). In fact, 1 mg extract/mL of MW Port corresponds to 0.67 µmol GAE/mL, while 1 mg extract/mL of GM and MW80 GM correspond to 0.49 µmol GAE/mL and 0.27 µmol GAE/mL, respectively. 0.25 mg extract/mL of MW Mt inhibited ROS generation more effectively than the correspondent concentration of all the other tested samples, resulting in 78% fluorescence relative to the untreated control in HaCaT and 39% in HFF, as opposed to fluorescence percentages >90% in HaCaT and >80% in HFF observed for other samples. Once again, TPC appears to be determinant in cellular antioxidant activity of the extracts, because 0.25 mg extract/mL of MW Mt corresponds to 0.39 µmol GAE/mL, as opposed to 0.12, 0.07 and 0.17 µmol GAE/mL of GM, MW80 GM and MW Port, respectively. This result agrees with all previous *in vitro* assays where red table wine lees extracts were the ones presenting the highest values in antioxidant assays and the lowest IC_{50} values in tyrosinase, elastase and MMP-1 assays.

An interesting detail should be noted concerning GM and MW80 GM: for both cell lines, at the lowest concentration of the extracts (0.25 mg extract/mL), MW80 GM showed a higher capacity for inhibition of ROS production than GM, with 92% *vs.* 97% fluorescence in HaCaT (p-value>0.05) and 83% *vs.* 91% in HFF (p-value<0.05); on the other hand, for the highest concentration of the extracts (2 mg extract/mL), GM showed better results, with 82% *vs.* 99% fluorescence relative to the untreated control in HaCaT (p-value<0.05) and 73% *vs.* 79% in HFF (p-value<0.05). These observations can be translated into the following hypothesis concerning phytochemical composition of the extracts: when phenolic concentration is low, the extract with higher anthocyanin content (MW80 GM) inhibits ROS production more effectively; whereas when phenolic concentration is higher, the extract with the best results is the one with highest TPC (GM), undermining the effect of anthocyanin content.

In order to evaluate the most immediate effects of the extracts on ROS production in cells upon addition of a stressor, cells were pre-incubated with the extracts for 1h prior addition of H_2O_2. Results are presented in Figure 3.7. C for HaCaT, and D for HFF. By comparing the two incubation periods (1h and 24h), it can be concluded that a more prolonged treatment of cells with the extracts yields better results in terms of prevention of ROS generation. This observation is probably due to a higher cellular uptake or membrane adhesion of phenolic compounds present in the extracts, when 24h incubation takes place. In both cell lines, MW Mt was yet again found to be the most effective extract, at 0.25 mg extract/mL.

Correlations of the effect of 0.25 mg extract/mL with TPC and TAC revealed differences depending on incubation time. For 1h incubation, in both HaCaT and HFF, correlation with TPC was slightly better than with TAC (R^2 of 0.9573 *vs.* 0.9553 in HaCaT, and 0.8953 *vs.* 0.8480 in HFF). On

the other hand, for an incubation period of 24h, correlations were better with TAC than with TPC (R^2 of 0.9415 *vs.* 0.8326 in HaCaT, and 0.9165 *vs.* 0.8900 in HFF). This could indicate that after a certain amount of time in contact with the cells, some phenolics, particularly anthocyanins, might bind to cell membranes, not being removed by washing steps. Indeed, it has been reported that flavonoids, a class of phenolics in which anthocyanins are included, interact with cell membranes [172,173], which supports this hypothesis.

When the extracts were co-incubated with the stressor (Figure 3.8.), results were much better than those observed for pre-incubation of cells with the extracts, with all tested concentrations presenting a significant ($p<0.0001$) decrease in ROS generation when compared to the untreated control. These findings suggest that there are compounds present in the extracts that are not capable of permeating the cell membrane even in the 24h incubation. Indeed, certain phenolic compounds may not be within specific structural limitations required for membrane permeation, and therefore do not reach intracellular space. These compounds may present additional antioxidant activity towards extracellular ROS, and their effect could only be noticed in the co-incubation approach. Such observations are consistent with those reported elsewhere, in which *Opuntia ficus-indica* extracts [174] and traditional Portuguese cherries extracts [175] reveal a stronger cellular antioxidant activity in co-incubation conditions rather than in the pre-incubation approach. High molecular weight phenolics, such as flavonoids and their respective conjugates, might be among the compounds contributing to the higher efficacy of the extracts on inhibition of ROS formation in co-incubation experiments, because of their low bioavailability. [176]

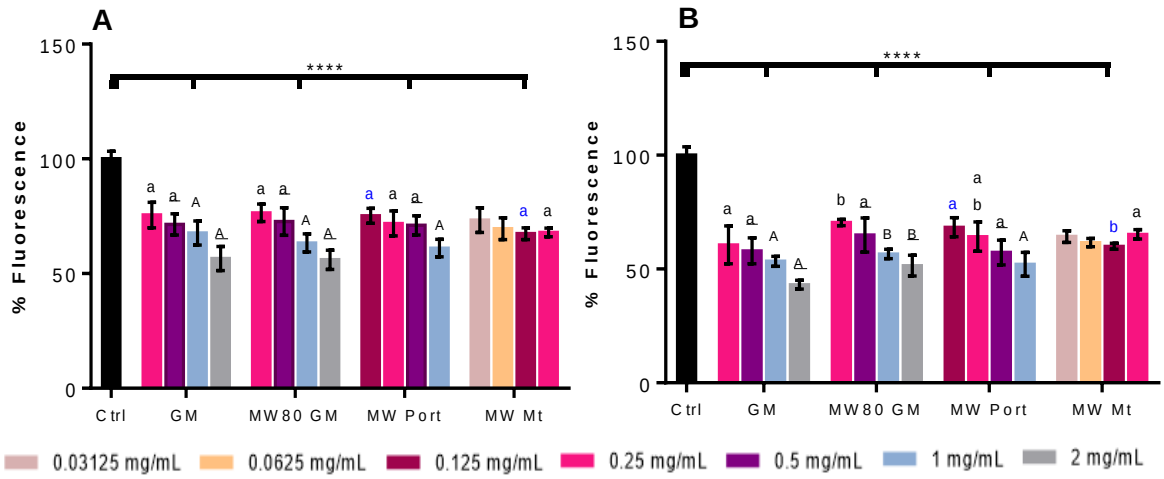

Figure 3.8. Co-incubation of (A) HaCaT and (B) HFF with the extracts and H_2O_2 for 1h – effect on total ROS generation. All concentrations of every extract significantly decreased fluorescence when compared with the untreated control where stress was also induced (**** p-value<0.0001). The same concentrations of different extracts were compared (blue lowercase letters for 0.125 mg/mL; black lowercase letters for 0.25 mg/mL; underlined lowercase letters for 0.5 mg/mL; uppercase letters for 1 mg/mL; underlined uppercase letters for 2 mg/mL); statistically different results (p-value<0.5) are identified with different letters. Results were obtained from two independent experiments.

In either cell line, differences between the same concentrations of different extracts were not significant in most cases. It would be expected that extracts with higher TPC would present higher antioxidant activity when all extracts were tested at the same concentration (mg extract/mL), yet this logic did not apply in the co-incubation case. It is possible that extracts with lower TPC contain specific phenolics with potent antioxidant capacity towards the radicals formed in these experimental conditions. This would lead to an overall similar effect of the different extracts (when tested at the same concentrations), relying on the antioxidant activity of specific phenolics rather than TPC. In fact, phenolic compounds may present varying antioxidant capacities towards different radicals (see section 3.1.2.), which supports this hypothesis.

Two different standards, malvidin-3-O-glucoside and quercetin, were submitted to the same experimental approaches in HaCaT and HFF, at four different concentrations (1, 5, 10 and 15 µM). These concentrations were found to be non-cytotoxic (data not shown) by the definition of cytotoxicity stated in ISO 10993-5. [163] The two compounds, belonging to the class of flavonoids, consist of an anthocyanin glycoside (malvidin-3-O-glucoside) and a flavonol aglycone (quercetin). Malvidin-3-O-glucoside was quantified in the extracts by HPLC method 1 using a standard calibration curve (Table 3.2.), hence the four chosen concentrations of malvidin-3-O-glucoside comprised those found in the highest tested concentrations of the extracts (3.25 µM in GM, 6.19 in MW Mt, 6.59 µM in MW80 GM, and 14.29 µM in MW Port). For comparison purposes, quercetin was tested at the same concentrations as malvidin-3-O-glucoside.

When cells were pre-incubated with the standards for 24h, malvidin-3-O-glucoside seemed slightly more effective than quercetin in reducing H_2O_2-induced ROS generation at the four tested concentrations and in both cell lines (Figure 3.9.), with fluorescence percentages relative to the untreated control ranging from 83% to 89% in HaCaT and from 79% to 88% in HFF, as opposed to 89–92% obtained for quercetin in HaCaT and 78–105% in HFF. Since both compounds are flavonoids, their ability to permeate membranes is low, yet they are likely to interact with the hydrophilic interface of lipid bilayers through the polar hydroxyl groups. [173] Malvidin-3-O-glucoside is a glycosylated flavonoid derivative, thus having more hydroxyl groups available in its structure than quercetin which is a flavonoid aglycone. Hence, the structure of malvidin-3-O-glucoside seems more likely to establish hydrophilic interactions with cell membrane surface, which could explain why the anthocyanin presented better results than quercetin in the pre-incubation experiment.

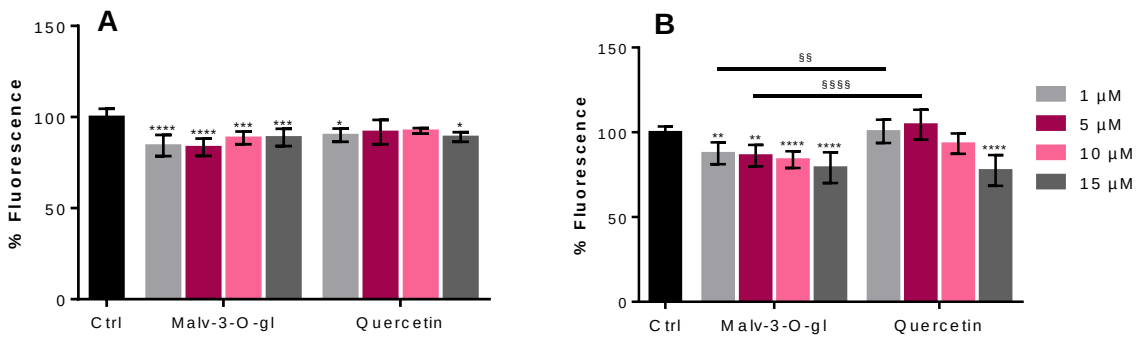

Figure 3.9. Pre-incubation of (A) HaCaT and (B) HFF with two different standards for 24h prior to addition of H_2O_2 – effect on total ROS generation. The symbol * indicates significance relative to the control (* p-value<0.05;*** p-value<0.001, **** p-value<0.0001); the symbol § indicates significance between the same concentration of the two standards (§§ p-value<0.01, §§§§ p-value<0.0001). Results were obtained from at least two independent experiments, except in the case of quercetin in HaCaT, where only one experiment was performed.

When standards were co-incubated with H_2O_2 (Figure 3.10.), inhibition of ROS generation was more effective than what was seen for pre-incubation experiments (Figure 3.9.). This effect is more pronounced in the case of quercetin, which reaches fluorescence percentages ≤62% in co-incubation, while the best result in pre-incubation experiments was 78%. This result is consistent with those obtained for the tested extracts, supporting the claim that flavonoids present in the extracts may play an important part in extracellular antioxidant activity. Moreover, quercetin revealed significantly higher effectiveness than malvidin-3-O-glucoside in reducing ROS production at all tested concentrations, with fluorescence percentages relative to the untreated control ranging from 85% to 62% in HaCaT and from 72% to 49% in HFF. In contrast, malvidin-3-O-glucoside reached fluorescence percentages ranging from 94% to 83% in HaCaT and from 87% to 72% in HFF. This is in agreement with the fact that quercetin is a generally better antioxidant than malvidin-3-O-glucoside in *in vitro* chemical assays, due to more favorable structural features. [60]

When comparing the results obtained for the extracts and malvidin-3-O-glucoside in co-incubation experiments, it is clear that there are other phenolic compounds apart from this anthocyanin contributing to the cellular antioxidant activity of the extracts. In HaCaT, the fluorescence percentages of the maximum tested concentration of extract relative to the untreated control were 57% for GM (3.25 µM malvidin-3-O-glucoside), 56% for MW80 GM (6.59 µM malvidin-3-O-glucoside), 61% for MW Port (14.29 µM malvidin-3-O-glucoside), and 68% for MW Mt (6.19 µM malvidin-3-O-glucoside). The fluorescence percentages obtained for co-incubation of HaCaT with the standard malvidin-3-O-glucoside were 94% for 1 µM, 93% for 5 µM, 86% for 10 µM, and 83% for 15 µM. In HFF, the fluorescence percentages of the maximum tested concentration of extract relative to the untreated control were 43% for GM, 51% for MW80 GM, 52% for MW Port, and 65% for MW Mt. As for the tested concentrations of malvidin-3-O-glucoside, the fluorescence percentages were 87% for 1 µM, 87% for 5 µM, 78% for 10 µM, and 72% for 15 µM. In all cases, the efficacy of the extracts in inhibiting ROS production, when co-incubated with H_2O_2, is higher

than that of the standard malvidin-3-O-glucoside, strongly suggesting that there must be other phenolics in the extracts contributing to the ROS-inhibiting effect.

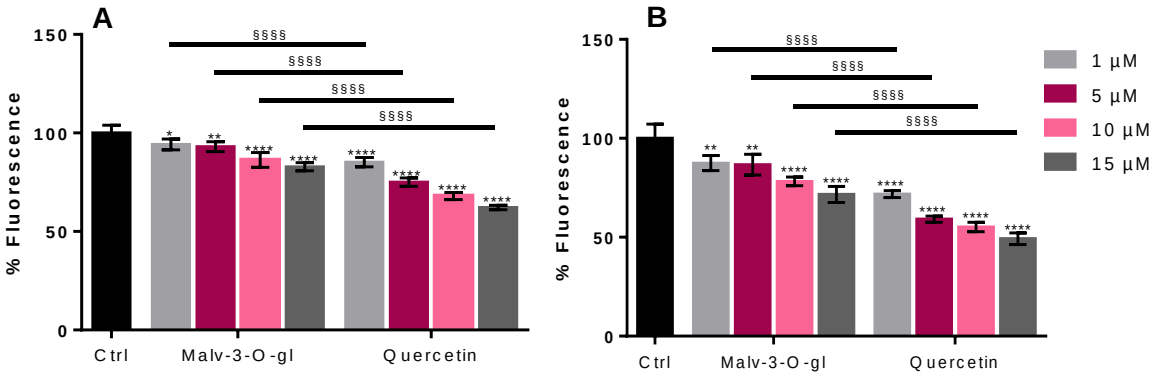

Figure 3.10. Co-incubation of (A) HaCaT and (B) HFF with two different standards (malvidin-3-O-glucoside and quercetin) and H_2O_2 for 1h – effect on total ROS generation. The symbol * indicates significance relative to the control (* p-value<0.05; ** p-value<0.01; **** p-value<0.0001); the symbol § indicates significance between the same concentration of the two standards (§§§§ p-value<0.0001). Results were obtained from at least two independent experiments.

Assessment of the protective effects of natural extracts or isolated compounds against H_2O_2-induced cytotoxicity is commonly performed. [167–169]

In this approach, cells were pre-incubated with the extracts for 24h hours, and then oxidative stress was induced with a H_2O_2. After 1h, MTS assay was performed and cell viability of the treated cells was compared to an untreated control where stress was also induced (Ctrl +). For this purpose, a concentration of stressor capable of inducing cytotoxicity was used, so that improvements in cell viability could be noticed. The concentrations of H_2O_2 chosen were 1 mM for HaCaT and 1.25 mM for HFF.

As can be seen in Figure 3.11., 1 mM H_2O_2 induced approximately 50% cytotoxicity in HaCaT, while 1.25 mM H_2O_2 caused a decrease of about 60% in HFF cell viability.

In HaCaT, at least the two highest concentrations of each extract caused a significant increase in cell viability relative to the positive control (Ctrl +), reaching even the levels of the negative control (Ctrl -), where no stress had been induced, in the case of MW Port at 1 mg extract/mL. When comparing the results obtained for 0.25 mg extract/mL of the four extracts, MW Mt performed significantly better, reaching a percentage of cell viability 1.7-fold higher than the positive control. Results obtained by the four extracts in this experiment, for 0.25 mg extract/mL, showed good correlation with those obtained for inhibition of H_2O_2-induced ROS generation (Figure 3.7. A) (R^2=0.9105), indicating that the compounds responsible for the reduced generation of ROS are probably the ones preventing ROS-induced cytotoxicity.

In HFF, hardly any improvements relative to the positive control were observed, as opposed to what happened with HaCaT. This could be explained by an excessive cytotoxicity caused by the

concentration of stressor used. If cell damage is too pronounced, the amount of phenolics applied might not be enough to counteract the deleterious effects of the induced oxidative stress. In addition, 0.25 mg extract/mL MW Mt seemed to potentiate H_2O_2-induced cell damage, which is difficult to explain. Phenolic compounds are renowned antioxidants; however, they can also show pro-oxidative effects in certain conditions. For instance, although phenolics can chelate transition metal ions, in some cases a redox reaction takes place instead, yielding reactive metal ions even more prone to participate in the Fenton chemistry, as well as phenolic intermediates (phenoxyl radicals) with pro-oxidant properties. Moreover, it is possible that a complexed metal ion retains its catalytic activity. [166,177,178] Considering these facts, we may hypothesize that the amount of H_2O_2-induced ROS led to an exhaustion of the antioxidant capacity of the phenolics present in the extract, triggering pro-oxidant effects that might have caused a further decrease in cell viability. Nevertheless, further studies must be carried out, with a lower concentration of H_2O_2, in order to better understand the protective effects of the extracts in HFF.

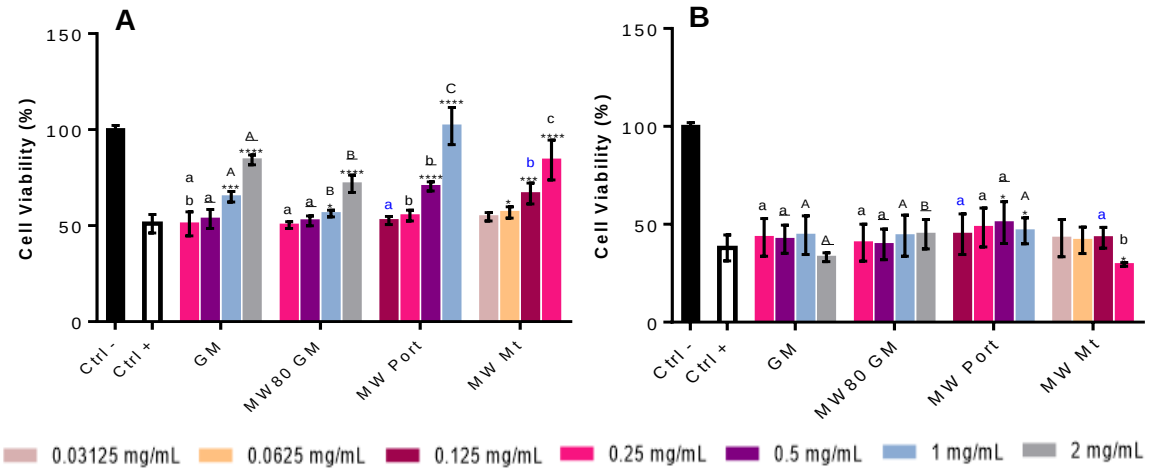

Figure 3.11. Pre-incubation of (A) HaCaT and (B) HFF with the extracts for 24h: influence on cell viability upon H_2O_2-induced stress. The symbol * indicates significance relative to the control where stress was induced, *i.e.* Ctrl + (*p-value<0.05, *** p-value<0.001, **** p-value<0.0001). The same concentrations of different extracts were compared (blue lowercase letters for 0.125 mg/mL; black lowercase letters for 0.25 mg/mL; underlined lowercase letters for 0.5 mg/mL; uppercase letters for 1 mg/mL; underlined uppercase letters for 2 mg/mL); statistically different results (p-value<0.5) are identified with different letters. Results were obtained from two independent experiments.

Regarding the two tested standards, protective effects against H_2O_2-induced cytotoxicity were not very pronounced in either cell line (Figure 3.12.). These findings suggest that the antioxidant effects of quercetin and malvidin-3-O-glucoside after 24h incubation are not enough to combat the cell injury caused by the concentration of H_2O_2 used. Hence, there must be other phenolics exerting the protective effect observed in the extracts, other than quercetin and malvidin-3-O-glucoside.

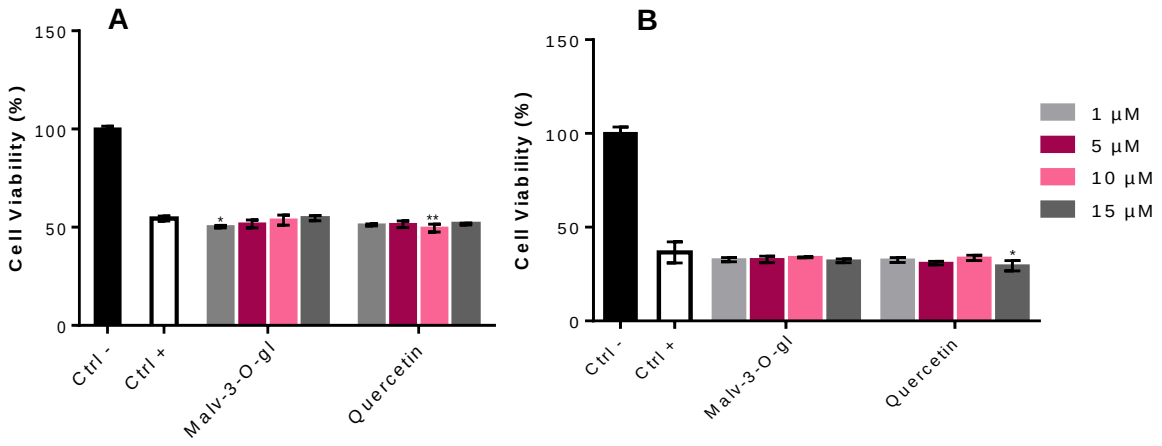

Figure 3.12. Pre-incubation of (A) HaCaT and (B) HFF with two standards for 24h: influence on cell viability upon H_2O_2-induced stress. The symbol * indicates significance relative to the control where stress was induced (* p-value<0.05, ** p-value<0.01). Preliminary results obtained from one experiment only.

3.2.3.3. Inhibition of Intrinsic ROS Production

Cells were pre-incubated with the extracts for 1 and 24h, and their capacity to inhibit intrinsic ROS production was evaluated. Results are represented in Figure 3.13.. Changes relative to the untreated control seem more relevant for an incubation period of 1h, especially in the case of HaCaT, suggesting that the immediate antioxidant effect of the extracts on intrinsic ROS may be more relevant than long-term antioxidant effects. The opposite was observed for inhibition of H_2O_2-induced ROS formation (Figure 3.7.). These findings could be explained by the fact that inhibition of intrinsic formation of ROS is probably carried out by phenolic compounds that are capable of permeating the cell membrane, in order to act in the intracellular compartment, whereas extrinsic ROS (induced by the stressor) also arise extracellularly, in which case a longer incubation would improve the antioxidant effect due to binding of antioxidant compounds to cell membranes. Results also suggest that some metabolism or exhaustion of phenolics entering the cell may take place, rendering them less active. This would explain the apparently lower capacity of the extracts to inhibit intrinsic ROS generation in the 24h incubation period.

Correlation of the effect of 0.25 mg/mL (concentration common to all extracts) of each extract with TPC was higher than with TAC for both cell lines and incubation times (R^2 values not shown), which is supported by the fact that anthocyanins have low bioavailability and are less likely to permeate cell membranes, and inhibit ROS production at an intrinsic level, than other phenolics.

Differences between the same concentrations of different extracts are not significant in most cases, possibly because of the diverse composition of the samples, leading to distinct antioxidant activities towards different ROS, as mentioned above, or because the amount of phenolic compounds with the ability to permeate cell membranes may vary depending on the extract. Nevertheless, the highest concentration of MW Mt (0.25 mg extract/mL) showed better results than the corresponding concentration of the other three tested extracts, resulting in fluorescence percentages ≤79%, as opposed to fluorescence percentages ≥94% observed for other

samples. This is probably because of the higher amount of compounds that are able to permeate cell membranes, for instance phenolic acids [179], present in MW Mt.

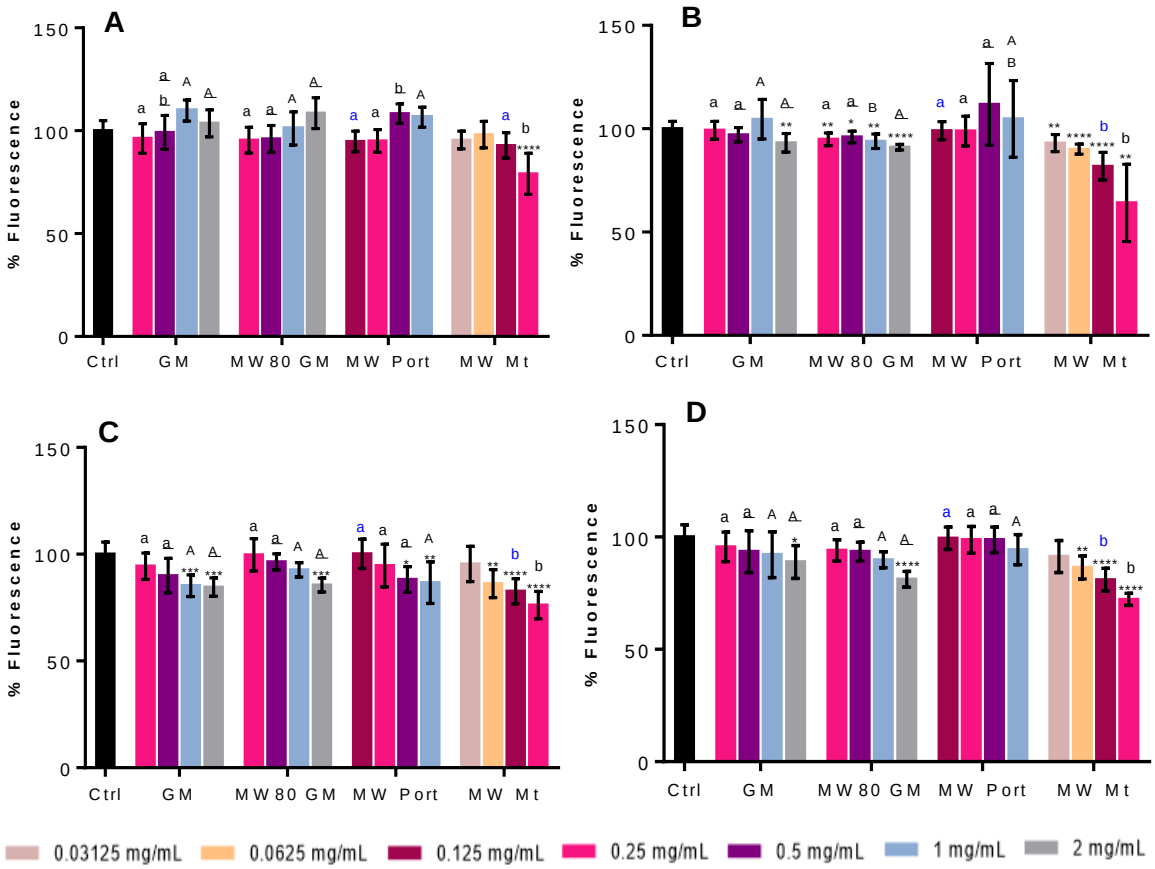

Figure 3.13. Pre-incubation of cells with the extracts for 24h and 1h – effect on intrinsic ROS generation. (A) 24h in HaCaT; (B) 24h in HFF; (C) 1h in HaCaT; (D) 1h in HFF. The symbol * indicates significance relative to the control (* p-value<0.05, ** p-value<0.01, *** p-value<0.001, **** p-value<0.0001). The same concentrations of different extracts were compared (blue lowercase letters for 0.125 mg/mL; black lowercase letters for 0.25 mg/mL; underlined lowercase letters for 0.5 mg/mL; uppercase letters for 1 mg/mL; underlined uppercase letters for 2 mg/mL); statistically different results (p-value<0.5) are identified with different letters. Results were obtained from at least two independent experiments.

The capacity of malvidin-3-O-glucoside and quercetin to reduce intrinsic ROS production was assessed, after 24h of incubation (Figure 3.14.). In HaCat, quercetin was more effective than malvidin-3-O-glucoside in inhibiting generation of intracellular ROS. Although both compounds are poorly bioavailable [176], this observation suggests that the quercetin may be more likely to permeate cell membranes than malvidin-3-O-glucoside. This makes sense because malvidin-3-O-glucoside is a positively charged compound, with a higher molecular weight and an increased polarity when compared to quercetin. Moreover, malvidin-3-O-glucoside increases intrinsic ROS levels instead of decreasing them. This observation could be explained if the concentrations of malvidin-3-O-glucoside, although determined as non-cytotoxic, were inducing some stress in the cells. This hypothesis should be evaluated in further studies.

Conversely, in HFF, only the highest concentration of the standards showed a significant decrease in intrinsic ROS production, with a fluorescence percentage of 78% relative to the untreated control for malvidin-3-O-glucoside, and 92% for quercetin. Furthermore, malvidin-3-O-glucoside appears more effective than the corresponding concentration of quercetin, although this difference is not statistically significant. However, this result comprises a large standard deviation, hence there is some uncertainty to it, and further experiments must be done in order to clarify this observation.

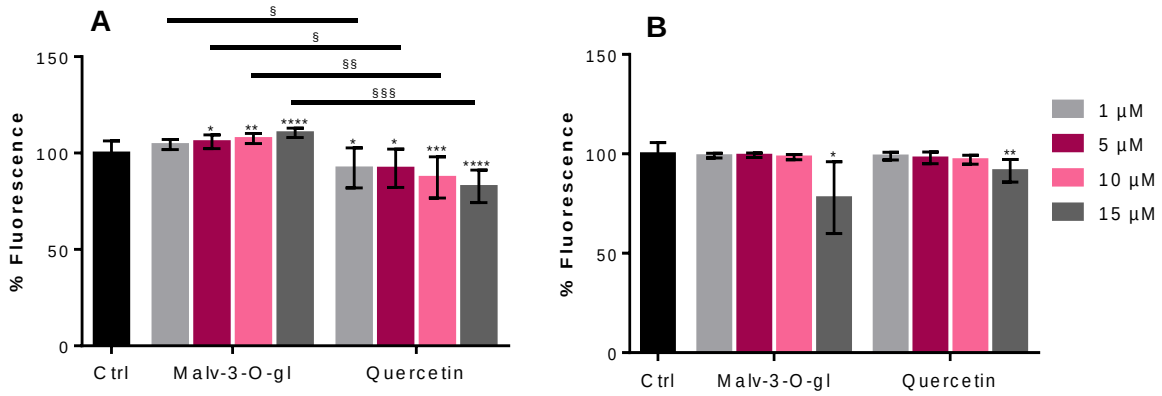

Figure 3.14. Pre-incubation of (A) HaCaT and (B) HFF with two different standards for 24h: effect on intrinsic ROS production. The symbol * indicates significance relative to the control (*p-value<0.05, ** p-value<0.01, *** p-value<0.001, **** p-value<0.0001); the symbol § indicates significance between the same concentration of different extracts (§ p-value<0.05, §§ p-value<0.01, §§§ p-value<0.001). Results were obtained from at least two independent experiments.

All results obtained in cell-based assays for 0.25 mg extract/mL (concentration common to all extracts) are summarized in Table 3.10.. Overall, results show that the extract obtained from red table wine lees following MW pretreatment of the raw material, MW Mt, is the most effective in inhibiting ROS generation at cellular level, both in the presence and in the absence of an oxidative stress inducer. Differences in the bioactivity of different extracts are observed, and may be justified by their distinct phenolic composition, both in qualitative and quantitative terms. Moreover, it can be concluded that flavonoids present in the extracts, namely malvidin-3-O-glucoside and quercetin, may play relevant roles in antioxidant protection of cells, particularly in what concerns to extracellular ROS.

Table 3.10. Summary of the results obtained for the selected extracts in cell-based assays, in terms of prevention of H_2O_2-induced ROS and intrinsic ROS generation, and protection against H_2O_2-induced cytotoxicity. For each assay, the extracts (at a concentration of 0.25 mg extract/mL) were rated by comparison with the untreated control. For prevention of ROS generation (fluorescence percentages relative to the untreated control): +++++ for <70%; ++++ for 70–75%; +++ for 75–80%; ++ for 80–85%; + for 85–90%; - for 90–95%; - - for 95–100%. For protection against H_2O_2-induced cytotoxicity (cell viability percentage): + for <50%; ++ for 50–60%; +++ for 60–70%; ++++ for 70–80%; +++++ for 80–90%. Results for HaCaT are represented in green, whereas results for HFF are represented in red.

		H_2O_2-induced ROS			Intrinsic ROS		Protection against H_2O_2-induced cytotoxicity
		Pre-incubation		Co-incubation	Pre-incubation		Pre-incubation
	Extract	1h	24h	1h	1h	24h	24h
Wine Lees	MW Mt	++ +++++	+++ +++++	+++++ +++++	+++ ++++	+++ +++++	+++++ +
	MW Port	- - -	- ++	++++ +++++	- - -	- - - -	++ +
Grape Marc	GM	- - -	- - -	+++ +++++	- - -	- - - -	++ +
	MW80 GM	- - -	- ++	+++ ++++	- - -	- - -	++ +

3.3. Impact of Formulation Process on the Stability and Antioxidant Activity of Conventional Grape Marc Extract

Phenolics are very attractive compounds for use in cosmetic products, not only because of their antioxidant capacity, but also because of their modulation effects on several biological endpoints. Unfortunately, phenolic compounds are unstable and susceptible to degradation by several parameters, such as pH, temperature, light and oxygen, among others. [180,181] In particular, anthocyanins are amongst the most vulnerable phenolics, as they require acidic pH conditions, are thermosensitive, and may interact with other compounds, such as the non-phenolic ascorbic acid or sugars, suffering degradation. [182–185] In addition, anthocyanins are likely to undergo self-association in solution in order to enhance stability; however, this phenomenon causes alterations in the color and composition of the solution. [186]

On the other hand, the poor bioavailability of phenolics, especially flavonoids, hampers their delivery to skin layers deeper than the *stratum corneum* [176,187], compromising the potential beneficial effects because the bioactive compounds may not reach their site of action. Moreover, the presence of hydrophilic substances other than phenolics may improve solubility, yet it can decrease skin permeation. [188]

To overcome these limitations, phenolic compounds are often incorporated into different formulations, with the main goals of increasing shelf-life, by protecting phenolics against adverse

environmental factors (oxygen, light, moisture, etc.), and bioavailability, by creating vehicles for administration.

Conventional grape marc extract (GM) was formulated by spray drying with three different carriers: maltodextrin (MD), whey protein isolate (WPI) and pea protein isolate (PPI), by the same process as described in the literature. [97] The three formulations were provided by the High Pressure Processes Group from the Department of Chemical Engineering and Environmental Technology, University of Valladolid, under the scope of the project "WineSense". In the present work, formulations were characterized in terms of phenolic and anthocyanin content, as well as chemical and cellular antioxidant activities.

Maltodextrin (MD) results from hydrolysis of corn starch to different degrees, and therefore is supplied with different dextrose equivalent (DE) values. DE reflects the level of hydrolysis, as it is a measure of the reducing capacity of a sugar product, expressed as a percentage of dextrose reducing capacity equivalents. MD is more commonly used in food products; however, because of its solubility and ability to bind several compounds, it is considered a good encapsulating agent that can also be used to stabilize cosmetic formulations. Proteins, such as WPI and PPI, have several characteristics and properties making them good candidates for usage as encapsulating agents with the ability to protect and stabilize core products. For instance, proteins contain a variety of functional groups in their structure allowing for interaction with numerous compounds and substances. At the same time, proteins possess amphiphilic properties that confer them emulsification and film-forming capacities. [189]

Grape marc conventional extract (GM) was formulated with the carriers by spray drying, as described elsewhere. [97,190]

3.3.1. Phytochemical Evaluation

TPC and TAC contained within formulation particles were evaluated, in order to determine the recovery rates of the formulation process. For this purpose, release of the extracts from the carrier had to be performed, which was achieved by dissolving each powder in a mixture of 50% (V/V) ethanol:water acidified to pH 1 with sulfuric acid. This procedure had already been optimized to disassemble the particles and release the extract to its full extent. [97]

TPC of the pure extract was found to be higher than TPC of the three formulations (Figure 3.15. A). This result is the reflection of an expected "concentration effect" of the formulations. This happens because the amount of carrier present in the formulations contributes to the mass of the dry product (extract:carrier ratio of 1:1), thus, in the absence of carrier (pure extract), the amount of phenolic compounds per gram of dry product is logically higher. TPC percentages of formulations relative to pure extracts TPC were 29% for GM:MD, 27% for GM:WPI and 36% for GM:PPI. Apart from the contribution of the carrier to the dry mass of the product, the lower TPC values of the formulations could be explained by the loss of a fraction of the extract during the formulation process, possibly due to the temperatures used in the process, as phenolic compounds are

susceptible to thermal degradation. This effect has already been observed by other authors. [191] In addition, these losses throughout the formulation process may alter the extract:carrier ratio.

Results obtained for TAC (Figure 3.15. B) are quite different from those obtained for TPC, as only GM:MD evidenced a modest, although significant, decrease in TAC when compared to GM (2.80 *vs.* 3.54 µmol malv-3-O-gl/g DB). This suggests that, despite the loss of anthocyanins during spray drying, the formulations may have protected the extract against degradation until the moment of the assay. As mentioned above, anthocyanins are more vulnerable to degradation by environmental factors than other phenolics in general, which would explain the lower than expected TAC value of the pure extract when compared to the formulated extract, because at the time of TAC determination, a significant fraction of GM anthocyanins might have already suffered degradation.

Grape marc extract formulated with MD provided a significantly higher TPC than with WPI (142 *vs.* 134 µmol GAE/g DB), whereas formulation with PPI had the highest TPC value (176 µmol GAE/g DB). Concerning TAC, formulations with PPI and WPI provided the highest values (3.71 and 3.39 µmol malv-3-O-gl/g DB, respectively), followed by MD (2.80 µmol malv-3-O-gl/g DB). These results are consistent with those found in the research work where the present formulation process was optimized. [97] The only discrepancy was that, in the present work, WPI formulation led to a higher TAC than MD formulation, possibly due to fluctuations in the process.

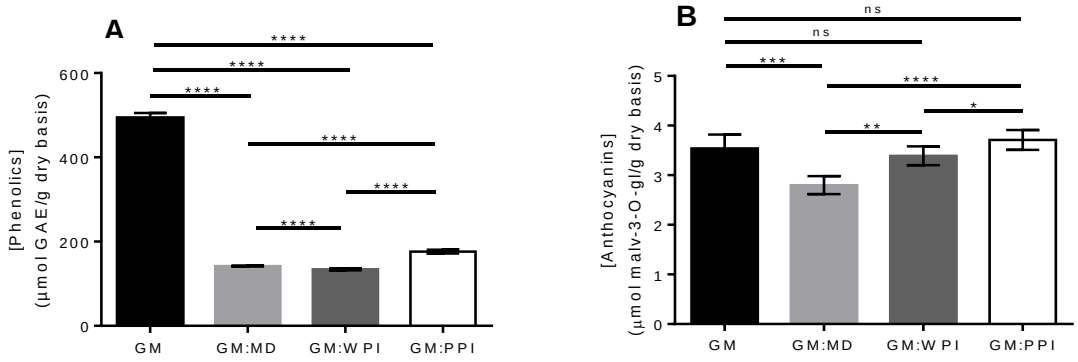

Figure 3.15. Total phenolic content (A) and total anthocyanin content (B) of the three formulations compared to that of the original extract (** p-value<0.01, **** p-value<0.0001, ns – non-significant). Results were obtained from at least three independent experiments.

3.3.2. Antioxidant Activity

Antioxidant capacity of the three formulations was determined by ORAC, HOSC and HORAC. Results for antioxidant capacity of the samples in the three assays were first presented as a function of the mass of the final formulation product (Figure 3.16. A). Because the mass of the product includes not only the encapsulated extract, but also the carrier ("concentration effect", mentioned in section 3.3.1.), it would be expected that the non-formulated extract would present a considerably higher antioxidant activity than the formulations when results were expressed per gram of dry product, as previously described for ORAC results in particles obtained by the same process. [97] Yet, results showed otherwise. The pure extract (GM) presented an HOSC value of

746 µmol TE/g DB, which was significantly different from that of GM:WPI (595 µmol TE/g DB) and GM:PPI (649 µmol TE/g DB), but not significantly different from that of GM:MD (826 µmol TE/g DB). The HORAC value of GM (305 µmol CAE/g DB) was higher than that of GM:PPI (233 µmol CAE/g DB), but statistically equal to the values obtained by GM:MD (277 µmol CAE/g DB) and GM:WPI (317 µmol CAE/g DB). The ORAC value of GM (481 µmol TE/g DB) was lower than those obtained for any of the formulations (≥ 682 µmol TE/g DB). These observations can be partially explained if we consider that the carriers used for formulation may present antioxidant properties, possibly interfering with the results. Indeed, it has been reported that whey protein preparations present reducing power, radical scavenging, and metal ion chelation abilities [192,193], and that pea protein isolate and hydrolysates also possess reducing power as well as radical scavenging abilities. [194,195] On the other hand, maltodextrins are carbohydrates presenting variable reducing capacity. In fact, maltodextrins are classified according to their dextrose equivalent (DE) reducing capacity. [196] Thus, it is possible that the presence of MD, WPI or PPI in the formulation may interfere with the results obtained in the antioxidant assays. In future work, the antioxidant capacity of the carriers used for formulation should be assessed, aiming at determining their contribution to the antioxidant values of samples.

However, although it is possible that the carriers might have interfered in the determination of antioxidant capacity of the formulations, this cannot fully explain the results. Thus, results were normalized and expressed as antioxidant values per micromoles of GAE (Figure 3.16. B), supposedly eliminating or at least attenuating the “concentration effect” caused by the carriers. After this normalization, it is clear that all the three formulations, presenting ORAC values ranging from 4.4 to 5.5 µmol TE/µmol GAE, HOSC values of 3.7–5.8 µmol TE/µmol GAE, and HORAC values between 1.3 and 2.4 µmol CAE/µmol GAE, had improved antioxidant capacities when compared to the non-formulated extract (1 µmol TE/µmol GAE in ORAC, 1.5 µmol TE/µmol GAE in HOSC, and 0.6 µmol CAE/µmol GAE in HORAC). This suggests that formulation increased the stability of the extract, by preserving antioxidant properties of the extract constituents, perhaps even potentiating the inherent antioxidant capacity of the extract. A similar effect of enhanced antioxidant activity was found when formulating epigallocatechin gallate (a flavanol/catechin derivative) [197], quercetin [198] or anthocyanins [199] with different carriers.

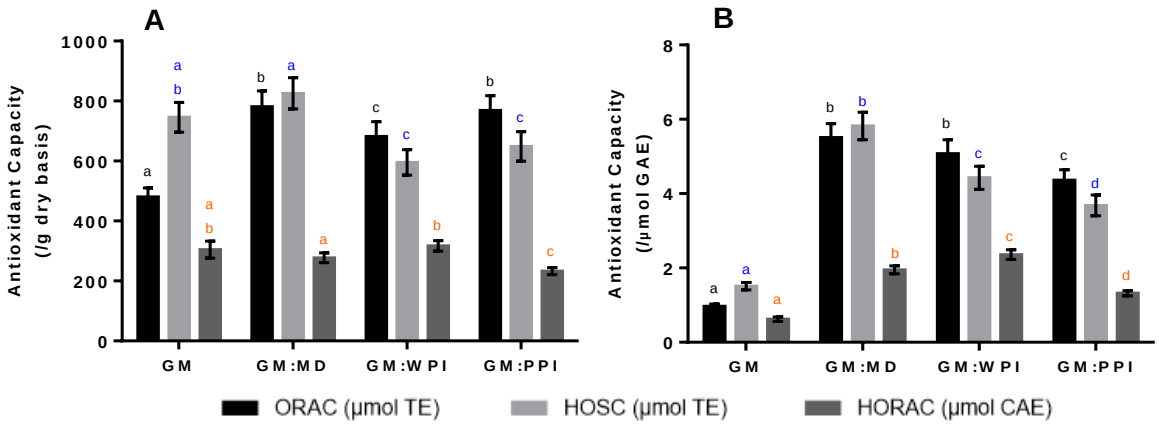

Figure 3.16. Antioxidant capacity of grape marc extract and respective formulations obtained in three different antioxidant activity assays, expressed per (A) gram of dry product and (B) per micromoles of GAE. Results identified with coincident letters, in each assay, are not significantly different; as opposed to results with different letters, which are significantly different with p-value<0.05 (ORAC – black, HOSC – blue, HORAC – orange). Results were obtained from at least three independent experiments.

3.3.3. Cytotoxicity Evaluation

Particle cytotoxicity depends on many parameters, such as size and composition, cell type, incubation time, etc. Nevertheless, a concentration higher than 1 mg/mL of particles is rarely used for cytotoxicity evaluations despite the cell line [97,200–203], thus cytotoxicity of the three formulations was assessed, in both HaCaT and HFF, in a concentration range between 0.01 and 1 mg formulation/mL (Figures 3.17. and 3.18.).

None of the tested concentrations caused a decrease in cell viability of either cell line. On the contrary, and similar to what was seen for the extracts (section 3.2.3.1.), the three formulations tended to enhance cell viability with increasing concentrations, in both cell lines. This effect has been observed for several types of particles in the same fibroblasts used in this work and in Caco-2 cell line. [203,204] An enhanced cell viability could be a result of several things: (1) the formulations have protective effects on the cells promoting cell survival/proliferation, (2) presence of remaining microorganisms in the particles due to ineffective sterilization, which may interfere with the MTS method, (3) interference of undissolved particles in absorbance readings, leading to an overestimation of cell viability, or (4) the formulations are inducing production of intracellular ROS, which are known to promote cell proliferation. In fact, one of the toxicity mechanisms of particulate systems is the induction of ROS production through several mechanisms, to an extent depending on inherent characteristics of the particles and cells. [205] Moreover, high amounts of ROS inflict damage to biomolecules, whereas moderate levels of ROS can cause alterations in cell functioning through activation and modulation of intracellular signaling, including MAPK pathway, leading to activation of transcription factors, such as AP-1 and NF-κB, which in turn are involved in the transcription of cell growth regulation genes. [206,207] Anyhow, in order to clarify these results and discard events (2) and (3), further studies must be performed to confirm sterility of the particles, and the possibility of interference in absorbance readings should be assessed.

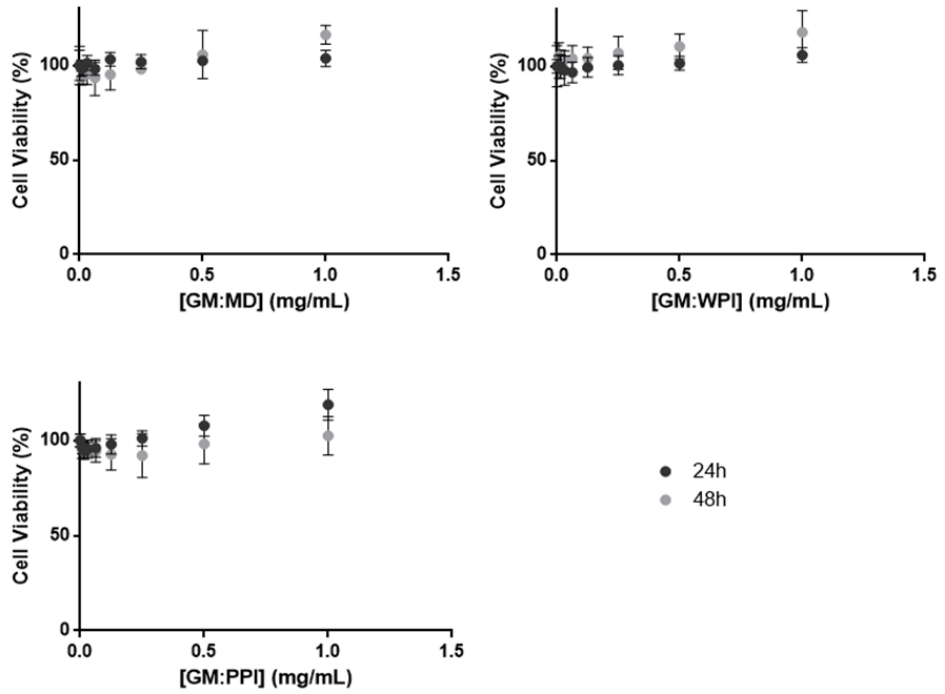

Figure 3.17. Cytotoxicity screening of the three formulations of grape marc extract (24 and 48 hours of incubation) in HaCaT. Results were obtained from at least three independent experiments. Results were obtained from at least two independent experiments.

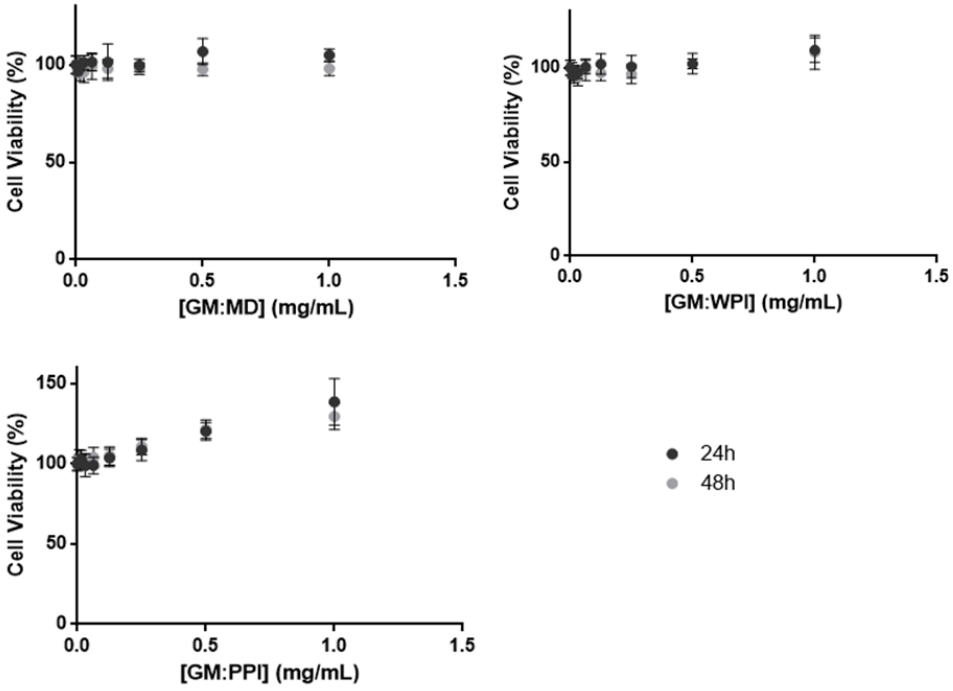

Figure 3.18. Cytotoxicity screening of the three formulations of grape marc extract (24 and 48 hours of incubation) in HFF. Results were obtained from at least two independent experiments. Results were obtained from at least three independent experiments. Results were obtained from at least two independent experiments.

3.3.4. Assessment of cytotoxicity through ROS production

To better understand the influence of the formulations on cell redox status, the effect of the samples on intrinsic ROS generation was evaluated. For comparison purposes between the formulations and the non-formulated extract, concentration of samples (GM and respective formulations) was normalized to mM GAE, and all the samples were tested at the same concentration for different incubation periods. The chosen concentration was 134 µM GAE, because it corresponds to the amount of GAE present in 1 mg formulation/mL (maximum concentration tested in cytotoxicity evaluation) of GM:WPI, the formulation presenting the lowest TPC value (section 3.3.1.).

Results for influence of the samples on intrinsic ROS generation are represented in Figure 3.19., in which the non-formulated extract revealed a slight tendency to decrease ROS generation with an increasing incubation time (92% fluorescence relative to the untreated control in HaCaT and 97% in HFF, for 24h incubation). This effect is not very pronounced given the low GM concentration tested (272 µg extract/mL, 0.134 µmol GAE/mL). Conversely, formulations, mainly GM:WPI and GM:PPI, significantly increased intrinsic ROS production, especially for the highest incubation period (24h), with fluorescence percentages of 120–156% relative to the untreated control in HaCaT and 108–134% in HFF, as opposed to 92% and 97% of GM, respectively. These results agree with those found in cytotoxicity evaluation of the formulations (section 3.3.3.), where all three samples promoted cell proliferation, especially GM:WPI and GM:PPI, possibly through induction of ROS. The effects of formulations on H_2O_2-induced ROS as well as H_2O_2-induced cytotoxicity, were also evaluated and are represented in Appendix B. Results are in agreement with those obtained for intrinsic ROS, further reaffirming the fact that formulations might be inducing cell proliferation through induction of ROS production.

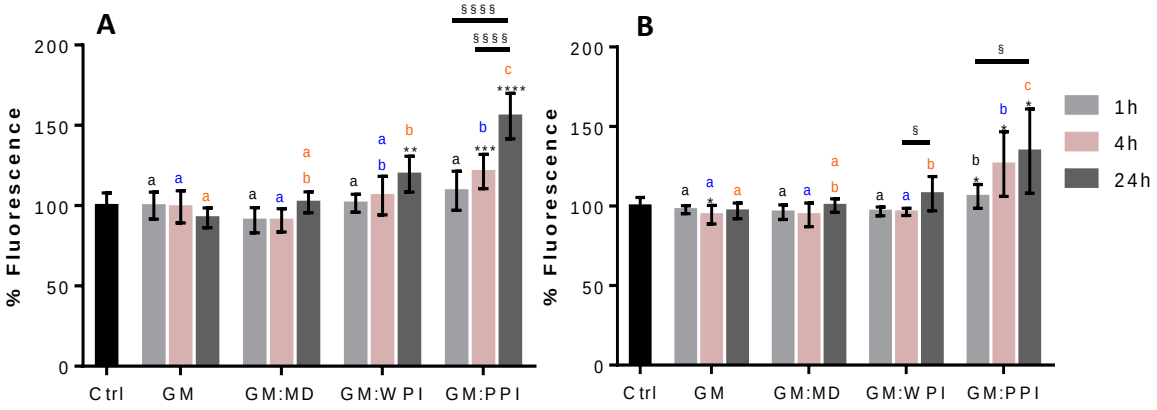

Figure 3.19. Pre-incubation (1h, 4h and 24h) of (A) HaCaT and (B) HFF with grape marc extract (GM) and its formulations with three different carriers – influence on intrinsic ROS production. The symbol * indicates significance relative to the control (* p-value<0.05, ** p-value<0.01, *** p-value<0.001, **** p-value<0.0001); the symbol § indicates significance between different incubation times of the same sample (§ p-value<0.05, §§§§ p-value<0.0001). The same incubation times of different samples were compared (1h – black, 4h – blue, 24h – orange); statistically different results (p-value<0.5) are identified with different letters. Results were obtained from two independent experiments.

Overall, it can be concluded that formulation of conventional grape marc extract with MD, WPI and PPI protects the capacity of the extract to scavenge peroxyl and hydroxyl radicals as well as its ability to chelate transition metal ions, as observed in ORAC, HOSC and HORAC results. Moreover, it is possible that the carriers themselves might reveal some antioxidant activity, potentiating the global antioxidant effect of formulations.

Furthermore, it was seen that formulations caused an increase in cell viability as measured by the MTS method, possibly through induction of ROS production, which in turn might activate transcription pathways leading to cell proliferation. Therefore, further studies must be carried out to better understand the effect of the tested formulations on keratinocytes and fibroblasts.

4. Conclusions

Wine industry generates large amounts of wastes, and the postulate that the several waste streams can still be valuable sources of bioactive compounds, particularly phenolics, led to the development of this project. In this work, extracts obtained from three winemaking waste stream matrices were assessed for bioactivity in targets relevant for application in cosmetics.

All extracts were found to be rich in phenolic compounds, including anthocyanins. Effects of MW pretreatment on wine lees matrices were more pronounced than on grape marc, generally yielding extracts with higher phenolic and anthocyanin content. Matarromera red table wine lees extracts presented the highest phenolic and anthocyanin contents, leading to distinguishably better results than all the other tested extracts in chemical, enzymatic and cellular assays. More specifically, Matarromera red table wine lees extracts obtained from the MW-pretreated matrix revealed the best results in terms of antioxidant activity as measured by three complementary assays (ORAC, HOSC, HORAC); tyrosinase, elastase and MMP-1 inhibitory capacity; and protection of human skin cells (keratinocytes and fibroblasts) against oxidative stress. Globally, MW pretreatment of raw materials appears to contribute to the efficiency of extraction processes, particularly in the case of wine lees matrices, enhancing phenolic and anthocyanin extraction.

Interestingly, although anthocyanins played an important part in the antioxidant capacity of the extracts in both chemical and cell-based assays, this subclass of flavonoids did not seem that much relevant in the inhibition of enzymes related to skin ageing (tyrosinase, elastase and MMP-1). In fact, flavonol aglycones seemed more important than anthocyanins (glycosylated anthocyanidins) in the inhibitory capacity of the extracts towards the mentioned enzymes, probably because of the steric hindrance presented by the latter, which hinders the interaction phenolic-enzyme.

The main conclusion of this thesis is that winemaking waste stream matrices, in particular wine lees, are indeed valuable sources of natural bioactive compounds with potential for application in cosmetic products with skin whitening and anti-ageing effects.

Formulation by spray drying technique with different carriers protected grape marc conventional extract against degradation, preserving and perhaps potentiating its antioxidant activity in chemical assays. However, effects of the formulations in skin cells in terms of cytotoxicity and ROS production must be further explored in order to clarify if the formulations are actually safe. Clear evidence that the formulations enhanced bioavailability of the extract was not found. Nevertheless, it should be stressed that appropriate formulation of natural extracts is an important approach to help maintaining stability and increase shelf life.

In future work, it would be interesting to assess the antioxidant capacity of the extracts towards singlet oxygen, which is an important ROS participating in biological damage involved in extrinsic skin ageing. Also, inhibitory effect of the extracts on other ECM proteases, such as MMP-3 (stromelysin), MMP-9 (gelatinase) and hyaluronidase, should be explored. In addition, the effects of individual phenolic compounds and combinations of compounds on biological targets could be

evaluated in order to identify synergistic or antagonistic interactions between compounds influencing the outcomes of the assays. Regarding cell-based assays, further studies of cellular antioxidant capacity of the extracts through impact on glutathione homeostasis, carbonyl protein formation, and impact on detoxifying enzymes (SOD, CAT, GPx) would be of interest. Furthermore, evaluation of the impact of the extracts on cellular levels of melanin, elastin, hyaluronan, collagen and ECM proteases should be performed. In addition, extracts could be screened for antimicrobial activity against the most relevant microorganisms enrolled in the contamination of cosmetic products, for possible application as alternative preservatives.

Finally, application of the tested extracts in cosmetic products requires further formulation. Besides, the final cosmetic product must undergo several tests in order to assure safety and efficacy.

5. References

[1] D.J. Gawkrodger, Dermatology - An Illustrated Colour Text, 2002.
[2] L. Celleno, F. Tamburi, Nutritional Cosmetics, 2009.
[3] W. Montagna, P.F. Parakkal, The structure and Function of Skin, Third edit, Academic Press, 1974.
[4] K. Vávrová, D. Henkes, K. Strüver, M. Sochorová, B. Skolová, M.Y. Witting, W. Friess, S. Schreml, R.J. Meier, M. Schäfer-Korting, J.W. Fluhr, S. Küchler, Filaggrin deficiency leads to impaired lipid profile and altered acidification pathways in a 3D skin construct., J. Invest. Dermatol. 134 (2014) 746–53.
[5] N.G. Markova, L.N. Marekov, C.C. Chipev, S.Q. Gan, W.W. Idler, P.M. Steinert, Profilaggrin is a major epidermal calcium-binding protein., Mol. Cell. Biol. 13 (1993) 613–25.
[6] X. Xiong, T. Wu, S. He, Physical forces make rete ridges in oral mucosa, Med. Hypotheses. 81 (2013) 883–886.
[7] P. Fratzl, Collagen: Structure and mechanics, an introduction, in: Collagen Struct. Mech., 2008: pp. 1–13.
[8] N. Dayan, SKIN AGING HANDBOOK: An Integrated Approach to Biochemistry and Product Development, William Andrew, Norwich, NY, USA, 2008.
[9] D.J.S. Hulmes, Building Collagen Molecules, Fibrils, and Suprafibrillar Structures, J. Struct. Biol. 137 (2002) 2–10.
[10] S.M. Mithieux, A.S. Weiss, Elastin, Adv. Protein Chem. 70 (2005) 437–461.
[11] G. Cotta-Pereira, F. Guerra Rodrigo, S. Bittencourt-Sampaio, Oxytalan, elaunin, and elastic fibers in the human skin, J. Invest. Dermatol. 66 (1976) 143–148.
[12] J.D. Esko, K. Kimata, U. Lindahl, Proteoglycans and Sulfated Glycosaminoglycans, in: Essentials Glycobiol., 2009: pp. 229–248.
[13] J.R. Fraser, T.C. Laurent, U.B. Laurent, Hyaluronan: its nature, distribution, functions and turnover., J. Intern. Med. 242 (1997) 27–33.
[14] D.H. Lee, J.H. Oh, J.H. Chung, Glycosaminoglycan and proteoglycan in skin aging, J. Dermatol. Sci. 83 (2016) 174–181.
[15] H. Hashizume, Skin aging and dry skin., J. Dermatol. 31 (2004) 603–609.
[16] B. Poljšak, R.G. Dahmane, A. Godić, Intrinsic skin aging: The role of oxidative stress, Acta Dermatovenerologica Alpina, Pannonica Adriat. 21 (2012) 33–36.
[17] A. Kammeyer, R.M. Luiten, Oxidation events and skin aging, Ageing Res. Rev. 21 (2015) 16–29.
[18] E. Birben, U.M. Sahiner, C. Sackesen, S. Erzurum, O. Kalayci, Oxidative stress and antioxidant defense., World Allergy Organ. J. 5 (2012) 9–19.
[19] M. Yaar, B.A. Gilchrest, Photoageing: Mechanism, prevention and therapy, Br. J. Dermatol. 157 (2007) 874–887.
[20] W. Ma, M. Wlaschek, I. Tantcheva-Poór, L.A. Schneider, L. Naderi, Z. Razi-Wolf, J. Schüller, K. Scharffetter-Kochanek, Chronological ageing and photoageing of the fibroblasts and the dermal connective tissue, Clin. Exp. Dermatol. 26 (2001) 592–599.
[21] G.J. Fisher, S. Kang, J. Varani, Z. Bata-Csorgo, Y. Wan, S. Datta, J.J. Voorhees, Mechanisms of photoaging and chronological skin aging., Arch. Dermatol. 138 (2002) 1462–70.
[22] J.F. Curtin, M. Donovan, T.G. Cotter, Regulation and measurement of oxidative stress in apoptosis, J. Immunol. Methods. 265 (2002) 49–72.
[23] M. Sárdy, Role of matrix metalloproteinases in skin ageing., Connect. Tissue Res. 50 (2009) 132–138.
[24] H.J. Ra, W.C. Parks, Control of matrix metalloproteinase catalytic activity, Matrix Biol. 26 (2007) 587–596.
[25] H. Nagase, R. Visse, G. Murphy, Structure and function of matrix metalloproteinases and TIMPs, Cardiovasc. Res. 69 (2006) 562–573.
[26] J. Wittenauer, S. MäcKle, D. Suβmann, U. Schweiggert-Weisz, R. Carle, Inhibitory effects of polyphenols from grape pomace extract on collagenase and elastase activity, Fitoterapia. 101 (2015) 179–187.

[27] M. Szendroi, G. Meimon, H. Bakala, C. Frances, L. Robert, G. Godeau, W. Hornebeck, On the presence of a metalloprotease in human skin fibroblasts that degrades the human skin elastic fiber system., J. Invest. Dermatol. 83 (1984) 224–229.
[28] N.F. Brás, R. Gonçalves, N. Mateus, P.A. Fernandes, M.J. Ramos, V. De Freitas, Inhibition of pancreatic elastase by polyphenolic compounds, J. Agric. Food Chem. 58 (2010) 10668–10676.
[29] U.K. Saarialho-Kere, E. Kerkelä, L. Jeskanen, T. Hasan, R. Pierce, B. Starcher, R. Raudasoja, A. Ranki, A. Oikarinen, M. Vaalamo, Accumulation of matrilysin (MMP-7) and macrophage metalloelastase (MMP- 12) in actinic damage, J. Invest. Dermatol. 113 (1999) 664–672.
[30] E.B. de Oliveira, M.C.O. Salgado, Pancreatic Elastases, in: Handb. Proteolytic Enzym., 2013: pp. 2639–2645.
[31] B. Korkmaz, M. Horwitz, D. Jenne, F. Gauthier, Neutrophil elastase, proteinase 3, and cathepsin G as therapeutic targets in human diseases, Pharmacol. Rev. 62 (2010) 726–759.
[32] N. Tsuji, S. Moriwaki, Y. Suzuki, Y. Takema, G. Imokawa, The role of elastases secreted by fibroblasts in wrinkle formation: implication through selective inhibition of elastase activity., Photochem. Photobiol. 74 (2001) 283–90.
[33] H. Takeuchi, T. Gomi, M. Shishido, H. Watanabe, N. Suenobu, Neutrophil elastase contributes to extracellular matrix damage induced by chronic low-dose UV irradiation in a hairless mouse photoaging model, J. Dermatol. Sci. 60 (2010) 151–158.
[34] Y. Okada, S. Watanabe, I. Nakanishi, J. Kishi, T. Hayakawa, W. Watorek, J. Travis, H. Nagase, Inactivation of tissue inhibitor of metalloproteinases by neutrophil elastase and other serine proteinases., FEBS Lett. 229 (1988) 157–60.
[35] Z. Chen, Y.S. Jin, K.K. Yeon, R.L. Se, H.K. Kyu, H.C. Kwang, C.E. Hee, H.C. Jin, Heat modulation of tropoelastin, fibrillin-1, and matrix metalloproteinase-12 in human skin in vivo, J. Invest. Dermatol. 124 (2005) 70–78.
[36] H. Nar, K. Werle, M.M. Bauer, H. Dollinger, B. Jung, Crystal structure of human macrophage elastase (MMP-12) in complex with a hydroxamic acid inhibitor., J. Mol. Biol. 312 (2001) 743–51.
[37] N. Morisaki, S. Moriwaki, Y. Sugiyama-Nakagiri, K. Haketa, Y. Takema, G. Imokawa, Neprilysin is identical to skin fibroblast elastase: Its role in skin aging and UV responses, J. Biol. Chem. 285 (2010) 39819–39827.
[38] U. Talas, J. Dunlop, S. Khalaf, I.M. Leigh, D.P. Kelsell, Human elastase 1: Evidence for expression in the skin and the identification of a frequent frameshift polymorphism, J. Invest. Dermatol. 114 (2000) 165–170.
[39] T.S.A. Thring, P. Hili, D.P. Naughton, Anti-collagenase, anti-elastase and anti-oxidant activities of extracts from 21 plants., BMC Complement. Altern. Med. 9 (2009) 27.
[40] J. Labat-Robert, A. Fourtanier, B. Boyer-Lafargue, L. Robert, Age dependent increase of elastase type protease activity in mouse skin effect of UV-irradiation, J. Photochem. Photobiol. B Biol. 57 (2000) 113–118.
[41] K.S. Girish, K. Kemparaju, The magic glue hyaluronan and its eraser hyaluronidase: A biological overview, Life Sci. 80 (2007) 1921–1943.
[42] Y.J. Kim, H. Uyama, Tyrosinase inhibitors from natural and synthetic sources: Structure, inhibition mechanism and perspective for the future, Cell. Mol. Life Sci. 62 (2005) 1707–1723.
[43] T.S. Chang, An updated review of tyrosinase inhibitors, Int. J. Mol. Sci. 10 (2009) 2440–2475.
[44] B. a Gilchrest, F.B. Blog, G. Szabo, Effects of aging and chronic sun exposure on melanocytes in human skin., J. Invest. Dermatol. 73 (1979) 141–143.
[45] G.T. Wondrak, M.K. Jacobson, E.L. Jacobson, Endogenous UVA-photosensitizers: mediators of skin photodamage and novel targets for skin photoprotection., Photochem. Photobiol. Sci. 5 (2006) 215–237.
[46] M.J. Davies, Singlet oxygen-mediated damage to proteins and its consequences, Biochem. Biophys. Res. Commun. 305 (2003) 761–770.
[47] S. Cho, M.H. Shin, Y.K. Kim, J.-E. Seo, Y.M. Lee, C.-H. Park, J.H. Chung, Effects of infrared radiation and heat on human skin aging in vivo., J. Investig. Dermatol. Symp. Proc. 14

(2009) 15–19.
[48] M.H. Shin, Y.J. Moon, J.E. Seo, Y. Lee, K.H. Kim, J.H. Chung, Reactive oxygen species produced by NADPH oxidase, xanthine oxidase, and mitochondrial electron transport system mediate heat shock-induced MMP-1 and MMP-9 expression, Free Radic. Biol. Med. 44 (2008) 635–645.
[49] S. Cho, M.J. Lee, M.S. Kim, S. Lee, Y.K. Kim, D.H. Lee, C.W. Lee, K.H. Cho, J.H. Chung, Infrared plus visible light and heat from natural sunlight participate in the expression of MMPs and type I procollagen as well as infiltration of inflammatory cell in human skin in vivo, J. Dermatol. Sci. 50 (2008) 123–133.
[50] J. Varani, D. Spearman, P. Perone, S.E. Fligiel, S.C. Datta, Z.Q. Wang, Y. Shao, S. Kang, G.J. Fisher, J.J. Voorhees, Inhibition of type I procollagen synthesis by damaged collagen in photoaged skin and by collagenase-degraded collagen in vitro., Am. J. Pathol. 158 (2001) 931–942.
[51] K. Yano, K. Kajiya, M. Ishiwata, Y.K. Hong, T. Miyakawa, M. Detmar, Ultraviolet B-Induced Skin Angiogenesis Is Associated with a Switch in the Balance of Vascular Endothelial Growth Factor and Thrombospondin-1 Expression, J. Invest. Dermatol. 122 (2004) 201–208.
[52] M.S. Kim, Y.K. Kim, K.H. Cho, J.H. Chung, Infrared exposure induces an angiogenic switch in human skin that is partially mediated by heat, Br. J. Dermatol. 155 (2006) 1131–1138.
[53] J.Y. Seo, S.H. Lee, C.S. Youn, H.R. Choi, G.E. Rhie, K.H. Cho, K.H. Kim, K.C. Park, H.C. Eun, J.H. Chung, Ultraviolet radiation increases tropoelastin mRNA expression in the epidermis of human skin in vivo, J. Invest. Dermatol. 116 (2001) 915–919.
[54] J.P. Ortonne, Pigmentary changes of the ageing skin., Br. J. Dermatol. 122 Suppl (1990) 21–28.
[55] V. Cheynier, P. Sarni-Manchado, S. Quideau, Recent Advances in Polyphenol Research, Wiley-Blackwell, 2012.
[56] R.H. Liu, Potential synergy of phytochemicals in cancer prevention: mechanism of action., J. Nutr. 134 (2004) 3479S–3485S.
[57] K. Khanbabaee, T. van Ree, Tannins: Classification and Definition, Nat. Prod. Rep. 18 (2001) 641–649.
[58] J.A. Nichols, S.K. Katiyar, Skin photoprotection by natural polyphenols: Anti-inflammatory, antioxidant and DNA repair mechanisms, Arch. Dermatol. Res. 302 (2010) 71–83.
[59] M. Guo, C. Perez, Y. Wei, E. Rapoza, G. Su, F. Bou-Abdallah, N.D. Chasteen, Iron-binding properties of plant phenolics and cranberry's bio-effects., Dalton Trans. (2007) 4951–61.
[60] C.A. Rice-Evans, N.J. Miller, G. Paganga, Structure-antioxidant activity relationships of flavonoids and phenolic acids, Free Radic. Biol. Med. 20 (1996) 933–956.
[61] D.B. Min, J.M. Boff, Chemistry and Reaction of Singlet Oxygen in Foods, Compr. Rev. Food Sci. Food Saf. 1 (2002) 58–72.
[62] P. Alov, I. Tsakovska, I. Pajeva, Computational studies of free radical-scavenging properties of phenolic compounds., Curr. Top. Med. Chem. 15 (2015) 85–104.
[63] O. Kutuk, M. Adli, G. Poli, H. Basaga, Resveratrol protects against 4-HNE induced oxidative stress and apoptosis in Swiss 3T3 fibroblasts., Biofactors. 20 (2004) 1–10.
[64] S.K. Manna, A. Mukhopadhyay, B.B. Aggarwal, Resveratrol Suppresses TNF-Induced Activation of Nuclear Transcription Factors NF- B, Activator Protein-1, and Apoptosis: Potential Role of Reactive Oxygen Intermediates and Lipid Peroxidation, J. Immunol. 164 (2000) 6509–6519.
[65] C.Y. Sun, Y. Hu, T. Guo, H.F. Wang, X.P. Zhang, W.J. He, H. Tan, Resveratrol as a novel agent for treatment of multiple myeloma with matrix metalloproteinase inhibitory activity, Acta Pharmacol Sin. 27 (2006) 1447–1452.
[66] P. Bernard, J.Y. Berthon, Resveratrol: An original mechanism on tyrosinase inhibition, Int. J. Cosmet. Sci. 22 (2000) 219–226.
[67] M. Erden Inal, A. Kahraman, T. Koken, Beneficial effects of quercetin on oxidative stress induced by ultraviolet A, Clin Exp Dermatol. 26 (2001) 536–539.
[68] H. Lim, P.K. Hyun, Inhibition of mammalian collagenase, matrix metalloproteinase-1, by naturally-occurring flavonoids, Planta Med. 73 (2007) 1267–1274.
[69] L. Sartor, E. Pezzato, I. Dell'aica, R. Caniato, S. Biggin, S. Garbisa, Inhibition of matrix-proteases by polyphenols: Chemical insights for anti-inflammatory and anti-invasion drug

design, Biochem. Pharmacol. 64 (2002) 229–237.
[70] S. Roy, S. Khanna, H.M. Alessio, J. Vider, D. Bagchi, M. Bagchi, C.K. Sen, Anti-angiogenic property of edible berries., Free Radic. Res. 36 (2002) 1023–1031.
[71] J.E. Kim, M.H. Shin, J.H. Chung, Epigallocatechin-3-gallate prevents heat shock-induced MMP-1 expression by inhibiting AP-1 activity in human dermal fibroblasts, Arch. Dermatol. Res. 305 (2013) 595–602.
[72] S.K. Katiyar, M.S. Matsui, C.A. Elmets, H. Mukhtar, Polyphenolic antioxidant (-)-epigallocatechin-3-gallate from green tea reduces UVB-induced inflammatory responses and infiltration of leukocytes in human skin, Photochem Photobiol. 69 (1999) 148–153.
[73] G.-S. Sim, B.-C. Lee, H.S. Cho, J.W. Lee, J.-H. Kim, D.-H. Lee, J.-H. Kim, H.-B. Pyo, D.C. Moon, K.-W. Oh, Y.P. Yun, J.T. Hong, Structure activity relationship of antioxidative property of flavonoids and inhibitory effect on matrix metalloproteinase activity in UVA-irradiated human dermal fibroblast., Arch. Pharm. Res. 30 (2007) 290–298.
[74] F. Afaq, D.N. Syed, A. Malik, N. Hadi, S. Sarfaraz, M. Kweon, N. Khan, M.A. Zaid, H. Mukhtar, Delphinidin, an Anthocyanidin in Pigmented Fruits and Vegetables, Protects Human HaCaT Keratinocytes and Mouse Skin Against UVB-Mediated Oxidative Stress and Apoptosis, J. Invest. Dermatol. 127 (2007) 222–232.
[75] P.N. Chen, S.C. Chu, H.L. Chiou, W.H. Kuo, C.L. Chiang, Y.S. Hsieh, Mulberry anthocyanins, cyanidin 3-rutinoside and cyanidin 3-glucoside, exhibited an inhibitory effect on the migration and invasion of a human lung cancer cell line, Cancer Lett. 235 (2006) 248–259.
[76] T. Pluemsamran, T. Onkoksoong, U. Panich, Caffeic acid and ferulic acid inhibit UVA-induced matrix metalloproteinase-1 through regulation of antioxidant defense system in keratinocyte HaCaT cells, in: Photochem. Photobiol., 2012: pp. 961–968.
[77] F. Jimenez, T.F. Mitts, K. Liu, Y. Wang, A. Hinek, Ellagic and tannic acids protect newly synthesized elastic fibers from premature enzymatic degradation in dermal fibroblast cultures, J Invest Dermatol. 126 (2006) 1272–1280.
[78] M.F. Melzig, B. Löser, S. Ciesielski, Inhibition of neutrophil elastase activity by phenolic compounds from plants, Pharmazie. 56 (2001) 967–970.
[79] D. Bagchi, C.K. Sen, M. Bagchi, M. Atalay, Anti-angiogenic, antioxidant, and anti-carcinogenic properties of a novel anthocyanin-rich berry extract formula, in: Biochem., 2004: pp. 75–80.
[80] T. Fujii, M. Wakaizumi, T. Ikami, M. Saito, Amla (Emblica officinalis Gaertn.) extract promotes procollagen production and inhibits matrix metalloproteinase-1 in human skin fibroblasts, J. Ethnopharmacol. 119 (2008) 53–57.
[81] M.A. Zaid, F. Afaq, D.N. Syed, M. Dreher, H. Mukhtar, Inhibition of UVB-mediated oxidative stress and markers of photoaging in immortalized HaCaT keratinocytes by pomegranate polyphenol extract POMx, Photochem. Photobiol. 83 (2007) 882–888.
[82] M.N. Aslam, E.P. Lansky, J. Varani, Pomegranate as a cosmeceutical source: Pomegranate fractions promote proliferation and procollagen synthesis and inhibit matrix metalloproteinase-1 production in human skin cells, J. Ethnopharmacol. 103 (2006) 311–318.
[83] H.M. Chiang, T.J. Lin, C.Y. Chiu, C.W. Chang, K.C. Hsu, P.C. Fan, K.C. Wen, Coffea arabica extract and its constituents prevent photoaging by suppressing MMPs expression and MAP kinase pathway, Food Chem. Toxicol. 49 (2011) 309–318.
[84] E. Bralley, P. Greenspan, J.L. Hargrove, D.K. Hartle, Inhibition of hyaluronidase activity by select sorghum brans., J. Med. Food. 11 (2008) 307–312.
[85] A.A. Karim, A. Azlan, A. Ismail, P. Hashim, S.S. Abd Gani, B.H. Zainudin, N.A. Abdullah, Phenolic composition, antioxidant, anti-wrinkles and tyrosinase inhibitory activities of cocoa pod extract., BMC Complement. Altern. Med. 14 (2014) 381.
[86] S.K. Mantena, S.K. Katiyar, Grape seed proanthocyanidins inhibit UV-radiation-induced oxidative stress and activation of MAPK and NF-kappaB signaling in human epidermal keratinocytes, Free Radic. Biol Med. 40 (2006) 1603–1614.
[87] E. Pastrana-Bonilla, C.C. Akoh, S. Sellappan, G. Krewer, Phenolic content and antioxidant capacity of muscadine grapes, J. Agric. Food Chem. 51 (2003) 5497–5503.
[88] E. Cantos, J.C. Espín, F.A. Tomás-Barberán, Varietal differences among the polyphenol

profiles of seven table grape cultivars studied by LC-DAD-MS-MS, J. Agric. Food Chem. 50 (2002) 5691–5696.
[89] C.A. Rice-Evans, L. Packer, Flavonoids in Health and Disease, Second edi, Marcel Dekker, Inc., New York, 2003.
[90] O. Bettini, C. Sloop, Eu-27. Wine Annual Report and Statistics 2015, (2015) 1–28. http://gain.fas.usda.gov/Recent GAIN Publications/Wine Annual_Rome_EU-28_3-16-2015.pdf.
[91] N. McCarthy, The Statistics Portal, World's Biggest Wine Prod. (2015).
[92] H. Johnson, J. Robinson, The World Atlas of Wine, 7th Editio, Octopus Publishing Group Ltd., n.d.
[93] J. Cipriano, Fermentação, Leveduras e Temperatura, Clube Vinhos Port. (2017). https://www.clubevinhosportugueses.pt/vinhos/fermentacao-leveduras-e-temperatura/ (accessed December 3, 2017).
[94] G. Zeppa, The Science and Technology of Wine Making, Dairy Sci. - Food Technol. (2007). https://www.dairyscience.info/index.php/science-and-technology-of-wine/124-the-science-and-technology-of-wine-making.html (accessed December 3, 2017).
[95] How is Port made?, Taylor's. (n.d.). http://www.taylor.pt/en/what-is-port-wine/how-is-port-made/ (accessed December 5, 2017).
[96] A. Teixeira, N. Baenas, R. Dominguez-Perles, A. Barros, E. Rosa, D.A. Moreno, C. Garcia-Viguera, Natural bioactive compounds from winery by-products as health promoters: A review, Int. J. Mol. Sci. 15 (2014) 15638–15678.
[97] T. Moreno, E. de Paz, I. Navarro, S. Rodríguez-Rojo, A. Matias, C. Duarte, M. Sanz-Buenhombre, M.J. Cocero, Spray Drying Formulation of Polyphenols-Rich Grape Marc Extract: Evaluation of Operating Conditions and Different Natural Carriers, Food Bioprocess Technol. (2016) 1–13.
[98] H.C. Ansel, W.P. Norred, I.L. Roth, Antimicrobial activity of dimethyl sulfoxide against Escherichia coli, Pseudomonas aeruginosa, and Bacillus megaterium., J. Pharm. Sci. 58 (1969) 836–839.
[99] L. Li, K.Y. Mak, J. Shi, C.H. Leung, C.M. Wong, C.W. Leung, C.S.K. Mak, K.Y. Chan, N.M.M. Chan, E.X. Wu, P.W.T. Pong, Sterilization on dextran-coated iron oxide nanoparticles: Effects of autoclaving, filtration, UV irradiation, and ethanol treatment, Microelectron. Eng. 111 (2013) 310–313.
[100] E. a Ainsworth, K.M. Gillespie, Estimation of total phenolic content and other oxidation substrates in plant tissues using Folin-Ciocalteu reagent., Nat. Protoc. 2 (2007) 875–877.
[101] V.L. Singleton, R. Orthofer, R.M. Lamuela-Raventós, Analysis of total phenols and other oxidation substrates and antioxidants by means of folin-ciocalteu reagent, Methods Enzymol. 299 (1998) 152–178.
[102] B.W. Bolling, Y.Y. Chen, A.G. Kamil, C.Y.O. Chen, Assay Dilution Factors Confound Measures of Total Antioxidant Capacity in Polyphenol-Rich Juices, J. Food Sci. 77 (2012).
[103] Total Monomeric Anthocyanin Pigment Content of Fruit Juices, Beverages, Natural Colorants, and Wines, AOAC Off. Method 2005.02. (2005).
[104] J. Lee, C. Rennaker, R.E. Wrolstad, Comparison of two methods for anthocyanin quantification, Acta Hortic. 810 (2009) 831–834.
[105] N. Mateus, A.M.S. Silva, J. Vercauteren, V. De Freitas, Occurrence of anthocyanin-derived pigments in red wines, J. Agric. Food Chem. 49 (2001) 4836–4840.
[106] D. Huang, B. Ou, M. Hampsch-Woodill, J.A. Flanagan, R.L. Prior, High-throughput assay of oxygen radical absorbance capacity (ORAC) using a multichannel liquid handling system coupled with a microplate fluorescence reader in 96-well format, J. Agric. Food Chem. 50 (2002) 4437–4444.
[107] R.P. Feliciano, M.N. Bravo, M.M. Pires, A.T. Serra, C.M. Duarte, L. V. Boas, M.R. Bronze, Phenolic content and antioxidant activity of moscatel dessert wines from the setúbal region in portugal, Food Anal. Methods. 2 (2009) 149–161.
[108] C.C. Trevithick, J. a Vinson, J. Caulfeild, F. Rahman, T. Derksen, L. Bocksch, S. Hong, a Stefan, K. Teufel, N. Wu, M. Hirst, J.R. Trevithick, Is ethanol an important antioxidant in alcoholic beverages associated with risk reduction of cataract and atherosclerosis?, Redox Rep. 4 (1999) 89–93.

[109] J. Moore, J.J. Yin, L. Yu, Novel fluorometric assay for hydroxyl radical scavenging capacity (HOSC) estimation, J. Agric. Food Chem. 54 (2006) 617–626.
[110] B. Ou, M. Hampsch-Woodill, J. Flanagan, E.K. Deemer, R.L. Prior, D. Huang, Novel fluorometric assay for hydroxyl radical prevention capacity using fluorescein as the probe, J. Agric. Food Chem. 50 (2002) 2772–2777.
[111] E.W.C. Chan, Y.Y. Lim, L.F. Wong, F.S. Lianto, S.K. Wong, K.K. Lim, C.E. Joe, T.Y. Lim, Antioxidant and tyrosinase inhibition properties of leaves and rhizomes of ginger species, Food Chem. 109 (2008) 477–483.
[112] L.M. Vermeer, C.A. Higgins, D.L. Roman, J.A. Doorn, Real-time monitoring of tyrosine hydroxylase activity using a plate reader assay, Anal. Biochem. 432 (2013) 11–15.
[113] A.J. Barrett, H. Kirschke, Cathepsin B, Cathepsin H, and cathepsin L., Methods Enzymol. 80 (1981) 535–561.
[114] K.-I. Shimokawa, M. Katayama, Y. Matsuda, H. Takahashi, I. Hara, H. Sato, Complexes of gelatinases and tissue inhibitor of metalloproteinases in human seminal plasma., J. Androl. 24 (2003) 73–7.
[115] G. Malich, B. Markovic, C. Winder, The sensitivity and specificity of the MTS tetrazolium assay for detecting the in vitro cytotoxicity of 20 chemicals using human cell lines, Toxicology. 124 (1997) 179–192.
[116] T.L. Riss, R.A. Moravec, A.L. Niles, S. Duellman, H.A. Benink, T.J. Worzella, L. Minor, Cell Viability Assays, 2004.
[117] K.L. Wolfe, H.L. Rui, Cellular antioxidant activity (CAA) assay for assessing antioxidants, foods, and dietary supplements, J. Agric. Food Chem. 55 (2007) 8896–8907.
[118] L. Wang, C.L. Weller, Recent advances in extraction of nutra- ceuticals from plants, Trends Food Sci. Technol. 17 (2006) 300–312.
[119] I. Elez Garofulić, V. Dragović-Uzelac, A. Režek Jambrak, M. Jukić, The effect of microwave assisted extraction on the isolation of anthocyanins and phenolic acids from sour cherry Marasca (Prunus cerasus var. Marasca), J. Food Eng. 117 (2013) 437–442.
[120] T.S. Ballard, P. Mallikarjunan, K. Zhou, S. O'Keefe, Microwave-assisted extraction of phenolic antioxidant compounds from peanut skins, Food Chem. 120 (2010) 1185–1192.
[121] V. Camel, Microwave-assisted solvent extraction of environmental samples, TrAC - Trends Anal. Chem. 19 (2000) 229–248.
[122] Z. Yang, W. Zhai, Optimization of microwave-assisted extraction of anthocyanins from purple corn (Zea mays L.) cob and identification with HPLC-MS, Innov. Food Sci. Emerg. Technol. 11 (2010) 470–476.
[123] C. Negro, L. Tommasi, A. Miceli, Phenolic compounds and antioxidant activity from red grape marc extracts, Bioresour. Technol. 87 (2003) 41–44.
[124] I.I. Rockenbach, E. Rodrigues, L.V. Gonzaga, V. Caliari, M.I. Genovese, A.E.D.S.S. Gonalves, R. Fett, Phenolic compounds content and antioxidant activity in pomace from selected red grapes (Vitis vinifera L. and Vitis labrusca L.) widely produced in Brazil, Food Chem. 127 (2011) 174–179.
[125] N.G. Baydar, G. Özkan, O. Sağdiç, Total phenolic contents and antibacterial activities of grape (Vitis vinifera L.) extracts, Food Control. 15 (2004) 335–339.
[126] M.S. Lingua, M.P. Fabani, D.A. Wunderlin, M. V. Baroni, In vivo antioxidant activity of grape, pomace and wine from three red varieties grown in Argentina: Its relationship to phenolic profile, J. Funct. Foods. 20 (2016) 332–345.
[127] Y. Tao, D. Wu, Q.A. Zhang, D.W. Sun, Ultrasound-assisted extraction of phenolics from wine lees: Modeling, optimization and stability of extracts during storage, Ultrason. Sonochem. 21 (2014) 706–715.
[128] J.A. Pérez-Serradilla, M.D. Luque de Castro, Microwave-assisted extraction of phenolic compounds from wine lees and spray-drying of the extract, Food Chem. 124 (2011) 1652–1659.
[129] A. Morata, M.C. Gómez-Cordovés, J. Suberviola, B. Bartolomé, B. Colomo, J.A. Suárez, Adsorption of anthocyanins by yeast cell walls during the fermentation of red wines, J. Agric. Food Chem. 51 (2003) 4084–4088.
[130] R.T. Branquinho, V.C.F. Mosqueira, E.K. Kano, J. De Souza, D.D.R. Dorim, D.A. Saúde-Guimarães, M. De Lana, HPLC-DAD and UV-spectrophotometry for the determination of

lychnopholide in nanocapsule dosage form: Validation and application to release kinetic study, J. Chromatogr. Sci. 52 (2014) 19–26.
[131] PhytoHub, www.phytohub.eu.
[132] Phenol-Explorer, www.phenol-explorer.eu.
[133] X. Wu, R.L. Prior, Systematic identification and characterization of anthocyanins by HPLC-ESI-MS/MS in common foods in the United States: Fruits and berries, J. Agric. Food Chem. 53 (2005) 2589–2599.
[134] A. Vallverdú-Queralt, N. Boix, E. Piqué, J. Gómez-Catalan, A. Medina-Remon, G. Sasot, M. Mercader-Martí, J.M. Llobet, R.M. Lamuela-Raventos, Identification of phenolic compounds in red wine extract samples and zebrafish embryos by HPLC-ESI-LTQ-Orbitrap-MS, Food Chem. 181 (2015) 146–151.
[135] M. Schwarz, P. Quast, D. Von Baer, P. Winterhalter, Vitisin A content in Chilean wines from Vitis vinifera cv. Cabernet Sauvignon and contribution to the color of aged red wines, J. Agric. Food Chem. 51 (2003) 6261–6267.
[136] M. Sanz, B. Fernández de Simón, E. Esteruelas, Á.M. Muñoz, E. Cadahía, M.T. Hernández, I. Estrella, J. Martinez, Polyphenols in red wine aged in acacia (Robinia pseudoacacia) and oak (Quercus petraea) wood barrels, Anal. Chim. Acta. 732 (2012) 83–90.
[137] T. Hernández, I. Estrella, D. Carlavilla, P.J. Martín-Álvarez, M.V. Moreno-Arribas, Phenolic compounds in red wine subjected to industrial malolactic fermentation and ageing on lees, in: Anal. Chim. Acta, 2006: pp. 116–125.
[138] M.P. Delgado De La Torre, F. Priego-Capote, M.D. Luque De Castro, Characterization and comparison of wine lees by liquid chromatography-mass spectrometry in high-resolution mode, J. Agric. Food Chem. 63 (2015) 1116–1125.
[139] P. Donato, F. Rigano, F. Cacciola, M. Schure, S. Farnetti, M. Russo, P. Dugo, L. Mondello, Comprehensive two-dimensional liquid chromatography–tandem mass spectrometry for the simultaneous determination of wine polyphenols and target contaminants, J. Chromatogr. A. 1458 (2016) 54–62.
[140] D. Blanco-Vega, F.J. López-Bellido, J.M. Alía-Robledo, I. Hermosín-Gutiérrez, HPLC-DAD-ESI-MS/MS characterization of pyranoanthocyanins pigments formed in model wine, J. Agric. Food Chem. 59 (2011) 9523–9531.
[141] A. Brito, C. Areche, B. Sepúlveda, E.J. Kennelly, M.J. Simirgiotis, Anthocyanin characterization, total phenolic quantification and antioxidant features of some chilean edible berry extracts, Molecules. 19 (2014) 10936–10955.
[142] M.N. Bravo, S. Silva, A. V. Coelho, L.V. Boas, M.R. Bronze, Analysis of phenolic compounds in Muscatel wines produced in Portugal, in: Anal. Chim. Acta, 2006: pp. 84–92.
[143] S. Hogan, L. Zhang, J. Li, S. Sun, C. Canning, K. Zhou, Antioxidant rich grape pomace extract suppresses postprandial hyperglycemia in diabetic mice by specifically inhibiting alpha-glucosidase., Nutr. Metab. (Lond). 7 (2010) 71.
[144] H.H. Tournour, M.A. Segundo, L.M. Magalhães, L. Barreiros, J. Queiroz, L.M. Cunha, Valorization of grape pomace: Extraction of bioactive phenolics with antioxidant properties, Ind. Crops Prod. 74 (2015) 397–406.
[145] W. Brand-Williams, M.E. Cuvelier, C. Berset, Use of a free radical method to evaluate antioxidant activity, LWT - Food Sci. Technol. 28 (1995) 25–30.
[146] P. Iacopini, M. Baldi, P. Storchi, L. Sebastiani, Catechin, epicatechin, quercetin, rutin and resveratrol in red grape: Content, in vitro antioxidant activity and interactions, J. Food Compos. Anal. 21 (2008) 589–598.
[147] M. Działo, J. Mierziak, U. Korzun, M. Preisner, J. Szopa, A. Kulma, The potential of plant phenolics in prevention and therapy of skin disorders, Int. J. Mol. Sci. 17 (2016).
[148] L. Mira, M. Tereza Fernandez, M. Santos, R. Rocha, M. Helena Florêncio, K.R. Jennings, Interactions of Flavonoids with Iron and Copper Ions: A Mechanism for their Antioxidant Activity, Free Radic. Res. 36 (2002) 1199–1208.
[149] J. CABANES, S. CHAZARRA, F. GARCIA-CARMONA, Kojic Acid, a Cosmetic Skin Whitening Agent, is a Slow-binding Inhibitor of Catecholase Activity of Tyrosinase, J. Pharm. Pharmacol. 46 (1994) 982–985.
[150] A. Karioti, A. Protopappa, N. Megoulas, H. Skaltsa, Identification of tyrosinase inhibitors from Marrubium velutinum and Marrubium cylleneum, Bioorganic Med. Chem. 15 (2007) 2708–

2714.
[151] L.-P. Xie, Q.-X. Chen, H. Huang, H.-Z. Wang, R.-Q. Zhang, Inhibitory effects of some flavonoids on the activity of mushroom tyrosinase., Biochem. Biokhimiia. 68 (2003) 487–91.
[152] H. Matsuda, H. Kuroda, M. Higashino, W. Chen, H. Tosa, M. Iinuma, M. Kubo, Studies of cuticle drugs from natural sources. III. Inhibitory effects of Myrica rubra on melanin biosynthesis, Biol,Pharm. 18 (1995) 1148–1150.
[153] J.Y. Jeong, Q. Liu, S.B. Kim, Y.H. Jo, E.J. Mo, H.H. Yang, D.H. Song, B.Y. Hwang, M.K. Lee, Characterization of melanogenesis inhibitory constituents of morus alba leaves and optimization of extraction conditions using response surface methodology, Molecules. 20 (2015) 8730–8741.
[154] I. Kubo, I. Kinst-Hori, S.K. Chaudhuri, Y. Kubo, Y. Sánchez, T. Ogura, Flavonols from Heterotheca inuloides: Tyrosinase inhibitory activity and structural criteria, Bioorganic Med. Chem. 8 (2000) 1749–1755.
[155] K. Shimizu, R. Kondo, K. Sakai, Inhibition of tyrosinase by flavonoids, stilbenes and related 4- substituted resorcinols: Structure-activity investigations, Planta Med. 66 (2000) 11–15.
[156] P.M. Starkey, A.J. Barrett, Human lysosomal elastase. Catalytic and immunological properties., Biochem. J. 155 (1976) 265–71.
[157] K.K. Lee, J.J. Cho, E.J. Park, J.D. Choi, Anti-elastase and anti-hyaluronidase of phenolic substance from Areca catechu as a new anti-ageing agent, Int. J. Cosmet. Sci. 23 (2001) 341–346.
[158] J. Shi, J. Yu, J.E. Pohorly, Y. Kakuda, Polyphenolics in grape seeds-biochemistry and functionality., J. Med. Food. 6 (2003) 291–299.
[159] B. Siedle, R. Murillo, O. Hucke, a Labahn, I. Merfort, Structure activity relationship studies of cinnamic acid derivatives as inhibitors of human neutrophil elastase revealed by ligand docking calculations., Pharmazie. 58 (2003) 337–339.
[160] B. Madhan, G. Krishnamoorthy, J.R. Rao, B.U. Nair, Role of green tea polyphenols in the inhibition of collagenolytic activity by collagenase, Int. J. Biol. Macromol. 41 (2007) 16–22.
[161] Y.J. Kim, H. Uyama, S. Kobayashi, Inhibition effects of (+)-catechin-aldehyde polycondensates on proteinases causing proteolytic degradation of extracellular matrix, Biochem. Biophys. Res. Commun. 320 (2004) 256–261.
[162] A. Hoh, K. Maier, Comparative Cytotoxicity Test with Human Keratinocytes, HaCaT cells, and Skin Fibroblasts to Investigate Skin-Irritating Substances, in: Cell Tissue Cult. Model. Dermatological Res., Springer-Verlag, 1993: pp. 341–347.
[163] I.O. for Standardization, ISO 10993-5, 2009.
[164] S. Sobočanec, V. Šverko, T. Balog, A. Šarić, G. Rusak, S. Likić, B. Kušić, V. Katalinić, S. Radić, T. Marotti, Oxidant/antioxidant properties of Croatian native propolis, J. Agric. Food Chem. 54 (2006) 8018–8026.
[165] E.G. Yordi, E.M. Pérez, M.J. Matos, E.U. Villares, Antioxidant and Pro-Oxidant Effects of Polyphenolic Compounds and Structure-Activity Relationship Evidence, in: J.B. and T. Bohn (Ed.), Nutr. Well-Being Heal., InTech, 2012: pp. 23–48.
[166] J. Bouayed, T. Bohn, Exogenous Antioxidants—Double-Edged Swords in Cellular Redox State: Health Beneficial Effects at Physiologic Doses versus Deleterious Effects at High Doses, Oxid. Med. Cell. Longev. 3 (2010) 228–237.
[167] A. Svobodová, J. Rambousková, D. Walterová, J. Vostalová, Bilberry extract reduces UVA-induced oxidative stress in HaCaT keratinocytes: A pilot study, BioFactors. 33 (2008) 249–266.
[168] J.Y. Choi, H. Kim, Y.J. Choi, A. Ishihara, K. Back, S.G. Lee, Cytoprotective activities of hydroxycinnamic acid amides of serotonin against oxidative stress-induced damage in HepG2 and HaCaT cells, Fitoterapia. 81 (2010) 1134–1141.
[169] M. Varasteh-kojourian, P. Abrishamchi, M.M. Matin, J. Asili, Antioxidant , cytotoxic and DNA protective properties of Achillea eriophora DC . and Achillea biebersteinii Afan . extracts : A comparative study, 7 (2017) 157–168.
[170] L.C. Dias, Effect of olive oil phenolic compounds against oxidative stress-induced injury in renal proximal tubule cells and keratinocytes, 2012.
[171] L. Liu, H. Xie, X. Chen, W. Shi, X. Xiao, D. Lei, J. Li, Differential response of normal human epidermal keratinocytes and HaCaT cells to hydrogen peroxide-induced oxidative stress,

Clin. Exp. Dermatol. 37 (2012) 772–780.
[172] H.S. Kim, M.J. Quon, J. a. Kim, New insights into the mechanisms of polyphenols beyond antioxidant properties; lessons from the green tea polyphenol, epigallocatechin 3-gallate, Redox Biol. 2 (2014) 187–195.
[173] H.T.T. Phan, T. Yoda, B. Chahal, M. Morita, M. Takagi, M.C. Vestergaard, Structure-dependent interactions of polyphenols with a biomimetic membrane system, Biochim. Biophys. Acta - Biomembr. 1838 (2014) 2670–2677.
[174] a Matias, S.L. Nunes, J. Poejo, E. Mecha, a T. Serra, P.J.A. Madeira, M.R. Bronze, C.M.M. Duarte, Antioxidant and anti-inflammatory activity of a flavonoid-rich concentrate recovered from Opuntia ficus-indica juice., Food Funct. 5 (2014) 3269–80.
[175] A.T. Serra, R.O. Duarte, M.R. Bronze, C.M.M. Duarte, Identification of bioactive response in traditional cherries from Portugal, Food Chem. 125 (2011) 318–325.
[176] S.H. Thilakarathna, H.P. Vasantha Rupasinghe, Flavonoid bioavailability and attempts for bioavailability enhancement, Nutrients. 5 (2013) 3367–3387.
[177] S. Azam, N. Hadi, N.U. Khan, S.M. Hadi, Prooxidant property of green tea polyphenols epicatechin and epigallocatechin-3-gallate: Implications for anticancer properties, Toxicol. Vitr. 18 (2004) 555–561.
[178] E.A. Decker, Phenolics: Prooxidants or Antioxidants?, Nutr. Rev. 55 (1997) 396–407.
[179] T.L. Farrell, L. Poquet, T.P. Dew, S. Barber, G. Williamson, Predicting phenolic acid absorption in Caco-2 cells: A theoretical permeability model and mechanistic study, Drug Metab. Dispos. 40 (2012) 397–406.
[180] I. Volf, I. Ignat, M. Neamtu, V. Popa, Thermal stability, antioxidant activity, and photo-oxidation of natural polyphenols, Chem. Pap. 68 (2014).
[181] M. Friedman, H.S. Jürgens, Effect of pH on the stability of plant phenolic compounds, J. Agric. Food Chem. 48 (2000) 2101–2110.
[182] S. Sipahli, V. Mohanlall, J.J. Mellem, Stability and degradation kinetics of crude anthocyanin extracts from H. sabdariffa, Food Sci. Technol. 37 (2017).
[183] S. Oancea, O. Drăghici, PH and thermal stability of anthocyanin-based optimised extracts of romanian red onion cultivars, Czech J. Food Sci. 31 (2013) 283–291.
[184] M.E. West, L.J. Mauer, Color and chemical stability of a variety of anthocyanins and ascorbic acid in solution and powder forms, J. Agric. Food Chem. 61 (2013) 4169–4179.
[185] M.J. Rein, Copigmentation reactions and color stability of berry anthocyanins, University of Helsinki, 2005.
[186] S. González-Manzano, C. Santos-Buelga, M. Dueñas, J.C. Rivas-Gonzalo, T. Escribano-Bailón, Colour implications of self-association processes of wine anthocyanins, Eur. Food Res. Technol. 226 (2008) 483–490.
[187] M.J. Abla, A.K. Banga, Quantification of skin penetration of antioxidants of varying lipophilicity, Int. J. Cosmet. Sci. 35 (2013) 19–26.
[188] J. Arct, A. Oborska, M. Mojski, A. Binkowska, B. Świdzikowska, Common cosmetic hydrophilic ingredients as penetration modifiers of flavonoids, Int. J. Cosmet. Sci. 24 (2002) 357–366.
[189] A. Madene, M. Jacquot, J. Scher, S. Desobry, Flavour encapsulation and controlled release - A review, Int. J. Food Sci. Technol. 41 (2006) 1–21.
[190] K. Cal, K. Sollohub, Spray drying technique. I: Hardware and process parameters, J. Pharm. Sci. 99 (2010) 575–586.
[191] J.A. Larrauri, P. Rupérez, F. Saura-Calixto, Effect of Drying Temperature on the Stability of Polyphenols and Antioxidant Activity of Red Grape Pomace Peels, J. Agric. Food Chem. 45 (1997) 1390–1393.
[192] A.S. Gad, Y.A. Khadrawy, A.A. El-Nekeety, S.R. Mohamed, N.S. Hassan, M.A. Abdel-Wahhab, Antioxidant activity and hepatoprotective effects of whey protein and Spirulina in rats, Nutrition. 27 (2011) 582–589.
[193] Q. Liu, B. Kong, J. Han, C. Sun, P. Li, Structure and antioxidant activity of whey protein isolate conjugated with glucose via the Maillard reaction under dry-heating conditions, Food Struct. 1 (2014) 145–154.
[194] B. Jiang, W.C. Obiro, Y. Li, T. Zhang, W. Mu, Bioactivity of Proteins and Peptides from Peas (Pisum sativum, Vigna unguiculata, and Cicer arietinum L), in: Bioact. Proteins Pept. as

Funct. Foods Nutraceuticals, 2010: pp. 273–287.
[195] N.S. Stanisavljević, G.N. Vukotić, F.T. Pastor, D. Sužnjević, Živko S. Jovanović, I.D. Strahinić, D.A. Fira, S.S. Radović, Antioxidant activity of pea protein hydrolysates produced by batch fermentation with lactic acid bacteria, Arch. Biol. Sci. 67 (2015) 1033–1042.
[196] D.L. Hofman, V.J. van Buul, F.J.P.H. Brouns, Nutrition, Health, and Regulatory Aspects of Digestible Maltodextrins, Crit. Rev. Food Sci. Nutr. 56 (2016) 2091–2100.
[197] V.S.S. Gonçalves, J. Poejo, A.A. Matias, S. Rodríguez-Rojo, M.J. Cocero, C.M.M. Duarte, Using different natural origin carriers for development of epigallocatechin gallate (EGCG) solid formulations with improved antioxidant activity by PGSS-drying, RSC Adv. 6 (2016) 67599–67609.
[198] V.S.S. Gonçalves, S. Rodríguez-Rojo, E. De Paz, C. Mato, T. Martín, M.J. Cocero, Production of water soluble quercetin formulations by pressurized ethyl acetate-in-water emulsion technique using natural origin surfactants, Food Hydrocoll. 51 (2015) 295–304.
[199] D.C. Estupiñan, S.J. Schwartz, G.A. Garzón, Antioxidant Activity, Total Phenolics Content, Anthocyanin, and Color Stability of Isotonic Model Beverages Colored with Andes Berry (Rubus glaucus Benth) Anthocyanin Powder, J. Food Sci. 76 (2011).
[200] F. Dechsakulthorn, A. Hayes, S. Bakand, L. Joeng, C. Winder, In vitro cytotoxicity assessment of selected nanoparticles using human skin fibroblasts, Proceeding 6th World Congr. Altern. Anim. Use Life Sci. (2007) 397–400.
[201] V.S.S. Gonçalves, P. Gurikov, J. Poejo, A.A. Matias, S. Heinrich, C.M.M. Duarte, I. Smirnova, Alginate-based hybrid aerogel microparticles for mucosal drug delivery, Eur. J. Pharm. Biopharm. 107 (2016) 160–170.
[202] V.S.S. Gonçalves, A.A. Matias, J. Poejo, A.T. Serra, C.M.M. Duarte, Application of RPMI 2650 as a cell model to evaluate solid formulations for intranasal delivery of drugs, Int. J. Pharm. 515 (2016) 1–10.
[203] M. Mori, P. V. Almeida, M. Cola, G. Anselmi, E. Mäkilä, A. Correia, J. Salonen, J. Hirvonen, C. Caramella, H.A. Santos, In vitro assessment of biopolymer-modified porous silicon microparticles for wound healing applications, Eur. J. Pharm. Biopharm. 88 (2014) 635–642.
[204] C. Saldanha do Carmo, C. Maia, J. Poejo, I. Lychko, P. Gamito, I. Nogueira, M.R. Bronze, A.T. Serra, C.M.M. Duarte, Microencapsulation of α-tocopherol with zein and β-cyclodextrin using spray drying for colour stability and shelf-life improvement of fruit beverages, RSC Adv. 7 (2017) 32065–32075.
[205] P.P. Fu, Q. Xia, H.-M. Hwang, P.C. Ray, H. Yu, Mechanisms of nanotoxicity: Generation of reactive oxygen species, J. Food Drug Anal. 22 (2014) 64–75.
[206] J.M. Matés, J.A. Segura, F.J. Alonso, J. Márquez, Intracellular redox status and oxidative stress: Implications for cell proliferation, apoptosis, and carcinogenesis, Arch. Toxicol. 82 (2008) 273–299.
[207] J.L. Martindale, N.J. Holbrook, Cellular response to oxidative stress: Signaling for suicide and survival, J. Cell. Physiol. 192 (2002) 1–15.

6. Appendix

Appendix A: Chromatographic profiles of one extract sample from each winemaking waste stream matrix at different wavelengths, obtained by the HPLC method 2. The presented scales are not representative of relative quantities of the compounds originating the peaks.

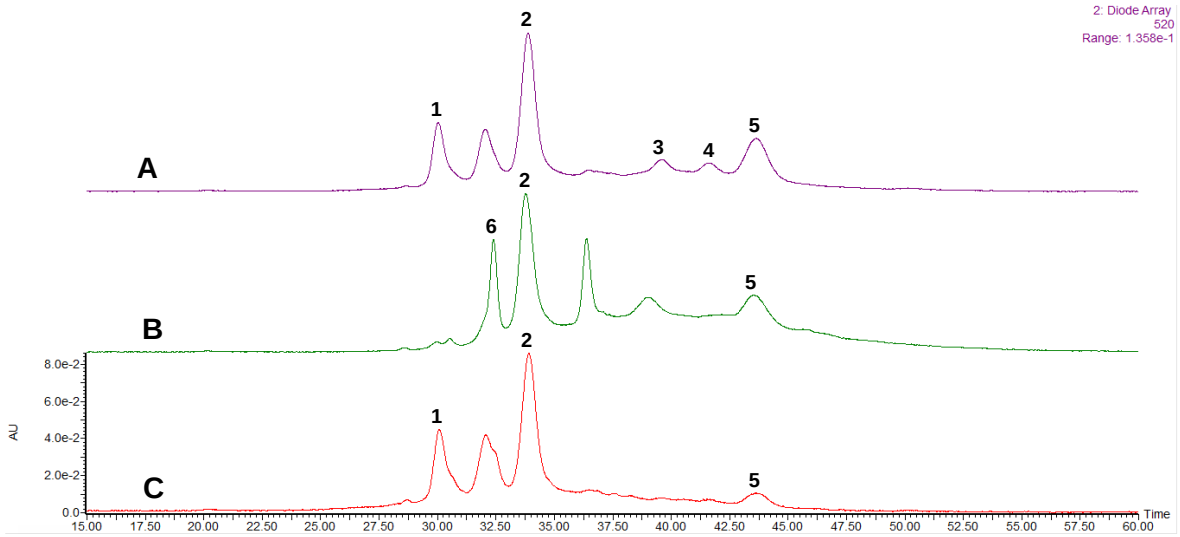

Figure 6.1. Chromatographic profiles of Mt (A), Port (B), and MW80 GM (C) at 520 nm.

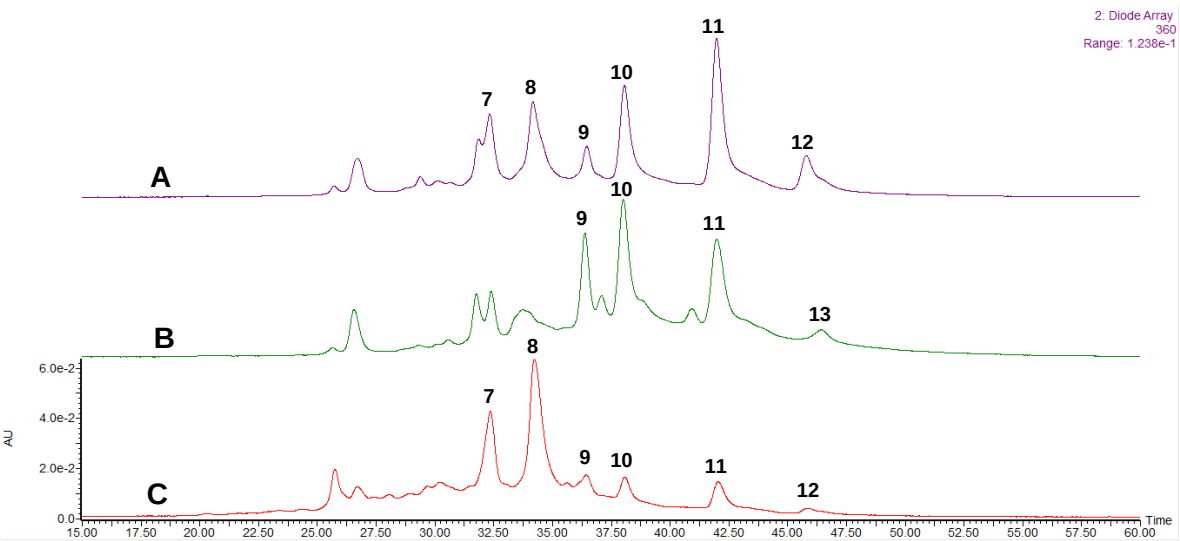

Figure 6.2. Chromatographic profiles of Mt (A), Port (B), and MW80 GM (C) at 360 nm.

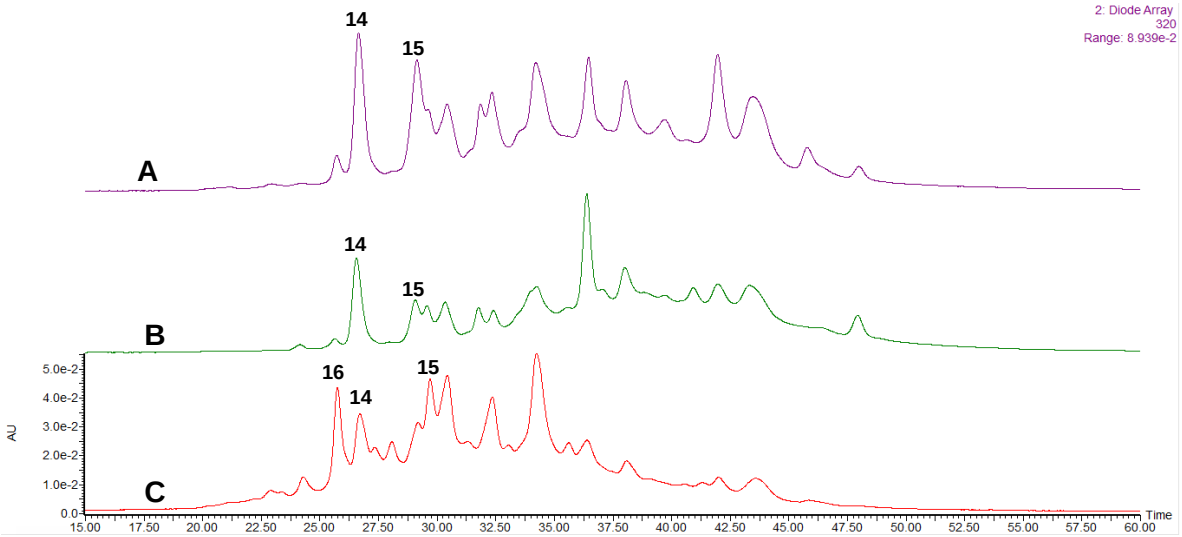

Figure 6.3. Chromatographic profiles of Mt (A), Port (B), and MW80 GM (C) at 320 nm.

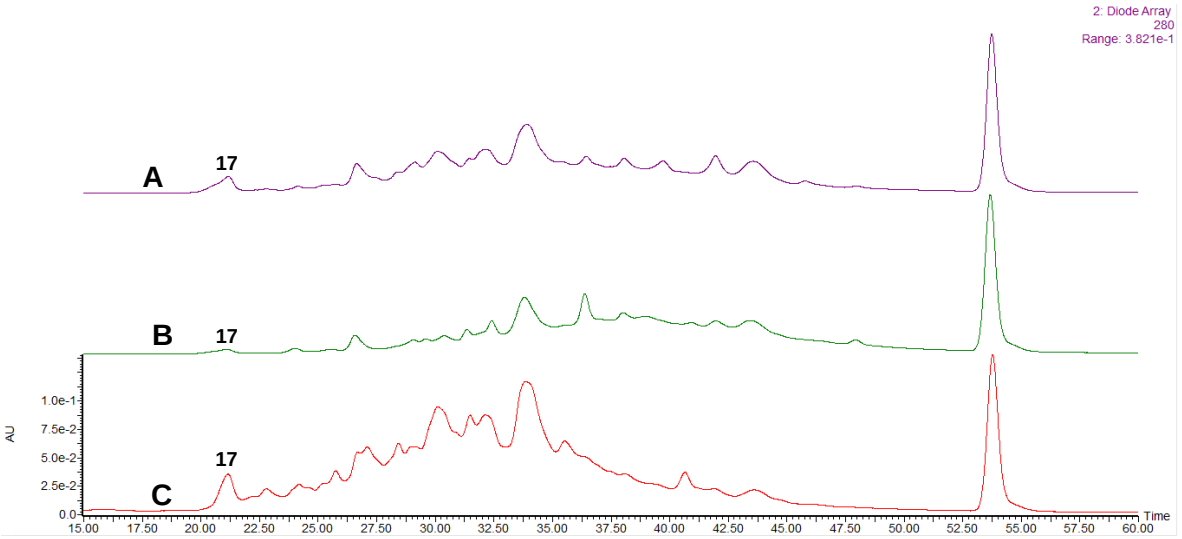

Figure 6.4. Chromatographic profiles of Mt (A), Port (B), and MW80 GM (C) at 280 nm.

Appendix B: Effect of grape marc conventional extract (GM) and respective formulations on H_2O_2-induced ROS and H_2O_2-induced cytotoxicity.

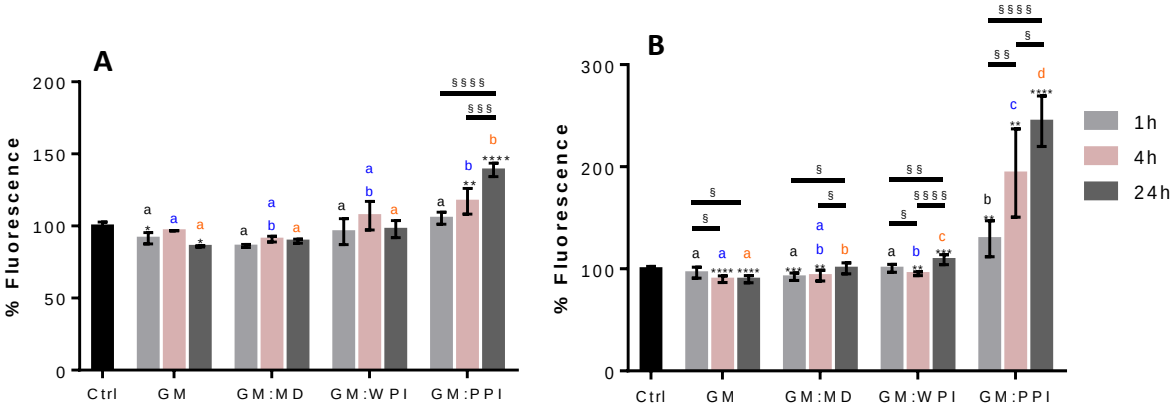

Figure 6.5. Pre-incubation (1h, 4h and 24h) of (A) HaCaT and (B) HFF with grape marc extract (GM) and its formulations with three different carriers prior addition of H_2O_2 – influence on total ROS production. The symbol * indicates significance relative to the control (* p-value<0.05, ** p-value<0.01, *** p-value<0.001, **** p-value<0.0001); the symbol § indicates significance between different incubation times of the same sample (§ p-value<0.05, §§ p-value<0.01, §§§ p-value<0.001, §§§§ p-value<0.0001). The same incubation times of different samples were compared (1h – black, 4h – blue, 24h – orange); statistically different results (p-value<0.5) are identified with different letters. Results were obtained from two independent experiments in HFF and only one experiment in HaCaT.

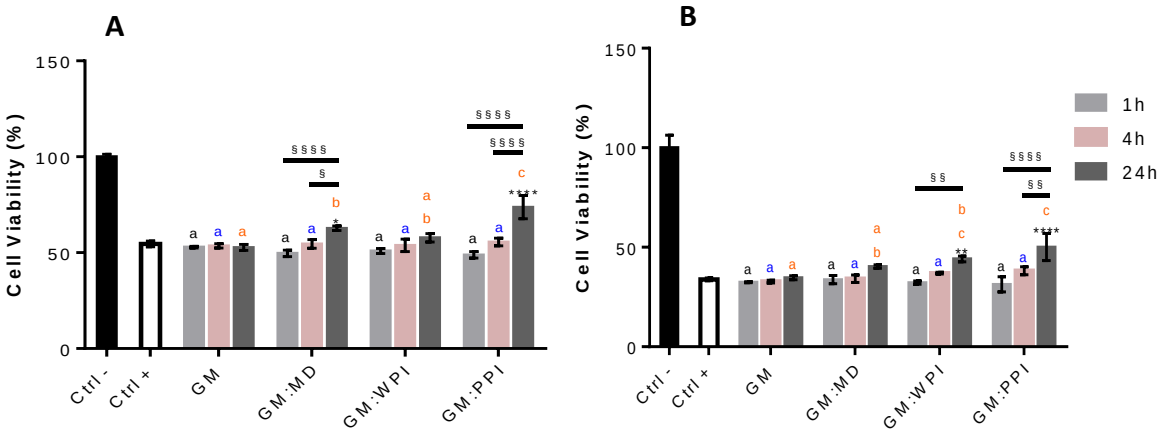

Figure 6.6. Pre-incubation (1h, 4h and 24h) of (A) HaCaT and (B) HFF with grape marc extract (GM) and its formulations with three different carriers: influence on cell viability upon H_2O_2-induced stress. The symbol * indicates significance relative to the control where stress was induced (* p-value<0.05, ** p-value<0.01, **** p-value<0.0001); the symbol § indicates significance between different incubation times of the same sample (§ p-value<0.05, §§ p-value<0.01, §§§§ p-value<0.0001). The same incubation times of different samples were compared (1h – black, 4h – blue, 24h – orange); statistically different results (p-value<0.5) are identified with different letters. Preliminary results obtained from one experiment only.